

Drug Delivery

ISSN: 1071-7544 (Print) 1521-0464 (Online) Journal homepage: www.tandfonline.com/journals/idrd20

Redefining intranasal brain delivery: from nasal entry to meaningful parenchymal and cellular exposure

Youngbeom Kim , Chae-Ok Yun & A-Rum Yoon

To cite this article: Youngbeom Kim , Chae-Ok Yun & A-Rum Yoon (2026) Redefining intranasal brain delivery: from nasal entry to meaningful parenchymal and cellular exposure, Drug Delivery, 33:1, 2738285, DOI: 10.1080/10717544.2026.2738285

To link to this article: https://doi.org/10.1080/10717544.2026.2738285

© 2026 The Author(s). Published by Informa UK Limited, trading as Taylor & Francis Group.

Published online: 01 Oct 2026.

Submit your article to this journal

Article views: 327

View related articles

View Crossmark data

Full Terms & Conditions of access and use can be found at
https://www.tandfonline.com/action/journalInformation?journalCode=idrd20

DRUG DELIVERY
2026, VOL. 33, NO. 1, 2738285
https://doi.org/10.1080/10717544.2026.2738285

Taylor & Francis
by informa

REVIEW ARTICLE

OPEN ACCESS Check for updates

Redefining intranasal brain delivery: from nasal entry to meaningful parenchymal and cellular exposure

Youngbeom Kim[a], Chae-Ok Yun[a,b,c,d,1] and A-Rum Yoon[a,b,c,1]

[a]Department of Bioengineering, College of Engineering, Hanyang University, Seoul, Republic of Korea; [b]Institute of Nano Science and Technology (INST), Hanyang University, Seoul, Republic of Korea; [c]Hanyang Institute of Bioscience and Biotechnology (HY-IBB), Hanyang University, Seoul, Republic of Korea; [d]GeneMedicine Co., Ltd, Seoul, Republic of Korea

ABSTRACT

Nose-to-brain (N2B) delivery is a promising noninvasive strategy to circumvent the blood–brain barrier (BBB). However, the clinical translation of N2B platforms remains hindered by a conceptual oversimplification that equates crude central nervous system (CNS) exposure with effective therapeutic delivery. This review reconceptualizes the N2B pathway as a stage-resolved sequential transport cascade extending from nasal entry to meaningful parenchymal and cellular access. We identify a critical imbalance in current formulation strategies, which have advanced two extreme poles, namely initial mucosal retention and epithelial permeation at one end and final target-cell engagement at the other, while leaving the intermediate post-epithelial gateways, including cerebrospinal fluid (CSF) and perivascular space (PVS)-mediated redistribution and deep intraparenchymal diffusion, as structural and interpretive blind spots. To bridge this gap, we propose an integrated engineering paradigm with three core design principles. First, multistage-aware design harmonizes sequential spatiotemporal functionalities within a single vehicle architecture. Second, disease-informed design integrates pathologically remodeled barrier states and glymphatic hydrodynamics into the formulation rationale. Third, cargo-informed design establishes the distinct biophysical identity and inherent liabilities of each payload, from small molecules to viral vectors and CRISPR machinery, as the primary engineering starting point. Finally, we advocate for a methodological standard demanding stage-specific validation of vehicle integrity, cross-boundary penetration, and functional target engagement, beyond compartment-blind whole-brain readouts. We further underscore the biofate and clearance of delivery systems as an emerging axis of safety and regulatory evaluation. Collectively, this framework provides a systematic basis for transitioning N2B engineering into a viable clinical modality.

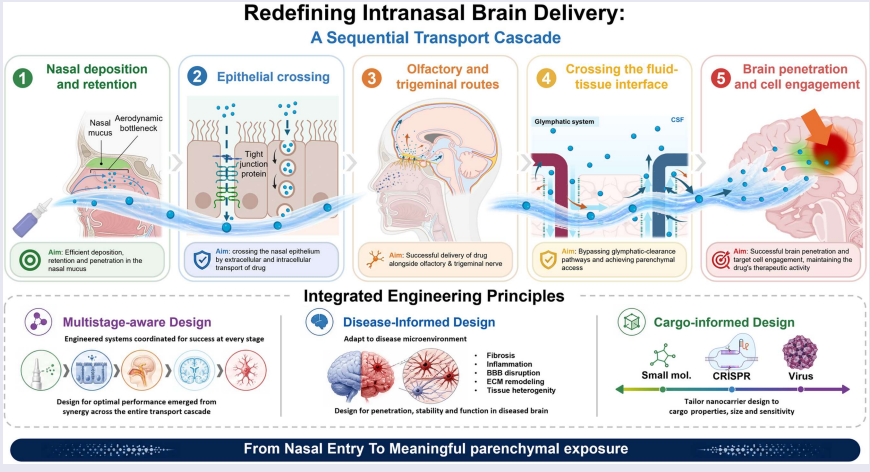

ARTICLE HISTORY

Received 23 July 2026
Revised 10 September 2026
Accepted 19 September 2026

KEYWORDS

Intranasal delivery; nose-to-brain delivery; blood–brain barrier; nanomedicine; CNS therapeutics

CONTACT Chae-Ok Yun chaeok@hanyang.ac.kr; chaeok1963@outlook.com; A-Rum Yoon ayoon@hanyang.ac.kr Department of Bioengineering, College of Engineering, Hanyang University, 222 Wangsimni-ro, Seongdong-gu, Seoul, 04763, Republic of Korea
[1] These authors contributed equally to this work as corresponding authors.

© 2026 The Author(s). Published by Informa UK Limited, trading as Taylor & Francis Group.
This is an Open Access article distributed under the terms of the Creative Commons Attribution-NonCommercial License (http://creativecommons.org/licenses/by-nc/4.0/), which permits unrestricted non-commercial use, distribution, and reproduction in any medium, provided the original work is properly cited. The terms on which this article has been published allow the posting of the Accepted Manuscript in a repository by the author(s) or with their consent.

1. Introduction

Recent global burden analyzes indicate that neurological conditions are now the leading cause of illness and disability, affecting more than three billion people globally (Steinmetz et al., 2024). Despite this substantial disease burden, therapeutic progress in central nervous system (CNS) disorders remains limited. A fundamental challenge lies in the difficulty of achieving sufficient and reproducible delivery of therapeutics to diseased brain regions. In particular, the blood–brain barrier (BBB) restricts the entry of over 98% of small-molecule drugs and virtually all macromolecular therapeutics, preventing many promising candidates from translating into effective CNS therapies (Pardridge 2005; Abbott et al. 2010). To bypass the BBB, invasive approaches such as intrathecal, intracerebroventricular, or convection-enhanced delivery are considered. However, their broader clinical use is constrained by procedural complexity, brain tissue injury, and the risk of infection (Lonser et al. 2015). To this end, nose-to-brain (N2B) delivery has emerged as a noninvasive approach with the potential to circumvent the BBB and offer broader clinical applicability and safer therapeutic access to the brain (Lochhead and Davis 2019; Wang et al. 2019; Keller et al. 2022).

The nasal route offers direct anatomical proximity to the CNS via neuroepithelial interfaces, avoids first-pass metabolism, and enables relatively rapid access to CNS-associated compartments (Lochhead and Davis 2019; Wang et al. 2019). Accordingly, interest in N2B delivery has expanded beyond small molecules to include peptides, proteins, antibodies, nucleic acids, and viral or virus-inspired delivery systems (Keller et al. 2022; Chung et al. 2023; Drath et al. 2025).

However, the translational significance of N2B delivery should not be overestimated based solely on route attractiveness (Yokel 2022). Clinically, approved intranasal CNS-related therapies remain largely limited to specific indications, such as treatment-resistant depression or seizure rescue, rather than serving as broadly applicable disease-modifying platforms (Higdon and Sperling 2021; Vasiliu 2023). This highlights a persistent gap between conceptual promise and mechanistically validated CNS delivery.

The imbalance in N2B delivery research arises from two fundamental issues in how the current research evaluates the delivery process. First, oversimplification of complexity of the delivery process to a single step process needs to be differentiated (Lochhead and Davis 2019; Wang et al. 2019; Yokel 2022). The assessment of the actual transport and tissue penetration processes following entry into the CNS is critical as cargo must not only cross the initial barriers but also traverse a complex sequence of physiological bottlenecks from cerebrospinal fluid (CSF) turnover and perivascular constraints to the dense extracellular matrix (Iliff et al. 2012; Xie et al. 2013; Spera et al. 2023). Second, equating simple CNS exposure with successful delivery can lead to inaccurate interpretation of delivery outcomes (Ahmad et al. 2017; Yokel 2022). Relying on crude metrics like total brain uptake fails to distinguish whether a therapeutic has penetrated the target tissue or is trapped in non-target compartments, such as the CSF or meninges (Lochhead et al. 2015; Ahmad et al. 2017; Lochhead and Davis 2019). Moreover, this superficial metric provides no evidence of whether the therapeutic has achieved functional engagement with the target cells.

In this context, the present review aims to propose a stage-resolved mechanistic and evaluative framework for N2B delivery (Lochhead and Davis 2019; Wang et al. 2019; Yokel 2022). Specifically, we reconceptualize the N2B pathway as a sequence of transport stages and associated bottlenecks, extending from nasal entry to meaningful parenchymal and cellular access. We further examine the current imbalance in the field, whereby early nasal barriers have been extensively studied, whereas post-entry transport and tissue-access processes remain comparatively under-integrated in both mechanistic discussion and experimental validation (Lochhead and Davis 2019; Wang et al. 2019; Yokel 2022; Drath et al. 2025). On this basis, we systematize the validation criteria required at each stage of delivery and thereby propose an evaluative framework capable of distinguishing meaningful delivery from simple exposure (Lochhead et al. 2015; Ahmad et al. 2017; Yokel 2022). Finally, we discuss how formulation design may need to evolve beyond single-barrier optimization toward multistage-aware, disease-informed, and cargo-informed strategies.

Collectively, this perspective seeks to redefine N2B delivery not as a simple brain-uptake outcome, but as a sequential transport process that must be resolved across anatomical compartments and biological scales to achieve meaningful therapeutic impact.

2. Intranasal delivery routes and stage-specific bottlenecks

2.1. Nasal deposition and retention

Efficient N2B delivery is determined by initial events within the nasal cavity. Accordingly, the proportion of the therapeutic agent deposited and retained within the nasal microenvironment, rather than the administered dose, is a key factor for effective N2B delivery (Illum 2000; Kimbell et al. 2007; Foo et al. 2007; Djupesland 2013; Gao et al. 2020; Seifelnasr et al. 2024). However, effective deposition in the olfactory region can be primarily hindered by the anatomical complexity inherent within the nasal cavity. The olfactory region, a primary target for N2B transport, is located in the superior-posterior nasal cavity and is difficult to access (Illum 2000; Djupesland 2013). The anterior nasal architecture acts as an aerodynamic bottleneck where the narrow passages and complex geometry cause droplets to impact and become trapped before reaching the olfactory cleft. Indeed, conventional nasal sprays typically deliver less than 1% of the dose to the olfactory region (Figure 1) (Kimbell et al. 2007; Foo et al. 2007; Djupesland 2013; Gao et al. 2020; Seifelnasr et al. 2024).

Once a therapeutic cargo bypasses this stringent aerodynamic filter and deposits in the target region, it immediately encounters the mucosal interface. The nasal mucosal barrier is not a simple aqueous surface. It is a viscoelastic hydrogel network composed of mucin glycoproteins (Cone 2009; Boegh and Nielsen 2015). To cross this mucosal barrier and access underlying nasal epithelium, a therapeutic cargo must effectively penetrate this layer. Thus, successful delivery depends on balancing local retention with the ability to diffuse through the mucus mesh. Alongside this physical filter, mucociliary clearance (MCC) acts as the primary kinetic constraint, functioning as a physiological defense mechanism that rapidly clears administered therapeutics toward the nasopharynx (Gizurarson 1993; Merkus et al. 1998). While mucus interactions dictate the spatial mobility of a formulation, MCC imposes a strict temporal limit on these interactions. The outcome of this stage is fundamentally predicated on how long the cargo can reside within the mucus and how rapidly it can penetrate through it. Consequently, mucus architecture and MCC are functionally

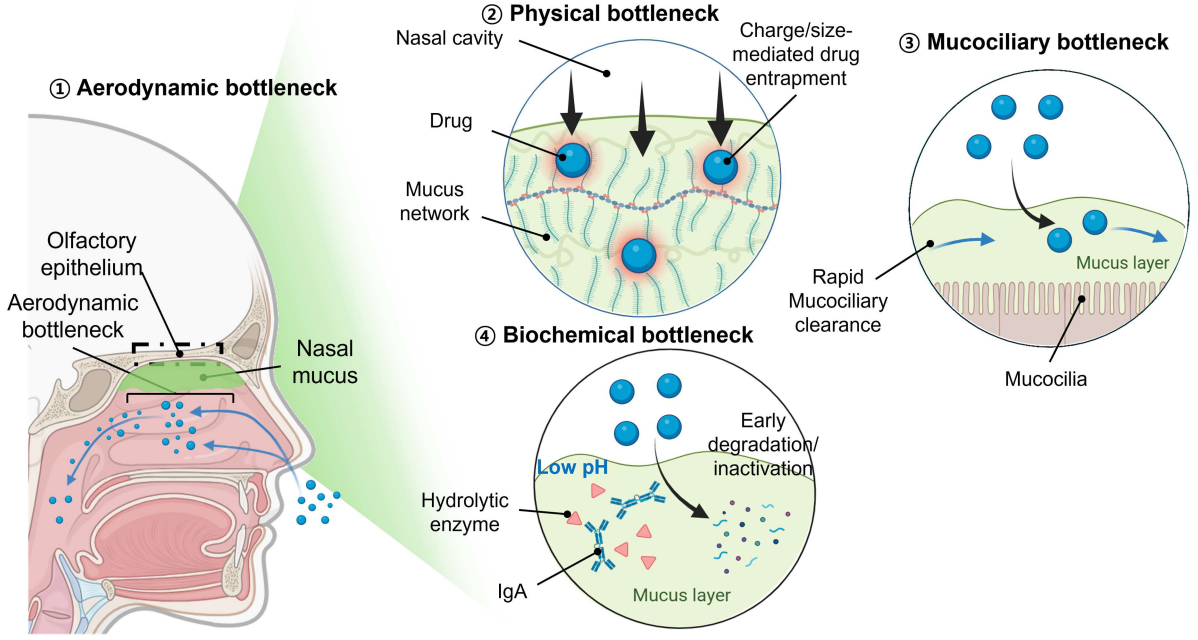

Figure 1. Bottlenecks at the nasal deposition and retention stage. Four sequential barriers restrict therapeutic cargo from reaching the olfactory epithelium. 1) An aerodynamic bottleneck is imposed by the anterior nasal geometry. 2) A physical bottleneck arises from charge- and size-mediated drug entrapment within the mucus network. 3) A mucociliary bottleneck is driven by rapid mucociliary clearance (MCC). 4) A biochemical bottleneck results from local immunoglobulin A (IgA), hydrolytic enzymes, and low pH that promote early cargo degradation and inactivation. These compounded early-stage losses determine the functionally available fraction of the administered dose that can advance to epithelial crossing. Created with BioRender.com.

distinguished, but cooperatively control diffusion, local residence, and clearance (Gizurarson 1993; Merkus et al. 1998; Cone 2009; Boegh and Nielsen 2015).

This mechanistic link between formulation properties, deposition, and clearance was quantitatively established in research showing correlation of nasal clearance rates with formulation characteristics. Harris et al. demonstrated that increasing methylcellulose concentration increased the mean droplet size from approximately 51 to 81 µm and 200 µm, respectively, which exerted a non-linear effect on retention (Harris et al. 1988). Specifically, while the 0.25% methylcellulose formulation successfully prolonged nasal residence, the 0.50% formulation paradoxically accelerated clearance. Crucially, the same study revealed that increased viscosity shifted deposition further anteriorly. This highlights that local residence and regional deposition are not independently tunable variables but rather mechanistically coupled phenomena.

Beyond physical and kinetic barriers, delivery is further constrained by the local biochemical microenvironment. The nasal cavity typically maintains slightly acidic to near-neutral pH. These specific pH and ionic conditions can significantly alter the stability and ionization state of sensitive cargoes (Gizurarson 1993; Keller et al. 2022). Building on these chemical constraints, the nasal mucosa also functions as an 'active metabolic barrier.' It contains various enzyme systems, such as cytochrome P450 and glutathione S-transferases, which directly degrade therapeutics such as peptides, proteins, and nucleic acids (Longo et al. 1986; Baron et al. 1988; Aceto et al. 1989; Gervasi et al. 1991). Additionally, the mucosal immune barrier, consisting of secreted antibodies and innate defenses, introduces biological constraints that can limit delivery efficiency and reproducibility, particularly for viral vectors or repeated dosing. Ensuring the biological and physicochemical integrity of cargo within this environment is an absolute prerequisite upon entry into this hostile nasal environment.

In summary, the administered dose alone does not determine brain exposure. These compounded early-stage losses dictate the true functionally available fraction. Only the minor fraction of the cargo that successfully navigates these aerodynamic, kinetic, and physicochemical hurdles can proceed to the next obligatory step: epithelial crossing (Gao et al. 2020; Seifelnasr et al. 2024).

2.2. Epithelial crossing

Once the therapeutic cargo breaches the superficial mucus layer, it immediately confronts the cellular front line, the nasal epithelium (Lochhead and Davis 2019; Yokel 2022; Drath et al. 2025; Qiu et al. 2025). It must cross the epithelial barrier to reach the lamina propria, thereby unlocking the downstream transport network. This critical stage marks the transition from surface exposure to true tissue penetration (Figure 2).

This epithelial crossing relies on two primary routes: extracellular and intracellular transport. Extracellular transport occurs via the paracellular route through the spaces between adjacent epithelial cells. However, this movement is immediately blocked by apical junctional complexes, specifically tight junctions. The dense network of transmembrane proteins like claudins and occludins seals the intercellular space into a formidable physical and electrostatic barrier. That resembles the molecular architecture found in the BBB (Steinke et al. 2008). The pore diameter of tight junctions in the nasal epithelium is approximately 0.4 to 0.8 nm, creating a size-exclusion threshold for passive paracellular diffusion (Sarin 2015). Consequently, these rigorous structural constraints ultimately restrict paracellular diffusion strictly to small (<1 kDa), hydrophilic solutes (Madara and Dharmsathaphorn 1985; Sarin 2015; Yokel 2022).

In contrast, the intracellular transport route can be further classified into two distinct pathways depending on the target cell type: epithelial transcellular passage and intraneuronal transport (Lin et al. 2016; Lochhead and Davis 2019; Yokel 2022; Drath et al. 2025; Qiu et al. 2025). The transcellular route, demanding direct migration of cargo through epithelial cells, incorporates transcellular transport via direct membrane passage and epithelial transcytosis via vesicle-mediated transport. Transcellular transport relies on passive partition and rapid intracellular diffusion, making it highly effective for small, lipophilic compounds (Illum 2000; Yokel 2022). In contrast, epithelial transcytosis is primarily utilized by larger biologics and nanoparticles to bypass tight junction limitations (Lin et al. 2016). Because this transcytotic pathway is an active biological process requiring sequential steps of apical uptake, intracellular routing, and basolateral release, it typically operates on a much longer timescale of tens of minutes to hours.

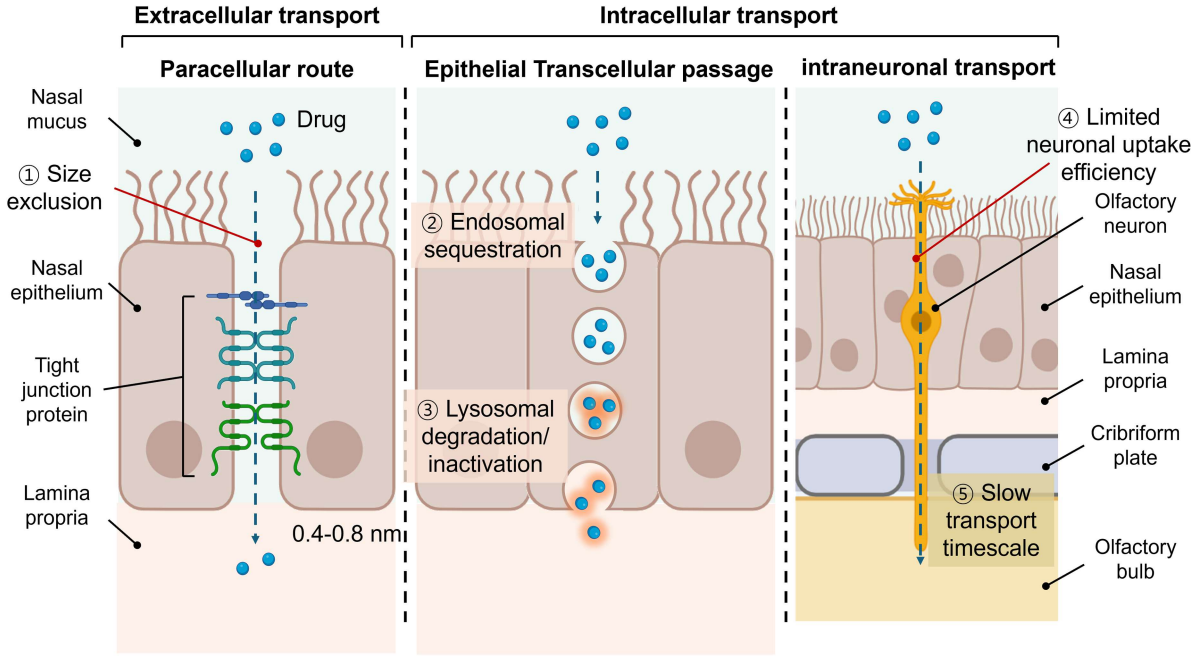

Figure 2. Overview of the three primary nasal epithelial crossing routes. The paracellular route and perineural bulk flow achieve central nervous system (CNS) exposure within seconds to minutes. Epithelial transcytosis operates on a timescale of 10 minutes to hours. Intraneuronal axonal transport requires hours to days. This timescale hierarchy determines which route governs the rapid initial CNS signal versus sustained cargo distribution. The mechanistic bottlenecks and cargo requirements for each route are summarized in Table 1. Created with BioRender.com.

Further, intraneuronal transport implies entry into olfactory or trigeminal neurons followed by axonal transport (Buchner et al. 1987; Yokel 2022). The maximum rate of axonal transport in olfactory nerve C-fibers has been quantified at up to 130 mm/day (Buchner et al. 1987), taking at least 45 minutes for a substance to reach the rat brain after intranasal administration. This biological pathway cannot account for rapid CNS exposure due to its inherent slowness requiring hours to days in larger species. This is distinguished from other types of fluid flow, such as paracellular or perineural bulk flow pathways. These routes can bypass intracellular sorting networks entirely, allowing therapeutic cargoes to be detected in the brain and CSF within 5 to 10 minutes post-administration (Lochhead and Davis 2019; Yokel 2022; Drath et al. 2025; Qiu et al. 2025). Nevertheless, intraneuronal axonal transport can be an alternative route for delayed, sustained drug distribution.

Consequently, the rapid initial CNS exposure is mechanistically governed by paracellular penetration coupled with CSF-associated bulk flow, achieving within minutes of intranasal administration (Lochhead and Davis 2019; Yokel 2022; Drath et al. 2025; Qiu et al. 2025). While transcytosis may proceed concurrently, its slower kinetics make it a minor wave of entry rather than the primary driver of immediate brain exposure (Table 1).

2.3. Olfactory and trigeminal routes

Upon entering the lamina propria, nasal anatomical divergence directs the cargo along either olfactory or trigeminal nerve-associated compartments (Crowe and Hsu 2022; Qiu et al. 2025). Specifically, crossing the olfactory epithelium guides the cargo toward the olfactory nerve bundles. By contrast, entry through the respiratory epithelium offers access to the trigeminal nerve pathways, alongside local tissue retention or systemic absorption (Lochhead and Davis 2019; Crowe and Hsu 2022).

The spatial trajectory of the olfactory pathway requires cargoes to migrate alongside olfactory nerve bundles toward the cranial compartment (Renner et al. 2012; Norwood and Zhang, 2019). Importantly, the foramina of cribriform plate, densely packed with nerve fibers, blood vessels, and connective tissue, does not offer an unobstructed passageway. Because this dense anatomical arrangement drastically reduces the

Table 1. Comparative features of major epithelial crossing pathways during intranasal delivery. For each of the three primary routes, the table lists the approximate transport timescale, the favored cargo physicochemical properties, and the primary mechanistic bottleneck: extracellular paracellular passage via tight junction (TJ) interstices, intracellular epithelial transcellular passage including transcytosis, and intraneuronal axonal transport via olfactory or trigeminal neurons. CPP, cell-penetrating peptide. NP, nanoparticle.

Route class	Specific pathway	Approx. timescale	Favored cargo properties	Major bottleneck	Ref
Extracellular transport	Paracellular route (via tight junction interstices)	Seconds to minutes	Small (<1 kDa) Hydrophilic	• Strict TJ pore size (0.4–0.8 nm) • Excludes macromolecules and vectors	Madara and Dharmsathaphorn (1985); Steinke et al. (2008); Sarin (2015); Yokel (2022)
Intracellular transport	Epithelial transcellular passage	10 minutes to hours	Macromolecules, biologics, nucleic acids CPP- or ligand-modified NPs	• Endosomal sequestration • Lysosomal degradation • Uncertain basolateral release • Slow transport • Unverified mechanism	Lin et al. (2016); Lochhead and Davis (2019); Yokel (2022); Crowe and Hsu (2022); Qiu et al. (2025)
	Intraneuronal transport	Hours to days	Neurotropic viruses Uptake-capable biologics	• Slow rate (~130 mm/day) • Impractical for acute delivery • Low neuronal uptake • Only for sustained delivery	Buchner et al. (1987); Yokel (2022)

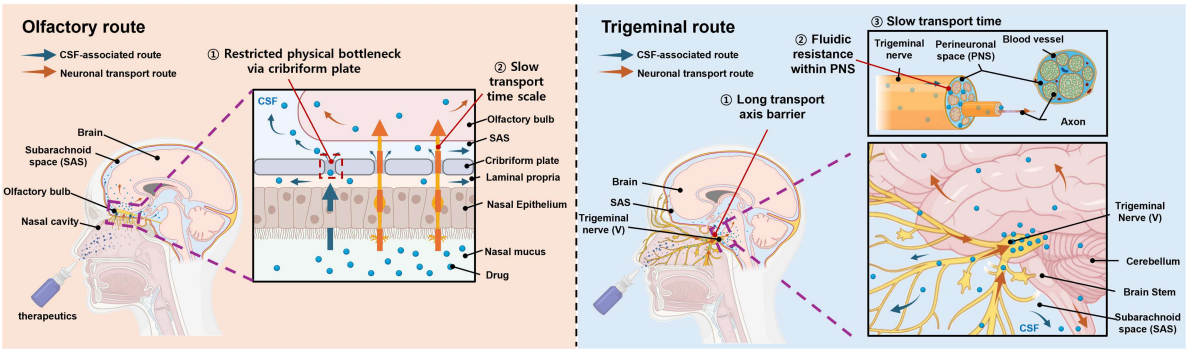

Figure 3. Anatomical trajectories and stage-specific bottlenecks of the olfactory and trigeminal routes. Along the olfactory route, cargo migrates alongside olfactory nerve bundles through the cribriform plate toward the subarachnoid space (SAS) and olfactory bulb, encountering three principal bottlenecks: 1) a restricted physical bottleneck at the densely packed cribriform plate foramina and 2) a slow transport timescale for intraneuronal axonal transit. Along the trigeminal route, cargo migrates through perineuronal spaces of the trigeminal nerve (V) toward the brainstem and cerebellum via the SAS, encountering two bottlenecks: 1) a long transport axis from the nasal cavity to the posterior CNS, 2) fluidic resistance within the perineuronal space (PNS), and 3) a slow transport timescale for perineural transit. The olfactory route preferentially targets anterior CNS structures via cerebrospinal fluid (CSF)-mediated redistribution, whereas the trigeminal route provides a conduit to the posterior and inferior CNS regions. Created with BioRender.com.

functionally available space, the cribriform plate acts as a highly restrictive physical bottleneck, forcing therapeutic cargoes to navigate through extremely narrow interstitial gaps to access the brain (Norwood and Zhang, 2019; Proulx 2021; Spera et al. 2023). Within this olfactory axis, transport mechanistically diverges into two distinct intraneuronal and extraneuronal pathways (Thorne et al. 2004; Renner et al. 2012; Drath et al. 2025). The intraneuronal route provides the advantage of direct delivery to the olfactory bulb, but its slow speed, restricted by motor protein velocities across microtubules, results in low efficiency. By contrast, extraneuronal pathways are closely coupled to the subarachnoid space (SAS) and CSF-associated compartments, facilitating rapid drug distribution within minutes in the early phase of delivery. Therefore, formulations should be designed to efficiently exploit the olfactory interface at the cribriform plate, which serves as a primary anatomical gateway for rapid CSF spread and anterior brain targeting (Figure 3) (Johnston et al. 2004; Nagra et al. 2006; Norwood and Zhang, 2019; Proulx 2021).

The trigeminal route initiates from the respiratory epithelium and forms a long transport axis along the peripheral nervous system toward the posterior CNS. Cargoes entering through the respiratory region reach compartments associated with terminal trigeminal fibers and migrate through the perineural, endoneurial, and epineurial spaces. They then progress along the larger trigeminal branches, including the ophthalmic (V1) and maxillary (V2) divisions, and the trigeminal ganglion, ultimately reaching the brainstem (Thorne et al. 2004; Lochhead and Davis 2019; Lochhead et al. 2019; Crowe and Hsu 2022). While cargoes that reach the brainstem may eventually redistribute into the SAS, this route functions to preferentially target the posterior and inferior regions of the CNS. Intranasally administered insulin, which localizes within the extracellular components and vessel-associated spaces of the trigeminal nerve layers, supports the existence of this peripheral-to-central transport axis (Lochhead and Davis 2019; Lochhead et al. 2019).

Ultimately, the olfactory route is ideal for anterior entry and rapid CSF-mediated spread, and the trigeminal route establishes a robust conduit to the posterior brainstem. Therefore, intranasal formulation must be strategically designed to target based on the spatial distribution of the intended neurological target (Thorne et al. 2004; Lochhead and Davis 2019; Lochhead et al. 2019; Crowe and Hsu 2022; Spera et al. 2023). As proof of concept, experimental models have shown that modifying the physicochemical properties of a therapeutic agent, such as altering its lipophilicity, molecular weight, or incorporating specific permeation enhancers, can actively shift its dominant transport trajectory between the olfactory-CSF and respiratory-trigeminal axes.

2.4. Crossing the fluid-tissue interface

Even after successful entry through olfactory- or trigeminal-associated pathways, therapeutic cargoes rarely reach the brain parenchyma. Instead, a substantial fraction redistributes into CNS-associated fluid compartments. This stage is not a passive intermediate step but an independent bottleneck that constrains subsequent parenchymal penetration (Figure 4) (Iliff et al. 2012; Xie et al. 2013; Iliff et al. 2013; Proulx 2021; Spera et al. 2023).

The primary bottleneck at this stage is defined by compartmental partitioning. Post-entry transport does not follow a linear path. The administered cargo undergoes multilineage distribution, splitting among local tissues, meningeal surfaces, and circulating fluid channels (Johnston et al. 2004; Nagra et al. 2006; Lochhead

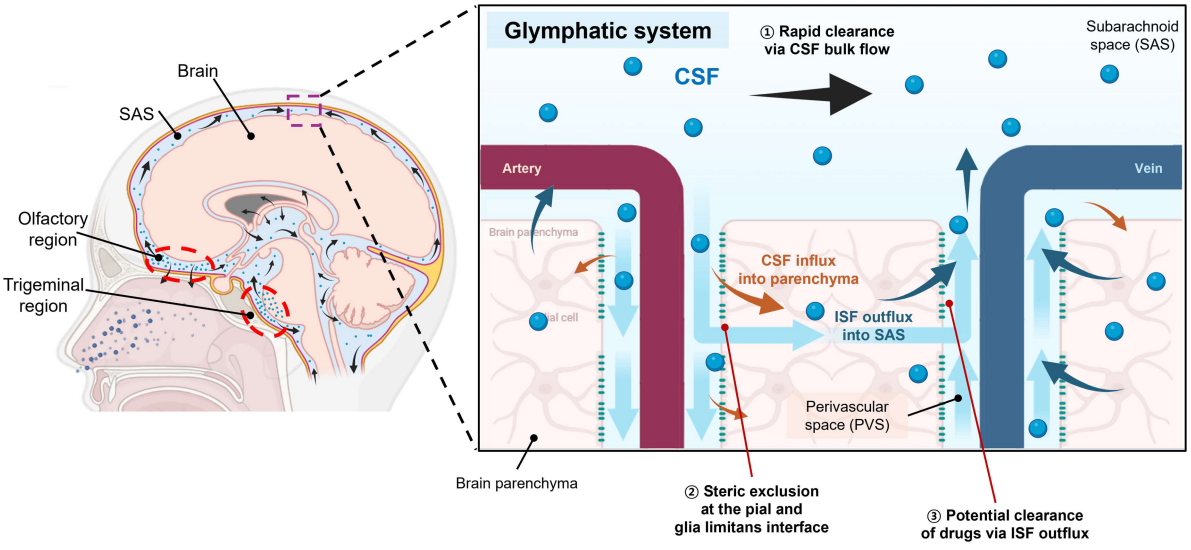

Figure 4. Bidirectional fluid dynamics at the CNS fluid-tissue interface. Schematic depicting the two opposing fluid exchange processes governing cargo redistribution between CNS fluid compartments and the brain parenchyma: cerebrospinal fluid (CSF) influx into the parenchyma and interstitial fluid (ISF) outflux into the subarachnoid space (SAS). The balance and directionality of these fluidic processes determine whether cargo that has entered the CSF or perivascular space (PVS) toward the deeper parenchyma or is diverted toward clearance pathways. Created with BioRender.com.

et al. 2015; Lochhead and Davis 2019; Lochhead et al. 2019; Proulx 2021; Spera et al. 2023). For instance, while a fraction of the cargo entering via the olfactory route may achieve direct local tissue exposure, another fraction redistributes along the cribriform plate interface into the SAS or CSF. Consequently, only a limited fraction accesses the deeper parenchyma through perivascular spaces (PVS) and CSF-interstitial fluid (ISF) exchange (Iliff et al. 2012; Iliff et al. 2013; Mestre et al. 2018). Similarly, trigeminal-associated cargoes are repartitioned between brainstem tissue regions and adjacent fluid-associated compartments. The critical constraint of preferential enrichment in a fluid compartment does not guarantee tissue penetration. This creates a weak link between fluidic redistribution and parenchymal access, and the process is vulnerable to redistribution, secondary repartitioning, and diversion towards lymphatic drainage (Johnston et al. 2004; Nagra et al. 2006; Lochhead and Davis 2019; Lochhead et al. 2019; Proulx 2021).

The directionality of cargo movement is actively driven by CSF bulk flow, PVS structural continuity, and localized pressure gradients, with the coordinated beating of ependymal cilia serving as the primary biological engine (Iliff et al. 2012; Xie et al. 2013; Iliff et al. 2013; Lochhead et al. 2015; Faubel et al. 2016; Mestre et al. 2018). Therefore, these intricate hydrodynamic and anatomical conditions can be another significant hurdle in the redistribution process. Unfortunately, these dynamic fluid mechanics are frequently overlooked in current literature, creating a major interpretive blind spot. When a CSF- or surface-associated signal is observed, this oversight makes it unclear whether the signal reflects sustained, productive transport toward the tissue or merely a transient state prior to clearance. Ultimately, the conversion of fluid redistribution into target tissue access is context-dependent, dictated by active local exchange dynamics rather than simple physical continuity between compartments (Iliff et al. 2012; Xie et al. 2013; Iliff et al. 2013; Mestre et al. 2018).

Thus, broad dissemination across fluid pathways must not be translated into tissue access. As CSF, SAS, and PVS are fundamentally fluid-associated compartments rather than the parenchyma itself, signals detected at the brain surface, meninges, ventricles, or perivascular regions must be interpreted independently of true intraparenchymal distribution (Iliff et al. 2012; Iliff et al. 2013; Lochhead et al. 2015; Mestre et al. 2018; Lochhead and Davis 2019). Therefore, the evaluation of delivery success must move beyond the mere observation of CNS entry to rigorously determine whether initial fluidic redistribution is structurally and functionally coupled to target tissue penetration.

2.5. Intraparenchymal extracellular diffusion: ECM and steric hindrance

The transition from fluidic exposure to deep tissue infiltration represents a formidable structural bottleneck in intranasal delivery. Accumulation in the CSF does not mean that a cargo will cross the fluid-tissue interface. The initial hurdle is the structural boundary separating fluid compartments from the parenchymal tissue. Cargoes that have reached the CSF or perivascular spaces (PVS) must cross formidable cellular and anatomical barriers, such as the pial surface, the glia limitans, or layers enriched in astrocytic endfeet, to reach the parenchyma (Iliff et al. 2012; Pizzo et al. 2018; Proulx 2021). These interfaces are selectively organized barriers composed of ECM and precise microarchitecture (Figure 5).

In vivo imaging and biodistribution studies utilizing large sizes of cargoes, such as monoclonal antibodies and viral vectors, frequently observe massive cargo accumulation trapped along the pial surface and within the PVS (Iliff et al. 2012; Pizzo et al. 2018). These findings show that the glia limitans and astrocytic endfeet form a size-exclusion filter, blocking large molecules from crossing out of fluid compartments. Consequently, the actual efficiency of parenchymal entry is strictly governed by the structural permeability of these boundaries, independent of the cargo concentration in the adjacent fluid. Even upon successfully crossing this interface, the brain parenchyma does not function as a free-diffusion space. High cell density, dense ECM, ISF flow, and electrostatic interactions impose strong physical limitations on cargo mobility. As a result, intraparenchymal spread is often highly restricted, confining the cargo to superficial layers or regions adjacent to entry points (Nance et al. 2012; Xie et al. 2013).

The in vivo diffusion studies utilizing multiple nanoparticle platforms have explicitly demonstrated that standard therapeutic carriers larger than the brain's ECM mesh size (typically ~100 nm), or those lacking dense surface passivation, are almost instantaneously immobilized by steric hindrance and adhesive forces, completely failing to penetrate deep tissue (Nance et al. 2012). Therefore, overcoming these extracellular

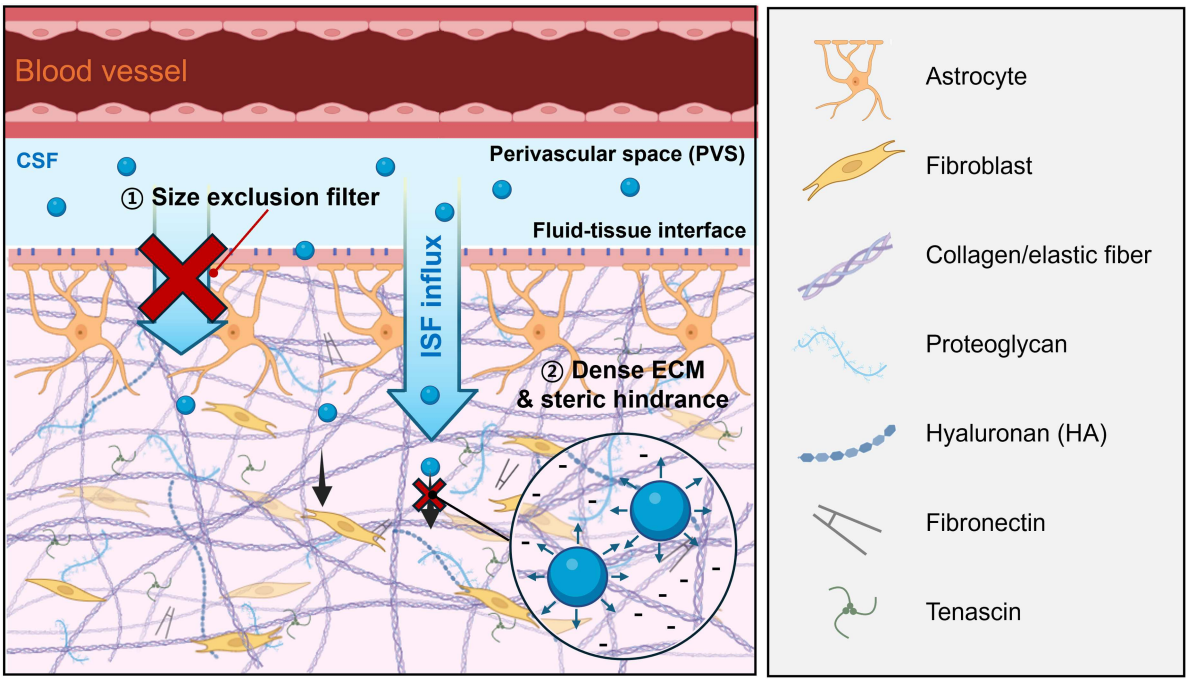

Figure 5. Structural barriers to intraparenchymal penetration at the fluid-tissue interface. Two biophysical obstacles restrict cargo from advancing from the perivascular space (PVS) into the brain parenchyma: 1) a size-exclusion filter imposed by the cellular and matrix architecture at the fluid-tissue interface, and 2) a dense extracellular matrix (ECM) composed of hyaluronan (HA), proteoglycans, tenascin, fibronectin, and collagen and elastic fibers that restricts intraparenchymal diffusion through steric hindrance. Astrocytes, fibroblasts, and blood vessels are depicted in their spatial arrangement at the PVS-parenchyma boundary, and ISF influx from the PVS into the parenchymal interstitium is indicated. Created with BioRender.com.

matrix restrictions and avoiding steric trapping are mandatory biophysical prerequisites for achieving homogeneous therapeutic distribution throughout the targeted brain structures.

2.6. Target-cell engagement and functional internalization

Crucially, deep intraparenchymal accumulation remains profoundly disconnected from cellular internalization (Zhuang et al. 2011; Alvarez-Erviti et al. 2011; Steinbach et al. 2016). While widespread tissue penetration is an absolute prerequisite, it is by no means a surrogate for productive target-cell engagement. The brain hosts diverse cell populations, including neurons, astrocytes, and microglia, each with distinct membrane properties and endocytic activities. Therefore, the cellular uptake efficiency of different cargoes can vary depending on the cell type. Cargoes will fail to exert a therapeutic effect if it only binds non-specifically to surfaces or are prematurely cleared by microglial phagocytosis (Zhuang et al. 2011). Thus, actual cellular internalization and functional engagement must be verified as a distinct, final hurdle separate from parenchymal penetration (Figure 6).

This multi-stage reality highlights the limitations of over-reliance on whole-brain homogenate data or bulk fluorescence to determine delivery success (Harmon et al. 2014; Lochhead et al. 2015; Ahmad et al. 2017; Lochhead and Davis 2019; Yokel 2022). Such 'regional exposure' metrics fail to distinguish whether a drug is merely trapped in perivascular or extracellular spaces, or it has entered intended target cells. Therefore, successful delivery requires strictly separating the evaluation of tissue accumulation from functional cellular engagement (Alvarez-Erviti et al. 2011; Harmon et al. 2014). The meaningful clinical translation of N2B delivery lies in providing clear mechanistic solutions for how a cargo will cross tissue boundaries, penetrate deeply into disease lesions, and ultimately engage with target cells (Lochhead and Davis 2019).

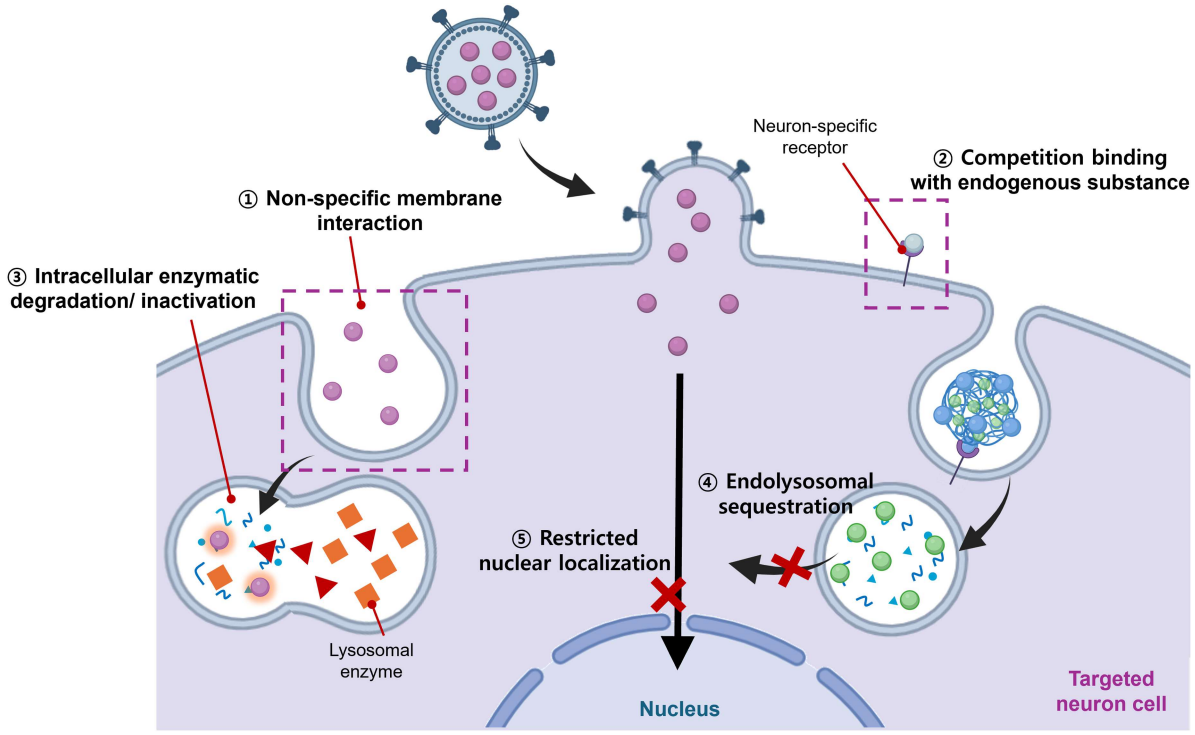

Figure 6. Five cellular-level barriers at the target-cell engagement stage. Even after intraparenchymal accumulation, therapeutic cargo must overcome the following sequential barriers: 1) non-specific membrane interactions that divert cargo from the intended receptor-bearing target cell, 2) competition with endogenous substances for binding at neuron-specific receptors, 3) intracellular enzymatic degradation and inactivation following uptake, 4) endolysosomal sequestration driven by lysosomal enzyme activity, and 5) restricted nuclear localization for gene-active payloads. These five barriers collectively define target-cell engagement as a distinct functional endpoint that cannot be inferred from parenchymal accumulation data alone. Created with BioRender.com.

3. Current formulation strategies to overcome stage-specific bottlenecks in N2B delivery

3.1. Physical interventions in the early nasal stage

3.1.1. Deposition optimization

Successful N2B delivery strategies should aim to maximize posterior nasal region, the gateway to effective brain delivery, rather than allowing formulations to mistarget the anterior impaction (Figure 7) (Kimbell et al. 2007; Foo et al. 2007; Djupesland 2013; Gao et al. 2020; Seifelnasr et al. 2024; Huang et al. 2024). The anterior nasal architecture, particularly the narrow 'nasal valve,' functions as a major aerodynamic filter that causes substantial dose loss to anterior impaction (Djupesland 2013). This limitation has been quantitatively validated by Kimbell et al., whose computational fluid dynamics (CFD) models showed that over 90% of standard 20–50 μm particles deposit anteriorly, though minor geometric or velocity adjustments can improve posterior access (Kimbell et al. 2007). Similarly, Foo et al. demonstrated using nasal replicas that narrowing the plume angle combined with a precise administration angle (shifting from 50° back to 30°) can dramatically boost turbinate deposition from ~15% to nearly 90%, highlighting the critical role of user positioning (Foo et al. 2007). To overcome these technique-dependent variances, Djupesland et al. introduced a breath-actuated bidirectional device that leverages the patient's exhaled air, this engineering approach successfully reduced anterior loss to ~14% and increased initial deposition in the critical superior–posterior region 3-fold from ~11% to ~32% (Djupesland et al. 2006). Collectively, these multi-level strategies have made anatomically targeted deposition the most mature engineering axis in N2B delivery.

Following anatomically targeted deposition, the second engineered axis focuses on local residence and mucus interaction (Gizurarson 1993; Merkus et al. 1998; Cone 2009; Boegh and Nielsen 2015). Even when deposition successfully occurs in anatomically favorable posterior regions, rapid MCC can wash away

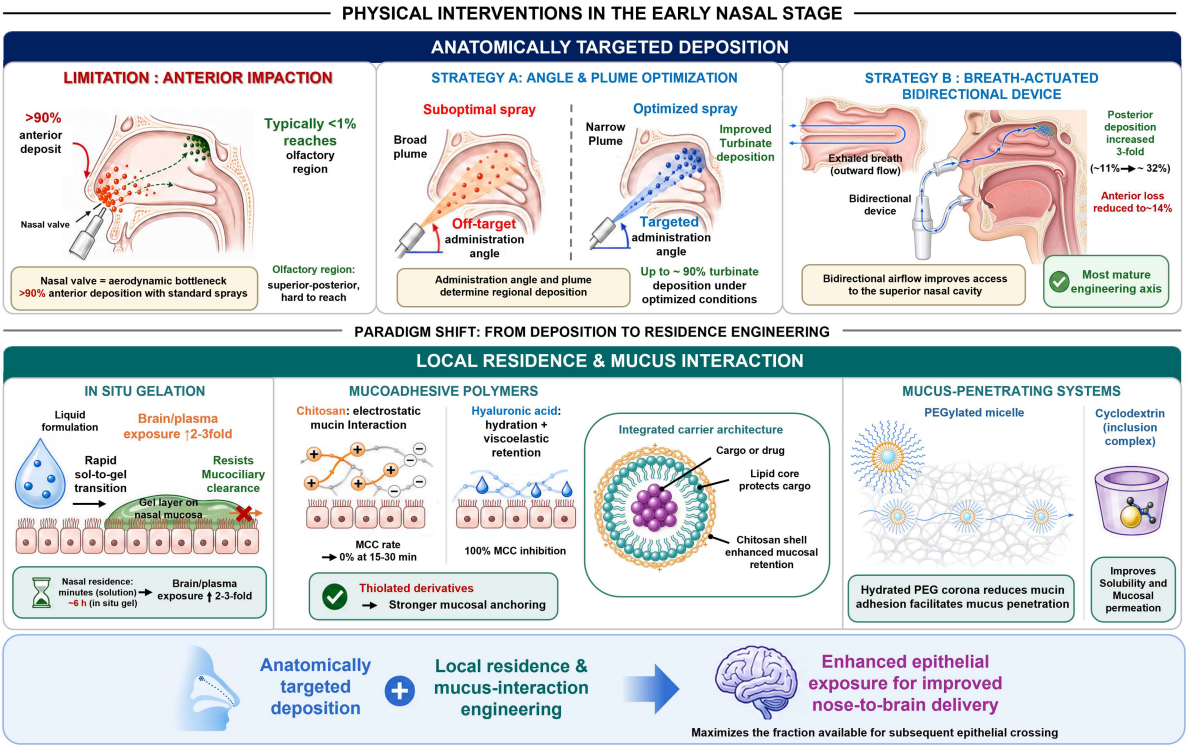

Figure 7. Physical interventions in the early nasal stage. Standard nasal sprays deposit over 90% of the dose in the anterior cavity, with typically less than 1% reaching the olfactory region. Anatomically targeted deposition is improved by optimizing administration angle and plume geometry or by using breath-actuated bidirectional devices, which increase posterior deposition approximately three-fold. Local residence is then engineered through in situ gelling, mucoadhesive polymers such as chitosan and hyaluronic acid, and mucus-penetrating systems including PEGylated micelles and cyclodextrin inclusion complexes. Together, anatomically targeted deposition and residence engineering maximize the fraction available for subsequent epithelial crossing. MCC, mucociliary clearance. PEG, polyethylene glycol. Created with Manus.

formulations within minutes, strictly restricting the opportunity for epithelial contact and subsequent transport. To actively circumvent this kinetic bottleneck, formulation engineering has shifted from simple solutions to advanced biomaterial platforms designed to prolong mucosal exposure.

3.1.2. In situ gelling systems

As a primary and direct strategy to prevent early-stage drug loss, researchers have extensively developed in situ gelling systems, which undergo a sol-to-gel transition after administration (Mehta et al. 2009; Qian et al. 2014). In situ gelling systems combine the ease of liquid administration with instantaneous viscosity enhancement upon mucosal contact, effectively locking the formulation in place to resist MCC. Mehta et al. engineered a thermosensitive, poloxamer/HPMC-based in situ gel co-loaded with pheniramine and phenylephrine for sinusitis therapy (Mehta et al. 2009). In vivo gamma scintigraphy demonstrated that this formulation extended the nasal residence time to approximately 6 hours, effectively overcoming the rapid mucosal clearance that eliminated the standard drug solution within just 15 minutes. Similarly, Qian et al. utilized a poloxamer-based thermosensitive in situ gel, which represents an advanced platform that autonomously forms a stable gel using the physiological temperature of the nasal cavity without external chemical triggers (Qian et al. 2014). They reported that this system delayed mucociliary transport by more than 6-fold, ultimately increasing plasma and brain exposure by approximately 2- to 3-fold compared to conventional formulation. Collectively, these studies have established in situ gelling systems as one of the most direct and quantitatively validated physical interventions to extend nasal residence (Mehta et al. 2009; Qian et al. 2014).

To overcome the inherent kinetic limitations of such single-stimulus hydrogels, specifically the delayed gelation time of thermosensitive poloxamers, dual-responsive or multi-triggered in situ gelling systems have been developed (Chen et al. 2019; Agrawal et al., 2020; Gadhave et al. 2021). This strategy fused thermosensitive poloxamers with ion-responsive polysaccharides, such as gellan gum or sodium alginate. Upon intranasal administration, these hybrid platforms encounter simultaneous dual-stimuli. The temperature (37 °C) mediates thermal micellization of the poloxamer chains and endogenous cations (Ca^+ and Na^+) within the nasal mucus fluid trigger immediate ionic cross-linking of the polysaccharide domains. This multi-responsive axis is engineered to exhibit highly specialized shear-thinning rheological behavior. Under the high shear stress generated during spray actuation or administration, these polymer networks line up to lower viscosity, ensuring optimal atomization and targeted deposition. However, the moment the formulation contacts the mucosal interface and the shear rate drops to zero, the dual triggers prompt a sol-to-gel phase transition within a second. This abrupt viscosity escalation effectively anchors the formulation into a robust 3D matrix before the mechanical mucociliary sweeping action can initiate, thereby securely locking the therapeutic payload at the olfactory gateway.

3.1.3. Mucoadhesive systems

Beyond simply modulating viscosity of cargo formulation, the engineering paradigm has advanced toward utilizing polymer-based mucoadhesive systems that actively resist MCC (Illum et al. 1994; Pritchard et al. 1996; Soane et al. 1999; Krauland et al. 2006). Chitosan and hyaluronic acid (HA) are the most representative mucoadhesive polymers due to their capacity for strong interfacial engagement with the hydrated mucus layer. Chitosan is a cationic polysaccharide containing protonatable primary amine groups that interact electrostatically with negatively charged sialic acid and sulfate residues in mucin glycoproteins (Aspden et al. 1997; Soane et al. 1999; Krauland et al. 2006). In the mucus environment, chitosan absorbs water and forms a gel-like interfacial layer, facilitating polymer-mucin interaction and prolonging nasal residence (Soane et al. 1999; Krauland et al. 2006). Importantly, conclusions regarding these natural polymers cannot be broadly generalized, as their physical behavior depends heavily on molecular weight and structural grades. For instance, lower-molecular-weight chitosan generally offers superior transmucosal permeation, whereas higher-molecular-weight variants provide stronger viscosity-driven mucoadhesion but weaker penetration (Chae et al. 2005; Bruinsmann et al. 2019). Therefore, explicitly reporting specific parameters, such as the exact molecular weight and degree of deacetylation for chitosan, or chain length for HA, is essential for reproducibility and meaningful cross-study comparisons. Aspden et al. directly evaluated this concept using ex vivo human nasal tissue treated with 0.25% chitosan salt solutions (Aspden et al. 1997). When nasally administered as a spray, chitosan transiently suppressed the mucociliary transport rate, reducing it to 0% of the baseline at 15 and 30 minutes before recovering by 90 to 120 minutes. This demonstrates that chitosan physically slows mucociliary transport.

Subsequently, chitosan was integrated into particulate formulation systems designed to retain cargo more effectively within the nasal cavity. Soane et al. extended this concept using chitosan polymer microspheres and compared the nasal clearance of different formulations in human volunteers (Soane et al. 1999). Specifically, chitosan microspheres significantly extended the nasal clearance half-life, achieving a 4- and 2-fold increase in retention time compared with a standard sodium fluorescein solution and unmodified chitosan solution, respectively (Soane et al. 1999). This study transitioned chitosan from a simple excipient to a polymer-based mucoadhesive platform, proving that particulate chitosan systems provide much stronger nasal residence.

Recent breakthroughs in N2B delivery highlight advanced hybrid platforms that structurally integrate the polycationic mucoadhesive functionality of chitosan with the robust protective capabilities of lipidic cores (Prego et al. 2006; Salade et al. 2017; Saini et al. 2021; Kapoor et al. 2025; Riani et al. 2026). Salade et al. developed an engineered nanoplatform for the N2B delivery of ghrelin by coating anionic liposomes with water-soluble quaternized chitosan (HTCC) (Salade et al. 2017). In this architecture, the internal liposomal core can electrostatically encapsulate and protect the peptide from nasal enzymatic degradation, while the external HTCC corona drives a significant increase in mucin adsorption capacity through enhanced electrostatic interactions. To validate these therapeutic advantages in vivo, Prego et al. evaluated chitosan-coated oily nanocapsules incorporating salmon calcitonin (sCT) as a model peptide (Prego et al. 2006). Following intranasal administration in rats, the sCT-loaded chitosan nanocapsules elicited a

significantly more potent and prolonged hypocalcemic effect compared to both uncoated nanoemulsions and simple chitosan-containing aqueous solutions. Furthermore, Saini et al. demonstrated the preclinical relevance of this hybrid engineering paradigm specifically for Alzheimer's disease models. They generated ferulic acid-loaded solid lipid nanoparticles (SLNs) coated with chitosan via ionic gelation (Saini et al. 2021). The functionalized chitosan shell drastically enhanced ex vivo mucoadhesive strength on the nasal mucosa. Critically, the chitosan-coated SLNs demonstrated a 7-fold increase in brain ferulic acid concentrations relative to the pure drug, while achieving a significantly superior brain-to-plasma ratio compared to uncoated SLNs, underscoring the necessity of the hybrid core-shell architecture for achieving sustained therapeutic efficiency within the nasal cavity. These series of studies indicates that the structural coupling of lipidic core entrapment with a peripheral chitosan coating yields a potent synergistic intervention capable of efficiently overcoming kinetic clearance barriers at the nasal interface and accelerating brain drug targeting (Prego et al. 2006; Salade et al. 2017; Saini et al. 2021).

Nevertheless, native chitosan and its particulate formulations have intrinsic limitations regarding their restricted mucoadhesive persistence. Their mucoadhesion relies on reversible physical mechanisms that are vulnerable to continuous mucus turnover (Soane et al. 1999; Krauland et al. 2006). To this end, chitosan has been modified to overcome these limitations. For example, Krauland et al. utilized thiolated chitosan (Krauland et al. 2006). Mechanistically, thiolation introduces sulfhydryl groups into the chitosan backbone, enabling the formation of strong covalent disulfide bonds with mucin glycoproteins. This creates a robust matrix that provides swelling-driven retention and sustained drug release. The thiolated chitosan microparticles provided sustained release of a peptide cargo over approximately 6 hours and boosted absolute bioavailability by approximately 3.5-fold compared to unmodified native chitosan microparticles. This specific case proves that thiolation of chitosan is a derivative advancement that successfully extends the limited mucoadhesive persistence of native chitosan microparticles and maximizes peptide delivery performance.

Native hyaluronic acid (HA) is also highly valued for its exceptional water-retention capacity and viscoelasticity, which facilitate hydration, lubrication, and prolonged mucosal contact (Pritchard et al. 1996). Pritchard et al. directly evaluated this property using an excised frog palate model to assess the mucociliary transport delaying effect of hyaluronic acid (Pritchard et al. 1996). In this study, native hyaluronic acid completely inhibited transport, demonstrating a $100.0 \pm 0.0\%$ reduction rate, which validates that native hyaluronic acid functions as a potent mucociliary transport-delaying polymer. To advance these platforms further, chemically modified variants have been introduced. For instance, Laffleur et al. proposed a chemical modification introducing a cysteine group into the HA backbone (Laffleur et al. 2023). Cysteine modification enables thiol disulfide exchange interactions with the cysteine-rich domains of mucus glycoproteins, thereby establishing strong covalent bonds with the mucus. Cysteine-modified HA increased mucoadhesive potential by 3.26-fold, ex vivo tissue bioadhesion by 1.4-fold, and the nasal residence time of a model cargo by 1.74-fold relative to unmodified HA, shifting the platform from simple hydration to robust interfacial retention.

However, recent advancements suggest that simply maximizing mucoadhesion is not always the optimal solution (Cone 2009; Boegh and Nielsen 2015; Porfiryeva et al. 2021). Excessively strong adhesion can trap the cargo within the mucus network, paradoxically impeding its transport to the nasal epithelium. Ultimately, factors such as particle size, surface charge, and interfacial properties determine whether a cargo diffuses through or becomes immobilized, making the mucus layer a formidable physicochemical filter. Recognizing this limitation has driven a paradigm shift toward ‘mucus-penetrating’ systems, designed to preserve the cargo's transport capacity while minimizing unproductive mucus interactions. Porfiryeva et al. directly compared mucoadhesive interpolyelectrolyte nanoparticles with PEGylated controls (Porfiryeva et al. 2021). They found that the PEGylated nanoparticles bypassed adhesion and instead exhibited smooth mucus-penetrating behavior on sheep nasal mucosa, proving to be a highly viable alternative for in vivo N2B delivery. Direct mechanistic evidence for this mucus-stabilizing advantage was provided by Bazargani et al., who demonstrated using PEGylated solid lipid nanoparticles that increasing PEGylation effectively prevented mucin-mediated trapping by reducing the formation of large aggregates when incubated in artificial nasal mucus for 20 minutes at 37 °C (Bazargani et al. 2025). This structural stabilization directly translated to enhanced transport capability, allowing the 15 percent PEGylated

formulation to dramatically increase apparent mucus permeability by 10.1 times without compromising cellular uptake in nasal epithelial cells.

3.1.4. Mucus-penetrating systems

Expanding upon this concept, native mucoadhesive polymers have been transformed into sophisticated mucus-penetrating platforms via strategic PEGylation (Ways et al. 2022; Gao et al. 2023). PEGylated chitosan-grafted amphiphilic micelles consist with chemically conjugating hydrophilic PEG chains and the cationic chitosan backbone. The highly localized positive surface charge of the primary amines is effectively masked at the outer particle interface. This steric and electrostatic shielding successfully prevents non-specific interactions with the negative domains of mucin glycoproteins, allowing the surface-tailored micelles to leverage their neutralized, highly hydrated corona to slip unimpeded through the mucosal meshwork. At the same time, the functional role of chitosan is repositioned within the nanostructure's interior. Beneath the protective PEG shell, the preserved primary amine groups of the chitosan backbone function as a potent electrostatic encapsulation core. This highly localized positive charge density drives spontaneous polyplex formation, aggressively packaging and protecting negatively charged biotherapeutic cargoes, such as therapeutic small interfering RNA (siRNA), messenger RNA (mRNA), or delicate peptide biologics, against aggressive nasal enzymatic degradation (Prego et al. 2006; Salade et al. 2017; Sava et al. 2020; Maniyamgama et al., 2025). Consequently, this hybrid architecture operates as a multifunctional vehicle. The outer PEG corona serves as a temporary stealth to bypass the mucociliary sweeping action, while the inner chitosan matrix acts as a robust, protective cage for fragile payloads, collectively ensuring highly efficient and structurally intact direct N2B transport.

The structural optimization of the mucus-penetrating strategies is not limited to polymeric backbones. Advanced lipid-based self-assembling systems have also emerged as a highly effective, physicochemical strategy to outmaneuver the mucosal barrier. As structurally stable colloidal systems typically prepared via high-pressure homogenization or microfluidics (Bonferoni et al. 2019; Bahadur et al. 2020), nanoemulsions offer a highly tunable platform that physicochemical properties dictate in vivo fate. Specifically, engineering the particle size below 200 nm significantly minimizes mucus entrapment and mucociliary clearance, thereby prolonging nasal residence time and maximizing epithelial uptake (Samaridou and Alonso 2018). Furthermore, tailoring the interfacial properties to achieve a zeta potential exceeding ±30 mV ensures robust colloidal stability, while introducing a positive surface charge facilitates strong electrostatic interaction with the negatively charged sialic acid residues of the nasal mucosa, effectively preventing premature dose loss (Chatterjee et al. 2019).

3.1.5. Cyclodextrin platforms

Importantly, this programmatic transition toward minimizing unproductive mucus interactions can be downscaled from particulate colloidal dispersions to the individual molecular level. Cyclodextrin-based platforms can also be conceptualized within this mucus-penetrating design axis (Rassu et al. 2015; Kali et al. 2024). Cyclodextrins act as amphiphilic penetration enhancers that utilize their lipophilic internal cavities to form inclusion complexes with drugs, thereby increasing aqueous solubility and preventing the cargo from being trapped in the mucin network to actively enhance mucus diffusion. Kali et al. comprehensively reviewed cyclodextrins and their derivatives as multifunctional delivery platforms, emphasizing that modified variants such as thiolated cyclodextrins can offer a diverse functional capability, including mucoadhesion, permeation enhancement, in situ gelation, and improved cellular uptake (Kali et al. 2024). Rassu et al. used methyl-*β*-cyclodextrin (MβCD) microparticles loaded with deferoxamine mesylate, a hydrophilic iron chelator drug (Rassu et al. 2015). The added methyl groups alter the hydrophobicity and steric environment around the cavity, enhancing complexation efficiency with drug molecules. In this study, MβCD microparticles showed approximately 1.6 times higher permeation capacity compared to deferoxamine alone and 13.6 times higher permeation capacity compared to the chitosan polymer. After intranasal administration in rats, MβCD microparticles demonstrated an approximately 3.8-fold higher drug concentration in the cerebrospinal fluid at 30 minutes post-administration compared to chitosan microparticles.

Taken together, these studies illustrate that local residence and mucus interaction constitute a critical early-stage bottleneck that the field has aggressively and extensively engineered. Through spray-angle modulation, in situ gelation, mucoadhesive polymer design, mucus-penetration engineering, and

researchers have established a multifaceted framework of strategies to delay clearance, maximize epithelial exposure, and ultimately drive delivery efficiency (Table 2) (Djupesland et al. 2006; Krauland et al. 2006; Qian et al. 2014; Rassu et al. 2015; Bonferoni et al. 2019; Agrawal et al., 2020; Porfiryeva et al. 2021; Kali et al. 2024). Consequently, as with anatomically targeted deposition, this stage represents a highly mature, experimentally tractable intervention axis supported by a wealth of quantitative and mechanistic evidence.

3.2. Biochemical and immunological constraints at the nasal interface

Beyond physical deposition and mucus interaction, intranasal delivery is also constrained by the biochemical and immunological environment of the nasal cavity (Figure 8) (Longo et al. 1986; Baron et al. 1988; Aceto et al. 1989; Gervasi et al. 1991; Sarkar 1992). Even when formulations are successfully deposited and retained locally, therapeutic cargoes may be exposed to enzymatic degradation, chemical destabilization, premature release, or immune-mediated inactivation before productive epithelial entry. This issue is particularly important for biologics, including peptides, proteins, nucleic acids, and viral vectors, whose structural integrity or biological activity can be rapidly compromised at the mucosal interface. Accordingly, biochemical instability and local immune exposure have become another actively targeted early-stage bottleneck in intranasal delivery.

3.2.1. Enzymatic protection

One of the earliest and most direct demonstrations of this barrier came from studies of intranasally administered peptides. Hussain et al. showed that leucine enkephalin peptide underwent extensive hydrolysis within the rat nasal cavity at physiologically relevant concentrations (Hussain et al. 1985). Intact peptide rapidly declined and the extent of absorption was estimated to be less than ~10%. Notably, co-administered competing peptides successfully mitigated this hydrolysis and enhanced absorption. This protective 'decoy' effect proved that the primary barrier to delivery was not the impermeability of the nasal membrane itself. In this context, peptide absorption is strongly limited by rapid enzymatic degradation before epithelial crossing can occur.

Recognition of this barrier led to active investigation of protease inhibition strategies. O'Hagan et al. showed that coadministration of the aminopeptidase inhibitor amastatin significantly enhanced intranasal absorption of biosynthetic human growth hormone in rats, increasing peak plasma levels by 278% and relative bioavailability to approximately 28.9%, whereas bestatin showed little benefit (O'Hagan et al. 1990). Hussain et al. demonstrated that *α*-aminoboronic acid derivatives markedly stabilized leucine enkephalin in the nasal cavity (Hussain et al. 1989). In the presence of boroleucine, more than 90% of intact peptide remained after 45 minutes and approximately 85% remained after 90 minutes. Together, these studies established that improving intranasal delivery often requires preserving cargo integrity long enough for absorption (Hussain et al. 1989; O'Hagan et al. 1990).

This same principle becomes even more critical for nucleic acid therapeutics (Howard et al. 2006; Fihurka et al. 2018). In addition to nuclease-mediated degradation, nucleic acid cargoes are vulnerable to electrostatic interactions with mucus, aggregation or premature unpackaging under ionic conditions, and inefficient intracellular release after cellular uptake. To overcome these vulnerabilities, cationic polymers have emerged as a crucial strategy. Because siRNA is a strongly negatively charged hydrophilic macromolecule, utilizing cationic polymers is essential to condense nucleic acid therapeutics, such as siRNA, antisense oligonucleotide (ASO), and mRNA into nanoscale dimensions, mask their negative charge, and promote both mucus penetration and cellular uptake (Howard et al. 2006). Fihurka et al. directly demonstrated that nanoparticle packaging can shield nucleic acid cargoes from nuclease access (Fihurka et al. 2018). While naked DNA was completely degraded within 20 minutes of DNase I treatment, silica nanoparticles successfully preserved over 90% of the DNA at 20 minutes and approximately 70% at 60 minutes. Howard et al. demonstrated that the chitosan siRNA nanoparticles improve structural stability of siRNA under physiological conditions. Crucially, repeated intranasal administration of this platform in transgenic mice reduced EGFP-positive epithelial cells by 43%, demonstrating that the formulation retains sufficient biological activity after nasal delivery to induce robust mucosal gene silencing (Howard et al. 2006).

Table 2. Formulation strategies targeting nasal deposition and mucosal retention. Strategies are organized by category, including deposition optimization, in situ gelling systems (single- and dual-stimulus), mucoadhesive systems such as chitosan, hyaluronic acid (HA), and hybrid lipid-polymer platforms, mucus-penetrating systems, and cyclodextrin platforms. The representative formulation component, applied cargo, disease model, and major limitation are listed for each approach. MCC, mucociliary clearance. CFD, computational fluid dynamics. SLN, solid lipid nanoparticle. HTCC, hydroxypropyltrimethylammonium chloride chitosan. MβCD, methyl-β-cyclodextrin. NP, nanoparticle.

Major category	Sub-category	Representative platform/ component	Applied cargoes	Major limitation	Ref
Deposition optimization	Aerodynamic control and device engineering	• CFD-guided spray optimization • Plume/administration angle adjustment • Bidirectional breath-actuated device	• CFD-modeled nasal spray droplets/particles • 99mTc-DTPA aerosol tracer	• Device- and technique-dependent • Sensitive to nasal anatomy, cycle, and positioning	Djupesland et al. (2006); Kimbell et al. (2007); Foo et al. (2007); Gao et al. (2020); Seifelnasr et al. (2024)
In situ gelling	Single-stimulus(thermosensitive)	• Methylcellulose gel • Thermosensitive poloxamer gel	• Desmopressin • Pheniramine • Phenylephrine • Tacrine	• Narrow optimal viscosity window • High viscosity impairing spray atomization • Non-linear viscosity-retention tuning required	Harris et al. (1988); Mehta et al. (2009); Qian et al. (2014)
	Dual-stimulus(thermo + ionic)	• Poloxamer/gellan gum • Poloxamer/sodium alginate hybrid gels	• Huperzine A • Amisulpride	• Increased formulation complexity • Limited in vivo N2B validation	Chen et al. (2019); Agrawal et al., 2020; Gadhave et al. (2021)
Mucoadhesive systems	Chitosan(solutions and microparticles)	• Chitosan solutions • Chitosan microspheres • Thiolated chitosan microparticles	• Insulin • Sodium fluorescein • Salmon calcitonin	• Reduced epithelial access from mucus trapping • Dependent on mucus hydration state • Reversible adhesion vulnerable to mucus turnover	(Illum et al. (1994); Soane et al. (1999); Krauland et al. (2006)
	Hyaluronic acid(native and cysteine-modified)	• Native HA • Cysteine-modified HA	• No active therapeutic cargo • Sodium fluorescein	• Added complexity from chemical modification • Uncharacterized mucus-penetration effect	Pritchard et al. (1996); Laffleur et al. (2023)
	Mucoadhesive–lipidhybrid(chitosan-shell + lipid core)	• HTCC-coated anionic liposomes • Chitosan-coated oily nanocapsules • Chitosan-coated SLNs	• Ghrelin • Salmon calcitonin • Ferulic acid	• Largely unverified intact-carrier brain delivery • Mucus-entrapment risk from cationic surfaces	Prego et al. (2006); Salade et al. (2017); Saini et al. (2021)
Mucus-penetrating systems	PEGylation-based(steric shielding)	• PEGylated interpolyelectrolyte NPs • PEGylated chitosan-amphiphilic micelles • PEGylated SLNs	• Haloperidol • Atazanavir • Elvitegravir • Drug-free chitosan-grafted polymer NPs	• Cargo-specific inclusion complexation • Limited N2B generalizability data	Porfiryeva et al. (2021); Ways et al. (2022); Gao et al. (2023); Bazargani et al. (2025)
Cyclodextrin platforms	Inclusion complexation(MβCD microparticles)	• Methyl-β-cyclodextrin • Microparticles	• Deferoxamine mesylate	• Highly cargo-specific inclusion complex formation • Limited N2B generalizability data	Rassu et al. (2015); Kali et al. (2024)

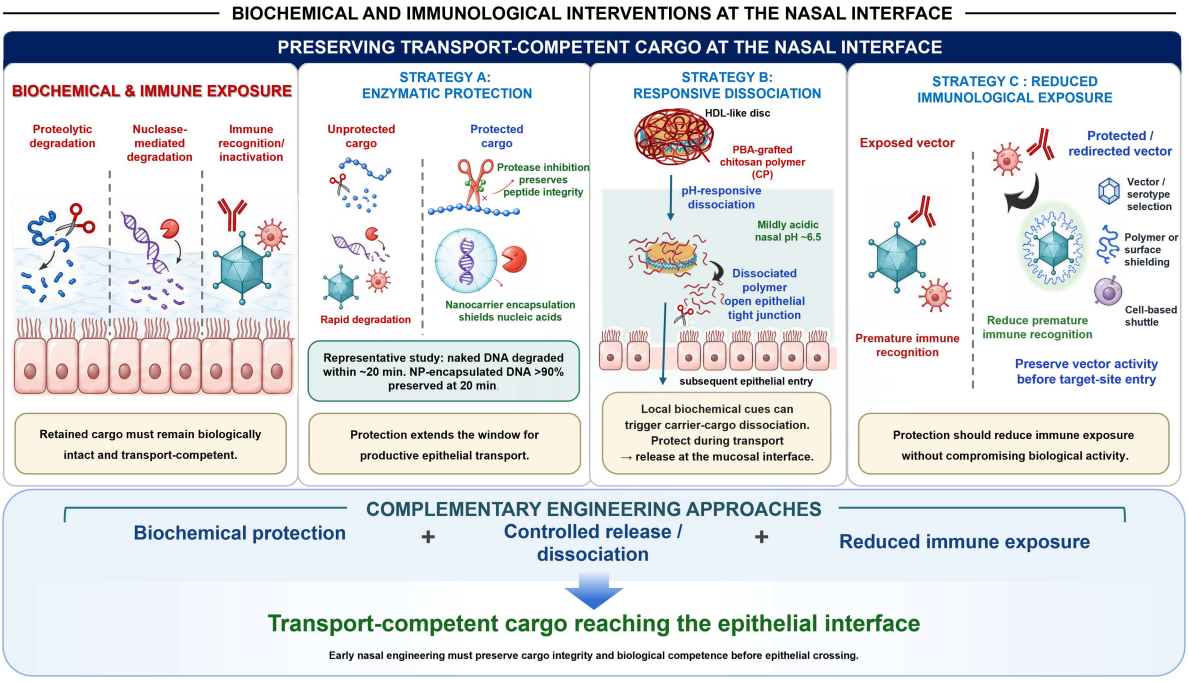

Figure 8. Biochemical and immunological interventions at the nasal interface. Retained cargo must remain biologically intact and transport-competent against proteolytic degradation, nuclease-mediated degradation, and immune recognition. Enzymatic protection through protease inhibition or nanocarrier encapsulation extends the window for productive epithelial transport, as illustrated by naked DNA degrading within approximately 20 minutes while nanoparticle-encapsulated DNA remains largely preserved. Responsive dissociation uses local biochemical cues, such as the mildly acidic nasal pH, to trigger carrier-cargo separation and release at the mucosal interface. Reduced immunological exposure through vector or serotype selection and surface shielding preserves vector activity before target-site entry. Created with BioRender.com and Manus.

3.2.2. Responsive dissociation

In contrast to shielding strategies that aim to preserve the intact carrier complex during mucosal transport, recent counterintuitive approaches have utilized the inherent biochemical properties of the nasal cavity to trigger interfacial dissociation, maximizing the penetration of the naked cargo (Zhang et al. 2023). In this novel strategy, the carrier acts merely as an 'escort,' safely transporting the cargo solely to the nasal wall and deliberately shedding it upon reacting to specific mucosal conditions. Zhang et al. developed a polymeric nanoDisc (polyDisc) system responsive to the slightly acidic microenvironment (pH ~6.5) of the nasal cavity for Alzheimer's disease treatment and showed that the carrier actively dissociated from the cargo at the mucosal interface. Specifically, they engineered a phenylboronic acid (PBA)-grafted chitosan polymer (CP) to package high-density lipoprotein discs (HDL-Disc). Their study demonstrated that the polyDisc actively depolymerized immediately upon reaching the mucosa, allowing the dissociated CP to exclusively act to open epithelial tight junctions while the carrier-free HDL-Disc slipped through the disrupted barrier to enter the brain. This design strategically subverts the biochemical constraints of the nasal cavity, utilizing the acidic environment not as a degradation threat but as a 'penetration switch,' thereby presenting a new paradigm in overcoming the initial nasal barrier by physically decoupling the roles of the carrier and cargo at the mucosal interface.

3.2.3. Immunological evasion

Local immune exposure represents a related but distinct early-stage constraint, particularly for biological and viral formulations that remain immunologically exposure state even when physically stabilized (Salzman et al. 1985; Quinn et al. 2011; Dey et al. 2016; El-Ayoubi et al. 2023; Zhao et al. 2025). In contrast to enzymatic degradation, which erodes cargo integrity directly, immune recognition can limit persistence, re-administration, and local tolerability. Quinn et al. showed that intranasally administered AAV12

effectively transduced the nasal epithelium while eliciting a lower immune response than AAV2, suggesting that a specific capsid variant can influence immune compatibility at the early stage of delivery (Quinn et al. 2011). Beyond serotype selection, delivery strategies have also been used to reduce extracellular immune exposure. Dey et al. used stem-cell-based shuttle systems to deliver oncolytic adenoviruses intranasally to glioblastoma, showing improved tumor-directed delivery after nasal administration (Dey et al. 2016). El-Ayoubi et al. likewise showed that optimized shuttle cells significantly improved intranasal delivery of oncolytic adenovirus to glioblastoma-bearing mice and extended survival (El-Ayoubi et al. 2023). In addition, polymer-coated viral systems such as the pH-sensitive polymeric oncolytic adenovirus reported by Zhao et al. may also reduce premature immune exposure before target-site activation (Zhao et al. 2025). Together, these findings show that early biochemical protection cannot be judged only by whether cargo survives. It must also be evaluated by whether the protective strategy reduces immunological visibility and extracellular loss without introducing a prohibitive local inflammatory burden at the nasal interface (Salzman et al. 1985; Quinn et al. 2011; Dey et al. 2016; El-Ayoubi et al. 2023; Zhao et al. 2025).

Viewed in this way, biochemical instability and local immune exposure occupy a distinct position from deposition or mucus residence. Whereas the earlier bottlenecks determine where and how long a formulation is present, this barrier determines whether the retained fraction remains biologically competent and immunologically tolerable. For this reason, the central challenge at this stage is not simply preservation in a generic sense, but preservation of a fraction that remains both transport-competent and locally acceptable (Table 3).

3.3. Epithelial crossing through modulating paracellular and transcellular entry

As outlined in Section 2.2, the epithelial crossing stage represents a critical branching point where several transport mechanisms, mostly the paracellular route (going between cells) and the transcellular route (going through cells), can either compete or cooperate (Figure 9). The specific route can dictate the downstream trajectory of cargo within the CNS (Lin et al. 2016; Lochhead and Davis 2019; Yokel 2022; Drath et al. 2025; Qiu et al. 2025).

3.3.1. Paracellular modulation

Faced with these competing pathways, researchers sought to target the paracellular route as the first line of approach, modulating apical junctional complexes to transiently increase paracellular permeability (Aungst 2012). This is supported by Min et al. who demonstrated that local hypoxic stimuli can significantly reduce transepithelial electrical resistance (TEER) and downregulate key junctional proteins such as ZO-1 and E-cadherin (Min et al. 2015). To this end, chitosan-based formulations have been engineered as an epithelial permeation enhancer. For instance, Zhang et al. showed that 0.5% chitosan markedly enhanced the in vitro permeability coefficient of FITC-labeled recombinant hirudin-2, a thrombin-inhibiting anticoagulant peptide, across excised nasal epithelium and increased its in vivo nasal bioavailability up to 8.26% compared to saline controls (Zhang et al. 2005). Moreover, combining chitosan with surfactants like SDS or Tween 80 further increased the nasal bioavailability of recombinant hirudin-2 up to 17.25%, while maintaining acceptable ciliotoxicity.

These early studies established that the epithelial layer should not be considered as a fixed boundary, but rather as dynamic gateway which is capable of modulation. This strategy has subsequently been refined using pH-resilient chitosan derivatives, ensuring functional efficacy across varied physiological conditions (du Plessis et al. 2010). Because unmodified chitosan retains its protonated and soluble state only under acidic conditions, its junction-opening capability is lost as the pH shifts toward neutral. To overcome this limitation, du Plessis et al. compared chitosan hydrochloride with highly quaternized *N*-trimethyl chitosan chloride (TMC) for intranasal insulin delivery. While all polymers enhanced insulin absorption at pH 4.40, only the highly quaternized TMC sustained its enhancing effect at pH 7.40, resulting in about 5-fold increase in insulin levels. This indicated that epithelial permeation is dependent on its ability to preserve ionization within the shifting physicochemical environment of the nasal cavity.

Beyond polymeric matrices, cyclodextrin-based platforms have emerged as chemical permeation enhancers that modulate epithelial membrane lipids and tight-junction organization (Marttin et al., 1999; Merkus et al., 1999; Yang et al. 2004). Cyclodextrins form complexes with membrane lipids which temporarily

Table 3. Formulation strategies for biochemical protection and immunological evasion at the nasal interface. Strategies are organized by category, including enzymatic protection via protease inhibitor co-administration or nanoencapsulation of nucleic acid cargoes, responsive dissociation via mucosal pH-triggered de-shielding, and immunological evasion via capsid variant selection or polymer-coated viral carriers. The applied cargo, disease model, and key limitation are listed for each approach. AAV, adeno-associated virus. PBA, phenylboronic acid. CP, chitosan polymer.

Major category	Sub-category	Representative platform/ component	Applied cargoes	Major limitation	Ref
Enzymatic protection	Co-administeredprotease inhibitors	• Competing substrate peptide • Amastatin • *α*-aminoboronic acid	• Leucine enkephalin • Biosynthetic human growth hormone	• No effect on mucus penetration, crossing, or targeting • Peptide- or enzyme-specific applicability	Hussain et al. (1985); Hussain et al. (1989); O'Hagan et al. (1990)
	Physical shielding viananoencapsulation (nucleic acids)	• Silica nanoparticles • Chitosan/siRNA nanocomplexes	• DNA oligonucleotides • EGFP-targeting siRNA	• Cationic-charge mucin entrapment • Incomplete intracellular release • Possible mucosal-fluid aggregation	Howard et al. (2006); Fihurka et al. (2018)
Responsive dissociation	Microenvironment-triggeredde-shielding (nasal interface)	• pH-responsive polymeric nanoDisc • PBA-grafted chitosan polymer	• HDL-Disc/apoA-I nanodisc	• Precise pH-trigger sensitivity required • Premature or incomplete dissociation under variable nasal pH	Zhang et al., (2023)
Immunological evasion	Capsid variant selection(for reduced innate immune recognition)	• AAV12 capsid	• AAV12-luciferase vector	• Species- and tissue-dependent immune compatibility • Possible loss of native infectivity with alternative capsids	Quinn et al., (2011)
	Cellular shuttles andpolymer-coated viralcarriers	• Stem-cell shuttle systems • pH-sensitive polymer-coated oncolytic adenovirus	• Oncolytic adenovirus • pH-sensitive polymer-coated oncolytic adenovirus	• Complex manufacturing • Safety and re-administration concerns • Possible infectivity loss before target arrival	Dey et al. (2016); El-Ayoubi et al. (2023); Zhao et al. (2025)

loosen the dense network of epithelial tight junctions and modulate localized epithelial membrane fluidity. Marttin et al. provided direct morphological evidence for structural changes in tight junctions using electron and confocal microscopy in the rat nasal respiratory epithelium following the application of methyl β-cyclodextrin (Marttin et al., 1999). Supporting these physical changes, Yang et al. reported that 5% dimethyl β-cyclodextrin induced the redistribution of the tight junction marker ZO-1 and decreased epithelial integrity to actively promote paracellular pathway opening (Yang et al. 2004). Crucially, this permeation-enhancing effect was fully reversible within 6 hours in vivo and effectively increased the absolute bioavailability of intranasal enoxaparin by approximately eight times. Based on these mechanisms, Merkus et al. demonstrated that dimethyl β-cyclodextrin significantly promoted the nasal absorption of insulin or ACTH analogs compared to liquid controls, achieving 70 to 100% bioavailability in mouse models (Merkus et al., 1999).

3.3.2. Matrix remodeling

The concept of barrier penetration has been expanded from intercellular gap opening in epithelial cells to enzymatic strategies that directly target the extracellular matrix structurally supporting them (Lochhead et al. 2015; Yokel 2022). Lochhead et al. demonstrated that matrix metalloproteinase-9 (MMP-9), which degrades tight junctions and extracellular matrix components, significantly increased the permeability of 10 kDa dextran across the olfactory epithelium, illustrating that modulating structural nasal epithelial permeability can actively enhance particle delivery (Lochhead et al. 2015). In a similar context, hyaluronidase has been also explored to increase tissue permeability (Danielyan et al. 2009; Galeano et al. 2018). The hyaluronidase pretreatment successfully facilitated nasal cellular uptake and maximized stem cell trafficking to the brain. However, there is a clear limitation in interpreting this as direct evidence of improved nasal epithelial permeability. It remains unclear whether the increased absorption is precisely due to enhanced penetration across the epithelial cell layer itself or the degradation of other tissue matrices located beyond

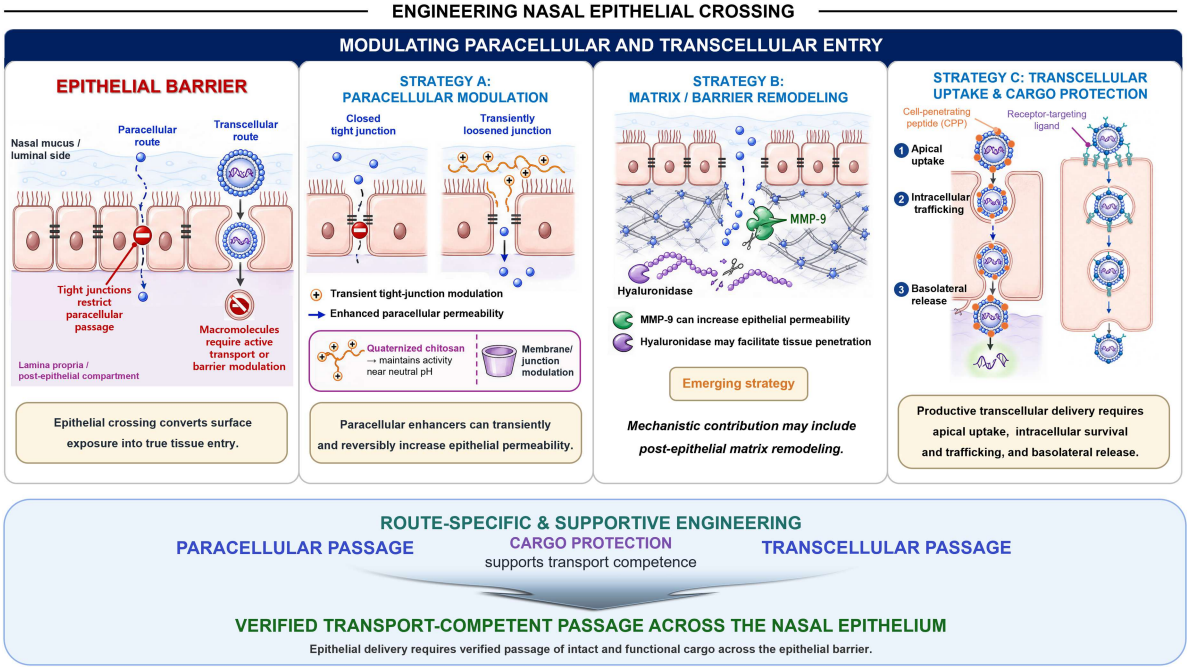

Figure 9. Engineering nasal epithelial crossing. Epithelial crossing converts surface exposure into true tissue entry, with tight junctions restricting paracellular passage and macromolecules requiring active transcellular transport or barrier modulation. Paracellular modulation transiently and reversibly loosens tight junctions, for example through quaternized chitosan that remains active near neutral pH. Matrix or barrier remodeling by enzymes such as matrix metalloproteinase-9 (MMP-9) or hyaluronidase may facilitate post-epithelial tissue penetration. Transcellular uptake and cargo protection require apical uptake, intracellular survival and trafficking, and basolateral release, supported by cell-penetrating peptides (CPPs) and receptor-targeting ligands. Created with Manus.

the epithelium. Furthermore, whether these macroscopic matrix-modifying pretreatments can directly enhance the absorption of synthetic nanomedicines or conventional small molecules has not yet been clearly reported. Consequently, verifying biological mechanisms for nanocarrier systems remains a critical objective requiring rigorous validation (Danielyan et al. 2009; Galeano et al. 2018; Yokel 2022).

3.3.3. Transcellular uptake

Another major strategy focused on utilizing transcellular uptake mechanisms (Malhotra et al., 2013; Lin et al. 2016). This approach is particularly critical for macrobiologics such as siRNA, mRNA, and plasmid DNA, which are intrinsically restricted from passive paracellular diffusion due to their large molecular weight and negative charge density (Howard et al. 2006; Malhotra et al., 2013; Lin et al. 2016). To overcome this limitation, cell-penetrating peptides (CPPs), which are cationic or amphipathic short amino acid sequences, are utilized to cross the epithelial cell membrane (Malhotra et al., 2013; Lin et al. 2016). Despite strategies targeting the transcellular route are increasing, most studies only demonstrate cellular uptake or brain distribution without directly proving epithelial transcytosis (Malhotra et al., 2013; Schlachet and Sosnik 2019; Yokel 2022). To claim transcytosis, it requires evidence such as apical internalization, intracellular vesicular trafficking, basolateral release, paracellular exclusion, and pathway inhibition. For example, Malhotra et al. engineered PEGylated chitosan nanoparticles, which were functionalized with dual MGF and TAT peptide tags, a representative CPPs, for siRNA delivery (Malhotra et al., 2013). In this system, chitosan provided mucoadhesive matrix, PEGylation offered steric stabilization, and the TAT and MGF peptide tags were integrated for membrane interaction and transcellular uptake. Although this system showed robust siRNA localization in the cerebral cortex and cerebellum within 4 hours of post-administration without inducing detectable neurotoxicity, it is a proof of concept for peptide-mediated brain delivery rather than direct proof of epithelial transcytosis. The underlying evaluation lacked the mechanistic resolution to differentiate transcellular crossing from paracellular, nerve-associated, or systemic pathways.

Ligand mediated uptake strategies present a similar methodological limitation (Schlachet and Sosnik 2019; Yokel 2022). Gabold et al. evaluated transferrin-decorated chitosan nanoparticles for nose-to-brain delivery of β-galactosidase as a model protein cargo (Gabold et al. 2023). In this study, transferrin was decorated on the surface of chitosan nanoparticles (CNs) after particle formation through copper-free click chemistry. This strategy minimizes undesired cargo-ligand interactions and allows modulation of surface ligands while preserving the protein cargo inside the nanoparticle. In an air–liquid interface (ALI) nasal epithelial model, encapsulation in chitosan nanoparticles increased cellular uptake of β-galactosidase, and transferrin decoration further enhanced uptake compared with non-decorated nanoparticles and free protein. However, such enhanced intracellular localization should not be equated with successful epithelial crossing. Confirming true receptor-mediated transcytosis requires rigorous tracking of the apical-to-basolateral transport of the intact cargo, definitive basolateral release, and the preservation of barrier integrity under competitive receptor-blocking conditions (Schlachet and Sosnik 2019; Yokel 2022).

3.3.4. Cargo protection

Even when cellular internalization is successfully achieved, it is not automatically translated into epithelial crossing, these nucleic acid cargoes remain highly vulnerable to endosomal sequestration and premature intracellular degradation (Howard et al. 2006; Malhotra et al., 2013; Harmon et al. 2014). To circumvent post-uptake endosomal sequestration, Harmon et al. applied CK30PEG-compacted plasmid DNA nanoparticles, utilizing a 30-mer poly-lysine peptide to package large nucleotide structures into a protective PEGylated shell (Harmon et al. 2014). Following intranasal administration, widespread eGFP expressions were observed along the rostral-caudal axis of the rat brain. By providing transgene expression as the delivery outcome, this study confirms that CK30PEG can preserve the cargo's structural integrity throughout the entire transport. This represents a critical frame evolution from strictly focused on maximizing initial epithelial uptake to designing carriers capable of sustaining cargo biological function throughout the post-entry stages.

In summary, the nasal epithelium has been aggressively engineered through tight-junction modulation, pH-resilient paracellular enhancers, CPP-assisted uptake, and endosomal-escape machinery (Marttin et al., 1999; Merkus et al., 1999; Yang et al. 2004; Zhang et al. 2005; Danielyan et al. 2009; du Plessis et al. 2010;

Aungst 2012; Malhotra et al., 2013; Min et al. 2015; Galeano et al. 2018; Schlachet and Sosnik 2019; Gabold et al. 2023). Despite these technological milestones, most literature concludes epithelial crossing success indirectly from downstream brain signals or reporter gene expression (Malhotra et al., 2013; Harmon et al. 2014; Schlachet and Sosnik 2019; Yokel 2022; Gabold et al. 2023). There are limited studies directly quantifying the exact fraction of cargo that traverses the epithelium in a transport-competent state. Although epithelial crossings are still one of the most intensively targeted parts of N2B formulation, paradoxically, they still require mechanical and biological validation (Table 4).

3.4. Post-epithelial gateways by navigating anatomical and fluidic pathways

This indicates that the immediate post-epithelial transport stage remains a critical gap and a completely uncharted territory in the design of drug delivery systems (Figure 10) (Yokel 2022; Drath et al. 2025). The mechanisms such as perineural transport along the olfactory and trigeminal nerves, CSF-mediated redistribution, and deep penetration into the brain parenchyma have received little attention in intranasal formulation design (Lochhead and Davis 2019; Yokel 2022; Drath et al. 2025). Although perineural transport into the brain is a well-established primary biological pathway following intranasal administration, there is a blank of formulation engineering that controls delivery efficiency by directly targeting the microfluidic or anatomical characteristics of these perineural spaces (Lochhead and Davis 2019; Lochhead et al. 2019; Spera et al. 2023). Indeed, several studies have highlighted the lack of evidence that nanosystems reach the brain parenchyma intact (Costa et al. 2019; Yokel 2020). While chitosan has been shown to enhance absorption from the nasal cavity into the brain or CSF, research demonstrating the intact translocation of nanoparticles deep into the brain parenchyma remains rare (Casettari and Illum 2014).

To overcome these barriers, pharmacological pretreatment strategies that modulate CSF dynamics and external physical-force-based approaches have been explored (Shingaki et al. 2009; Shingaki et al. 2010; Chen et al. 2014; Ye et al. 2021; Ye et al. 2023; Koh et al. 2026). In an intriguing example of chemical modulation, Shingaki et al. demonstrated that decreasing CSF production by acetazolamide, a carbonic anhydrase inhibitor, significantly increased the CSF concentrations of intranasally administered 5-fluorouracil and methotrexate. This approach offers a promising option for targeted drug delivery by inhibiting CSF production to reduce drug clearance. Additionally, approaches that physically overcome fluidic resistance using external electromagnetic forces or ultrasound are being explored. Ye et al. first demonstrated that transcranial magnetic stimulation (TMS)-generated pulsed magnetic fields, applied concurrently with intranasal administration of magnetic nanoparticles, can actively drive particles across the cribriform plate and into the brain parenchyma, achieving approximately two-fold greater brain delivery compared to passive intranasal administration alone (Ye et al. 2023). Building on this proof of concept, Koh et al. subsequently conjugated temozolomide to superparamagnetic iron oxide nanoparticles (TMZ-SPIONs) and guided them intranasally to an intracranial glioblastoma site using TMS, demonstrating that magnetically directed N2B delivery significantly prolonged survival in xenograft mouse models while requiring less than one-tenth of the conventional drug dose (Koh et al. 2026). Separately, focused ultrasounds have been employed to augment intranasal delivery through distinct mechanisms. The active propulsion of anti-PD-L1 antibodies into the brainstem via ultrasound-enhanced delivery, or the hemisphere-specific enhancement of DNA nanoparticle gene expression through ultrasound pretreatment, suggests that physical energy can potently facilitate parenchymal penetration (Chen et al. 2014; Ye et al. 2021). However, these approaches remain supplementary strategies that overcome hydrodynamic resistance through dependence on external devices, and their clinical scalability is constrained by the need for specialized equipment and precise spatial targeting (Chen et al. 2014; Ye et al. 2021; Ye et al. 2023; Koh et al. 2026).

The strategy for achieving brain parenchymal penetration through the formulation's integral physicochemical properties, without external devices, involves biomimetic systems based on high-density lipoprotein (HDL) or apoA-I nanodiscs (Zhang et al. 2023). Designed to be ultrasmall, these nanodiscs biologically mimic the endogenous lipid transport pathways that are naturally present within the brain. This characteristic prevents non-specific entanglement from steric hindrances of the densely interwoven extracellular matrix (ECM), enabling them to penetrate deep into brain tissue. The N2B delivery of ASO-loaded apoA-I nanodiscs resulted in neuron-specific accumulation along the anterior–posterior axis (Aly et al. 2023). While ASO alone reached the perivascular space but failed to breach the matrix barrier, the

Table 4. Formulation strategies for enhancing epithelial crossing. Strategies are organized by category, including paracellular modulation via tight junction opening using chitosan, *N*-trimethyl chitosan chloride (TMC), or cyclodextrin platforms, enzymatic matrix remodeling using MMP-9 or hyaluronidase, transcellular uptake via CPP-modified or receptor-decorated nanoparticles, and post-uptake endosomal escape. The applied cargo, disease model, and principal limitation are noted for each approach. CPP, cell-penetrating peptide. MβCD, methyl-*β*-cyclodextrin. DMβCD, dimethyl-*β*-cyclodextrin. MMP-9, matrix metalloproteinase-9. NP, nanoparticle. PLGA, poly(lactic-co-glycolic acid).

Major category	Sub-category	Representative platform/ component	Applied cargoes	Major limitation	Ref
Paracellular modulation	Chitosan/TMC(TJ opening)	• Chitosan solutions • *N*-trimethyl chitosan chloride • Chitosan + surfactant	• Recombinant hirudin-2 • Insulin	• Epithelial irritation and ciliotoxicity at high dose • Non-specific permeability increase • Native chitosan inactive at neutral pH	Zhang et al. (2005); du Plessis et al. (2010)
	Cyclodextrins(membrane lipid interaction)	• Methyl-*β*-cyclodextrin • Dimethyl-*β*-cyclodextrin	• Enoxaparin • Insulin • ACTH analogs	• Non-selective permeability without N2B specificity • Possible epithelial irritation with prolonged use	Marttin et al., 1999; Merkus et al., 1999; Yang et al. (2004)
Matrix remodeling	Enzymatic ECM modulation (MMP-9/hyaluronidase)	• MMP-9 • Hyaluronidase solution	• Texas Red–labeled dextran • Mesenchymal stem cells	• Ambiguous epithelial-crossing versus matrix-remodeling effect • Safety concerns from broad enzymatic pretreatment • Limited validation for synthetic nanocarriers	Danielyan et al. (2009); Lochhead et al. (2015); Galeano et al. (2018); Yokel (2022)
Transcellular uptake	CPP-modified nanoparticles (membrane interaction& endocytosis)	• TAT/MGF-tagged PEGylated Chitosan NP • CPP-modified PLGA NPs	• siRNA • Fluorescent PLGA NPs	• Enhanced uptake not proving transcytosis • Insufficient transport-route resolution • Endosomal-trapping risk	Malhotra et al., 2013; Steinbach et al. (2016)
	Receptor-decoratednanoparticles (selective epithelial uptake)	• Transferrin-decorated chitosan NPs	• *β*-Galactosidase	• Intracellular localization not proving apical-to-basolateral transcytosis • Basolateral-release and receptor-blocking controls required	Gabold et al. (2023)
Cargo protection (post-uptake)	Nucleic acid condensationand endosomal escape	• CK30PEG-compacted plasmid DNA NPs • Chitosan/siRNA NPs	• eGFP plasmid DNA • EGFP-targeting siRNA	• Functional readout not identifying the crossing route • Unresolved endosomal escape and cell-type specificity	Howard et al. (2006); Harmon et al. (2014)

nanodisc formulation capitalized on its superior matrix permeability to significantly reduce target gene expression in the cortex and striatum, thereby proving functional neural delivery. Furthermore, Zhang et al. engineered HDL discs to actively release under the mildly acidic conditions of the nasal cavity, capture amyloid-*β* within the brain parenchyma, and induce clearance mechanisms (Zhang et al. 2023). This approach drastically reduced amyloid-*β* accumulation in the brain parenchyma by up to 97.3% following administration.

Ultimately, the post-epithelial gateway, which governs the behavior of the cargo following epithelial transit, is the defining point of effective drug delivery. It dictates the precise compartmental distribution of the cargo and its capacity to penetrate the brain parenchyma (Nance et al. 2012; Pizzo et al. 2018; Yokel

2022; Drath et al. 2025). However, strategies driven purely by intranasal formulation engineering remain severely lacking compared with the research advancements seen in other routes of administration (Costa et al. 2019; Yokel 2020; Yokel 2022; Drath et al. 2025). Therefore, this is the key area that must be addressed as a priority in future formulation development (Table 5).

3.5. Cellular internalization and functional delivery

After reaching the brain parenchyma, the final goal in N2B delivery is precise engagement at the target site that aligns with the cargo's therapeutic mechanism (Figure 11) (Zhuang et al. 2011; Alvarez-Erviti et al. 2011; Harmon et al. 2014; Steinbach et al. 2016). The definition of successful delivery must vary depending on the characteristics of the cargo. Further, many cargoes, such as small molecules, peptides, siRNA, ASOs, plasmid DNA, and viral vectors, must enter disease-relevant cells to exert their functional activity, whereas other therapeutics act on extracellular targets and therefore do not require cellular internalization.

3.5.1. Receptor-mediated targeting

The most representative approach is receptor-mediated uptake which actively internalizes the cargo into cells by introducing specific ligands onto the carrier surface (Gabold et al. 2023). It targets receptors overexpressed on the surface of specific diseased cells or brain-related cells. Ferritin is an endogenous protein complex that stores iron in the body (Fan et al. 2012; Moglia et al. 2021). It forms a natural

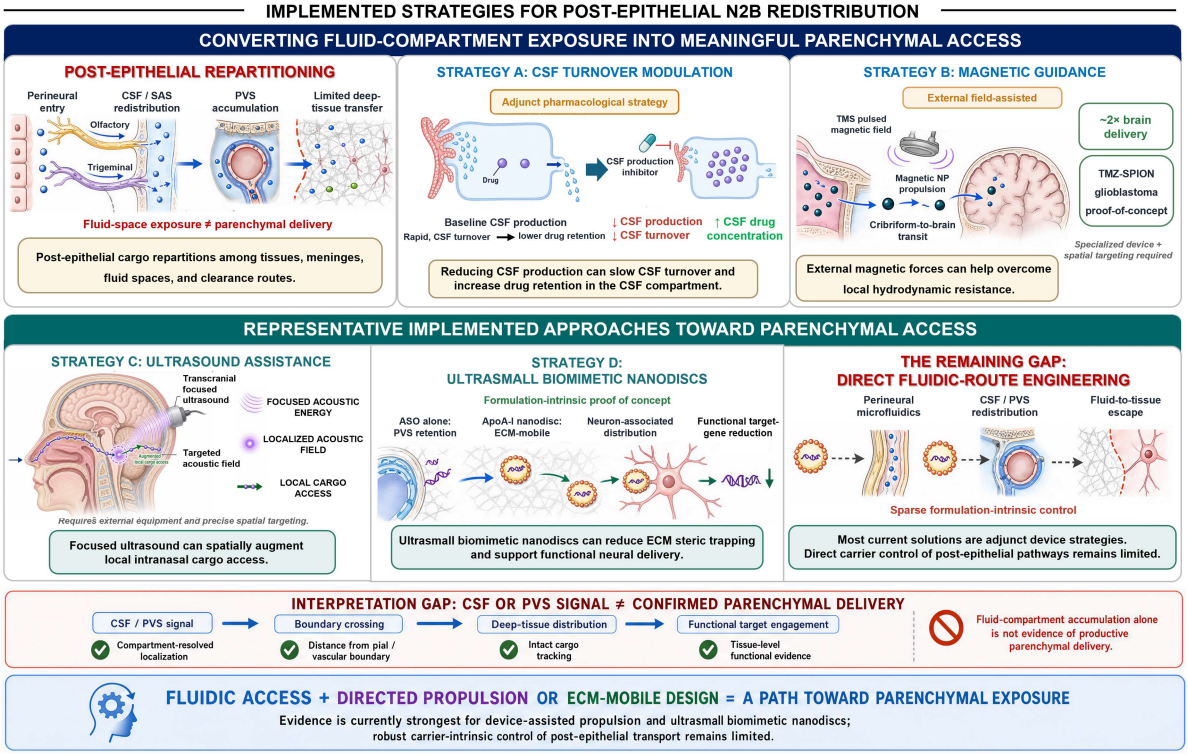

Figure 10. Implemented strategies for post-epithelial N2B redistribution. After epithelial crossing, cargo repartitions among perineural spaces, cerebrospinal fluid (CSF), subarachnoid space (SAS), perivascular space (PVS), and clearance routes, such that fluid-space exposure does not equate to parenchymal delivery. Adjunct approaches include pharmacological modulation that reduces CSF turnover to increase drug retention, magnetic guidance and focused ultrasound to overcome local hydrodynamic resistance, and ultrasmall biomimetic nanodiscs that reduce ECM steric trapping and support functional neural delivery. A key interpretation gap remains, as CSF or PVS signal is not equivalent to confirmed parenchymal delivery and requires compartment-resolved localization, boundary crossing, deep-tissue distribution, and functional target engagement. Direct carrier-intrinsic control of post-epithelial pathways remains limited relative to device-assisted strategies. SAS, subarachnoid space. PVS, perivascular space. ECM, extracellular matrix. SPION, superparamagnetic iron oxide nanoparticle. ASO, antisense oligonucleotide. Created with Manus.

Table 5. Formulation strategies targeting post-epithelial fluidic pathways and parenchymal penetration. Strategies are organized into three categories: pharmacological CSF modulation via acetazolamide-mediated carbonic anhydrase inhibition, external physical force-assisted delivery including TMS-guided magnetic nanoparticles and focused ultrasound (FUS)-enhanced delivery, and formulation-intrinsic approaches including biomimetic HDL-like nanodiscs and ECM-compatible ultrasmall carriers. The applied cargo, disease model, and principal limitation are listed for each approach. CSF, cerebrospinal fluid. PVS, perivascular space. TMS, transcranial magnetic stimulation. FUS, focused ultrasound. ECM, extracellular matrix. ASO, antisense oligonucleotide.

Major category	Sub-category	Representative platform/component	Applied cargoes	Major limitation	Ref
Biochemical/ pharmacological	CSF productionmodulation	• Acetazolamide	• 5-Fluorouracil • Methotrexate	• Safety evaluation of CSF-homeostasis perturbation required • CSF enrichment not equal to parenchymal penetration	Shingaki et al. (2009), (2010)
External physical forces	Transcranial magneticguidance	• Transcranial magnetic pulses • PEGylated magnetic nanoparticles	• PEGylated magnetic NPs • Temozolomide-conjugated SPIONs	• Device- and tissue-specific safety calibration • Limited clinical scalability	Ye et al. (2023); Koh et al. (2026)
	Focused ultrasound-enhanced delivery	• Focused ultrasound	• Anti-PD-L1 antibody	• Parameter-sensitive safety (heating, cavitation) • Specialized equipment required • Evidence mainly preclinical	Chen et al. (2014); Ye et al. (2021)
Formulation-intrinsic strategies	Biomimetic HDL-likeparenchymal-penetratingcarriers	• ApoA-I nanodiscs • pH-responsive HDL-Disc	• Huntingtin-lowering ASO • HDL-Disc/polyDisc	• Disease- and cargo-specific design • Uncertain generalizability to larger biologics or vectors • Limited intranasal validation	Zhang et al. (2023); Aly et al. (2023)
	ECM-compatible surfaceengineering (parenchymal diffusion)	• Densely PEGylated, ultra-small nanoparticles • neutral/low-adhesion surface	• Densely PEGylated polymeric NPs • Intrathecal antibodies/large-protein tracers	• Evidence mainly from direct brain-injection models • No dedicated intranasal validation • Steric optimization alone insufficient at the pial-glial interface	Iliff et al. (2012); Nance et al. (2012); Pizzo et al. (2018)

nanoscale cage structure, making it highly suitable for loading therapeutic drugs. Fan et al. and Moglia et al. demonstrated that H-ferritin nanocages target TfR1-rich brain tumor cells without any artificial chemical modifications. This intrinsically receptor-recognizing nanocage improves drug delivery to brain tumor cells, increasing cellular uptake by more than 7-fold. Furthermore, when applied to glioma therapy, this approach increased the cargo concentration in the tumor-bearing hemisphere by 5-fold and reduced tumor volume by up to 74% following intranasal administration (Marrocco et al. 2024).

Another major pathway to target is the lactoferrin (Lf)-lactoferrin receptor (LfR) axis. LfRs are abundantly expressed on the surface of major CNS-related cells, including brain vascular endothelial cells (Hu et al. 2009; Bi et al. 2016; Zhao et al. 2018). Thus, Lf-decorated carriers may facilitate receptor-associated entry into brain tissue and neural cells. Hu et al. demonstrated that Lf-conjugated PEG-PLA nanoparticles induced receptor-associated uptake in mouse brain microvascular endothelial cells and showed a 3-fold improvement in brain delivery efficiency *in vivo* compared with non-targeted PEG-PLA nanoparticles (Hu et al. 2009). Zhao et al. developed an Lf-modified nanostructured lipid carrier (Lf-NLC) loaded with nimodipine, a poorly water-soluble calcium-channel blocker, and showed enhanced receptor-mediated uptake and brain-targeting performance (Zhao et al. 2018).

Building on the same receptor-ligand logic, recent work has begun to extend N2B targeting from broad brain accumulation toward defined anatomical regions and individual cell types, although this remains an emerging capability. At the regional level, Rao et al. constructed hypothalamus-directed nanoparticles bearing a modified (Trp7, β-Ala8)-neurokinin A (4–10) ligand against the hypothalamic neurokinin three receptor (NK3R), which drove preferential uptake into hypothalamic cells after intranasal administration

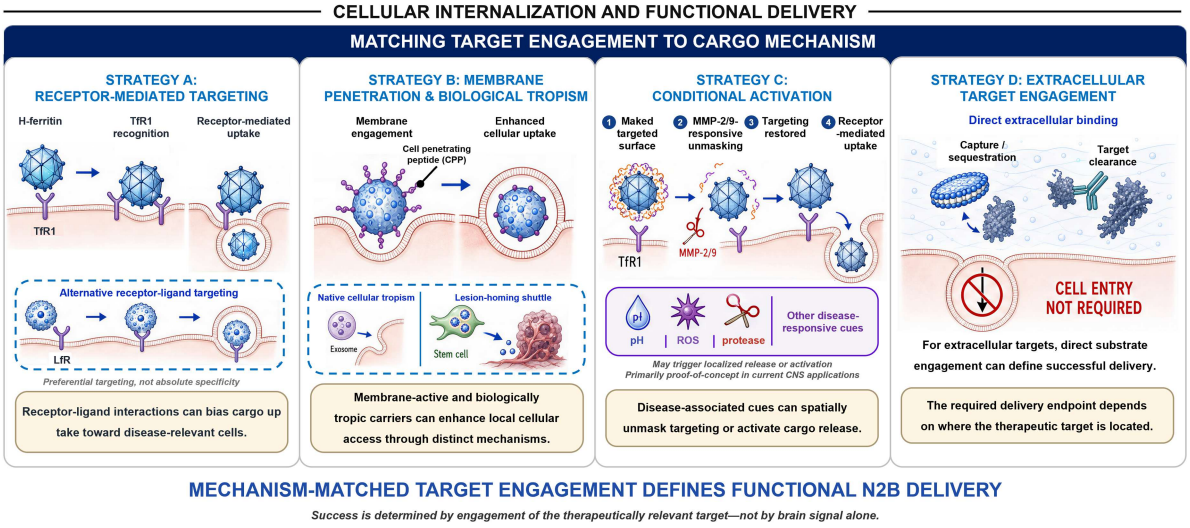

Figure 11. Cellular internalization and functional delivery. Successful delivery is defined by engagement of the therapeutically relevant target rather than by brain signal alone, so the required endpoint depends on where the target is located. Receptor-mediated targeting biases cargo toward disease-relevant cells through receptor-ligand interactions, such as H-ferritin with transferrin receptor 1 (TfR1) or lactoferrin with its receptor. Membrane penetration and biological tropism enhance local cellular access through cell-penetrating peptides, exosomal tropism, or cell-based shuttles. Conditional activation uses disease-associated cues, including pH, reactive oxygen species (ROS), and proteases, to spatially unmask targeting or activate cargo release, whereas extracellular target engagement can define successful delivery without cellular entry. TfR1, transferrin receptor 1. LfR, lactoferrin receptor. MMP, matrix metalloproteinase. Created with Manus.

(Rao et al. 2024). Route-dependent bias offers a complementary handle, as olfactory transport favors rostral structures whereas trigeminal input preferentially reaches caudal regions such as the brainstem, so that ligand choice and administration route can jointly shape regional distribution (Lochhead and Davis 2019; Crowe and Hsu 2022; Spera et al. 2023). At the cellular level, surface ligands can steer carriers toward particular glial populations. Transferrin and lactoferrin decoration has been used to bias uptake toward astrocytes and tumor-associated glia, and intranasal platforms that reprogram microglia through lactoferrin-functionalized carriers or exploit the microglial tropism of exosomes have been demonstrated in neuroinflammatory and neurodegenerative models (Zhuang et al. 2011; Dlamini et al. 2026). These examples indicate that region- and cell-type-selective N2B delivery is feasible in principle, yet current selectivity derives largely from receptor abundance and anatomical routing rather than from absolute molecular specificity, leaving precise single-target engagement an open challenge.

3.5.2. Membrane penetration

Receptor-independent, cell-penetrating peptide (CPP)-mediated membrane engagement strategies are also widely utilized (Malhotra et al., 2013; Lin et al. 2016; Steinbach et al. 2016; Khafagy et al. 2020). CPPs are short amino acid sequences with strong positive charges or amphiphilicity. CPPs interact electrostatically with the negatively charged components of the cell membrane surface, temporarily loosening the membrane structure or inducing active endocytosis (Lin et al. 2016; Steinbach et al. 2016; Khafagy et al. 2020). Steinbach et al. demonstrated that when various CPPs such as penetratin, EB1, and MPG were introduced into PLGA nanoparticles, the energy-dependent and clathrin-mediated cell internalization of the nanoparticles improved by 48- to 64-fold compared to unmodified NPs (Steinbach et al. 2016). Lin et al. utilized LMWP, an arginine-rich CPP, to promote the brain entry of protein cargoes. Using horseradish peroxidase (HRP) and β-galactosidase (β-gal) as functional enzyme cargoes, they further showed that LMWP-linked enzymes retained measurable enzymatic activity in brain tissue, with significantly higher activity than their native, non-modified counterparts (Lin et al. 2016). Furthermore, Khafagy et al. co-administered leptin with penetratin, a type of CPP, and demonstrated not only brain accumulation but also

CNS pharmacodynamic signaling, including STAT3 phosphorylation and leptin receptor stimulation (Khafagy et al. 2020).

Another strategy uses the native tropism of exosomes or cells (Zhuang et al. 2011; Dey et al. 2016; El-Ayoubi et al. 2023). Zhuang et al. intranasally administered exosome-encapsulated curcumin and observed exosome-positive signals in a substantial fraction of microglia, the target brain cells, within 1 hour (Zhuang et al. 2011). Further, it delayed brain inflammation and tumor growth. Dey et al. and El Ayoubi et al. intranasally administered an oncolytic adenovirus using a stem cell with migration characteristics toward the glioma microenvironment (Dey et al. 2016; El-Ayoubi et al. 2023). This approach is a unique strategy that extends survival not through target cell endocytosis, but by guiding the therapeutic viral cargo to the lesion via the tumor-homing behavior of a living carrier.

3.5.3. Conditional activation

There are also conditional activation strategies that regulate cargo release or receptor accessibility in response to the lesion or disease microenvironment (Marrocco et al. 2024; Zhao et al. 2025). The-0504 is a carrier designed to activate exclusively within the target tissue (Marrocco et al. 2024). The PASE shielding domain is a protective polypeptide module that masks the TfR1-binding surface of H-ferritin (HFt) and suppresses premature receptor binding until it is removed by MMP-2/9-mediated linker cleavage in the glioma microenvironment. Consequently, the exposed HFt is internalized by TfR1-overexpressing tumor cells, where it releases its payload (Genz-644282) to inhibit topoisomerase I. Ultimately, this single formulation can induce tumor receptor targeting and protease-responsive activation. In addition, protease-responsive linkers can be designed to remove shielding groups or release payloads using lesion-associated enzymes such as MMP-2/9, cathepsins, and legumain.

Tumor microenvironments of glioma often exhibit lower pH, higher ROS, and higher protease activity than normal tissues (Marrocco et al. 2024; Zhao et al. 2025). Therefore, pH-responsive systems can induce carrier disassembly and cargo release in an acidic tumor microenvironment or endosomal pH. For instance, the polyDisc system developed by Zhang et al. exploits the mildly acidic nasal and endosomal pH to trigger carrier depolymerization, enabling selective cargo release at the target interface (Zhang et al. 2023). Similarly, protease-responsive platforms exploit lesion-associated enzymes such as MMP-2/9 to trigger shielding removal and selective cargo activation, as exemplified by the ferritin-based The-0504 nanovector described above (Marrocco et al. 2024). Further, ROS-responsive linkers can accelerate drug release in lesion areas with high oxidative stress. Zhang et al. demonstrated this principle by engineering thioketal-crosslinked nanoparticles loaded with puerarin, a neuroprotective natural flavonoid, and decorated with a mitochondria-targeting peptide (SS-31) (Zhang et al. 2023). These nanoparticles were intranasally administered via the nose-to-brain pathway in a middle cerebral artery occlusion (MCAO) rat model of ischemic stroke. The thioketal linker enabled H_2O_2-dependent drug release, with cumulative release reaching approximately 48% under oxidative conditions compared to only 18% at baseline. In MCAO rat models, this approach reduced infarct volume approximately 3-fold compared to untreated controls, while alleviating oxidative stress and restoring mitochondrial function. These strategies can be applied not only in tumor targeting but also in CNS diseases where the lesion microenvironment is altered, such as neuroinflammation, ischemic injury, and neurodegenerative lesions (Zhuang et al. 2011; Marrocco et al. 2024; Zhao et al. 2025). Even though stimuli-responsive platforms, such as protease-sensitive ferritin-based nanovectors and pH- or photo-responsive polymeric viral systems, have been actively explored, their application remains largely confined to the experimental proof-of-concept stage in CNS tumor therapy (Marrocco et al. 2024; Zhao et al. 2025).

3.5.4. Extracellular engagement

On the other hand, direct binding or clearance of extracellular misfolded protein aggregates or neurotoxic assemblies can establish sufficient therapeutic outcomes without requiring cellular uptake (Zhang et al. 2023; Li et al. 2025). The HDL-Disc-based polyDisc system developed by Zhang et al. functions not only as a carrier but also as a therapeutic unit that captures amyloid-β (Zhang et al. 2023). It can induce clearance mechanisms in the central and peripheral nervous systems, achieving a 97.3% reduction in brain parenchymal and a 73.5% reduction in vascular amyloid-β accumulation following intranasal administration. This logic extends to antibody-based agents that engage soluble or aggregated species in the interstitial space.

Kamei et al. intranasally co-administered an anti-amyloid-β antibody with L-penetratin, achieving more efficient brain delivery than intravenous injection and improving spatial learning in aged App knock-in mice, while the increased soluble amyloid-β pool was consistent with suppressed plaque formation and microglia-associated clearance (Kamei et al. 2022).

Full-length antibodies carry an Fc effector domain that can provoke inflammatory or microhemorrhagic responses, motivating the exploration of antibody fragments. Cattepoel et al. showed that an anti-amyloid-β single-chain variable fragment (under 30 kDa) entered the cortex and hippocampus after chronic intranasal treatment, bound directly to parenchymal and vascular plaques, and reduced plaque burden and cerebral amyloid angiopathy without the Fc-mediated liabilities of the parent immunoglobulin (Cattepoel et al. 2011). Beyond binding-based sequestration, catalytic peptides can degrade aggregates enzymatically. Hatakawa et al. reported that JAL-TA9, a nine-residue catalytide hydrolyzing amyloid-β42, reached the cerebrospinal fluid at a concentration 4.8-fold higher than in plasma after intranasal administration, with direct transport percentages above 90% across the olfactory bulb, frontal, and occipital regions (Hatakawa et al. 2025). These strategies share a defining feature: the endpoint is engagement with an extracellular substrate rather than intracellular delivery (Table 6).

3.6. Biofate and clearance of N2B delivery systems

The preceding strategies address how a delivery system overcomes each sequential bottleneck, yet its ultimate fate within the brain is governed by the biomolecular identity it acquires in transit rather than by its as-synthesized properties alone. Surface charge and charge density are the primary determinants of this acquired identity (Illum et al. 1994; Pritchard et al. 1996; Soane et al. 1999; Krauland et al. 2006). In the nasal cavity, highly cationic lipid nanoparticles (LNPs) adsorb negatively charged mucins to form an adhesive corona that, while prolonging residence, can entrap the carrier and consign it to mucociliary clearance before epithelial transit (Aspden et al. 1997; Soane et al. 1999). Consistent with this, a systematic screen of ionizable lipid nanoparticles showed that a positive surface charge enhances nose-to-brain delivery by prolonging nasal residence and driving brain-specific mRNA expression, underscoring surface charge as a tunable determinant of N2B efficiency (Yu et al. 2026). Once the carrier reaches the perineural spaces or CSF, this layer evolves as mucosal proteins are exchanged for endogenous components such as apolipoproteins and albumin. The identity of the acquired proteins can steer subsequent handling. In plasma and blood–brain barrier models, apolipoprotein E (ApoE) adsorption promotes recognition by low-density lipoprotein receptors (LDLRs), and an analogous route may operate in the N2B context, whereas enrichment with opsonins instead favors phagocytic removal by macrophages and, in the CNS, microglia (Wagner et al. 2012; Vu et al. 2019). The corona therefore acts less as a fixed design feature than as a determinant of where, and how rapidly, a carrier is ultimately cleared.

Understanding how these systems exit the brain is as important as understanding their entry. Clearance proceeds through several parallel routes that extend beyond the enzymatic hydrolysis of peptides, proteins, and oligonucleotides. Convective exchange along the glymphatic system moves solutes between the CSF and the interstitial fluid, after which macromolecules and intact carriers drain from the CNS largely through meningeal lymphatic vessels and perineural routes crossing the cribriform plate toward the cervical lymph nodes (Chae et al. 2024). Notably, this outflow is anatomically concentrated. A discrete arachnoid region surrounding the olfactory bulbs was recently shown to contain abundant fenestrations that serve as principal exit portals for CSF into the olfactory meningeal lymphatics, a pathway conserved in non-human primates and markedly diminished with aging (Hong et al. 2026). For low-molecular-weight species released from a carrier, efflux transporters at the blood–brain barrier, most notably *P*-glycoprotein, actively pump substrates from the parenchyma back into the blood, a route that acts on the freed payload rather than on the intact nanocarrier (Cox et al. 2023). The nanocarriers themselves are instead handled predominantly by glial phagocytosis and perivascular drainage. These convective, lymphatic, cellular, and transporter-mediated pathways collectively set the residence time of a delivery system, which in turn defines both its therapeutic window and its potential for unintended accumulation.

This balance between residence and removal carries direct safety and toxicological implications central to regulatory evaluation (Keller et al. 2022). Given that the N2B route deposits material along the olfactory and trigeminal pathways and that repeated dosing is often required for chronic CNS conditions, impaired or

Table 6. Formulation strategies for target-cell engagement and functional delivery. Strategies are organized by category, including receptor-mediated targeting via the H-ferritin/TfR1 and lactoferrin (Lf)/LfR axes, CPP-mediated membrane engagement, tropism-guided delivery via exosomes or stem-cell shuttles, disease microenvironment-responsive conditional activation, and extracellular substrate engagement without requiring cellular uptake. The applied cargo, disease model, and major limitation are listed for each approach. CPP, cell-penetrating peptide. LfR, lactoferrin receptor. TfR1, transferrin receptor 1. MMP-2/9, matrix metalloproteinase-2/9. NP, nanoparticle.

Major category	Sub-category	Representative platform/component	Applied cargoes	Major limitation	Ref
Receptor-mediated targeting	H-ferritin/TfR1 axis(intrinsic receptorrecognition)	• H-ferritin nanocages • MMP-2/9-cleavable PASE-shielded ferritin nanovectors	• Genz-644282 • Gold/iron-oxide payloads in H-ferritin nanocages	• TfR1 expression varying across tumor and normal tissue • Endogenous-transferrin competition • MMP-2/9 activation needing confirmed enzyme gradients	Fan et al. (2012); Moglia et al. (2021); Marrocco et al. (2024)
	Lactoferrin/LfR axis(brain endothelial andneuronal targeting)	• Lactoferrin-conjugated PEG-PLA NPs • Lactoferrin-functionalized lipid nanocarriers	• Coumarin-6 • Nimodipine • Rotigotine	• Endogenous-lactoferrin competition • Receptor expression varying by disease and cell type • Lack of intranasal-specific mechanistic data	Hu et al. (2009); Zhao et al. (2018)
Membrane penetration	CPP-mediatedmembrane engagement(receptor-independent)	• CPP-modified PLGA NPs , • LMWP-conjugated proteins • Leptin + penetratin co-administration	• Fluorescent PLGA NPs • Horseradish peroxidase • β-Galactosidase • Leptin	• Reduced selectivity from non-specific membrane interaction • Endosomal-trapping risk • Organ- or circuit-level pharmacodynamic proof required	Malhotra et al., 2013; Lin et al. (2016); Steinbach et al. (2016); Khafagy et al. (2020)
	Native tropism-guideddelivery (exosomes/stem cells)	• Exosome-encapsulated curcumin • Stem-cell shuttle systems	• Curcumin • Oncolytic adenovirus	• Complex manufacturing • Variable carrier viability • Difficult biodistribution control • Limited control of final intracellular delivery	Zhuang et al. (2011); Dey et al. (2016); El-Ayoubi et al. (2023)
Conditional activation	Disease microenvironment-responsive targeting(protease/pH/NIR)	• pH-sensitive and photothermal polymeric oncolytic adenovirus • NIR-light-activated CRISPR-Cas9/RNP formulation	• Oncolytic adenovirus • CRISPR-Cas9 RNP	• Dependent on confirmed pathological microenvironment • Premature de-shielding risk • Preclinical proof-of-concept stage only • Device compatibility required for light-responsive systems	Simões et al. (2024); Zhao et al. (2025)
Extracellular engagement	Extracellular substratebinding and clearance(no cellular uptake required)	• PolyDisc/HDL-Disc, conceptually related extracellular aggregate-binding biologics or scavenger systems	• HDL-Disc/polyDisc • Anti-amyloid/anti-tau biologics or aggregate-binding systems	• Restricted to extracellular targets • Scarce evidence for long-term recovery and clearance specificity • Largely conceptual or disease-class-dependent	Zhang et al. (2023); Li et al. (2025)

saturated clearance raises the prospect of progressive nanomaterial accumulation in the olfactory bulb and perivascular compartments, sustained microglial activation, and local injury to the nasal epithelium. Conversely, because the same lymphatic outflow that clears waste can also remove a therapeutic before it acts, delivery and clearance must be considered as coupled design constraints rather than in isolation. Regulatory agencies accordingly expect biofate and safety profiles to be comprehensively evaluated alongside therapeutic efficacy. This includes not only biodistribution and systemic persistence, but also potential immunogenicity (both innate mucosal responses and systemic neutralizing immunity), neuroinflammation markers (astrogliosis and chronic microglial activation), and the overall reversibility of localized tissue effects.

4. Future perspectives: overcoming the translational barriers in N2B delivery

4.1. Multistage-aware design

The clinical landscape of intranasal CNS therapy reveals a pronounced translational imbalance. Agents that have reached regulatory approval are almost exclusively low-molecular-weight small molecules delivered as nasal sprays, including esketamine for treatment-resistant depression (Daly et al. 2018), zavegepant for acute migraine (Lipton et al. 2023), and midazolam and diazepam for seizure clusters (Detyniecki et al. 2019; Wheless et al. 2021). Peptide-based candidates, such as intranasal insulin for Alzheimer's disease, remain confined to early clinical testing (Craft et al. 2020). In contrast, the nanoplatform-based systems that dominate preclinical innovation, spanning chitosan nanoparticles, lipid nanoparticles, ferritin nanocages, and biomimetic nanodiscs, have yet to advance beyond rodent models (Zhang et al. 2023; Aly et al. 2023; Marrocco et al. 2024). This disparity indicates that formulation sophistication alone has not translated into clinical progress, pointing to unresolved barriers in the transport cascade rather than in cargo design. Successful N2B delivery strategies should aim to maximize posterior access, the gateway to effective brain delivery, rather than allowing formulations to mistarget the anterior region (Yokel 2022; Crowe and Hsu 2022; Drath et al. 2025). A fundamental engineering oversight driving this translational gap is the scarcity of formulation strategies that actively target post-epithelial fluidic and tissue-access pathways (Yokel 2020; Yokel 2022). These pathways range from the immediate post-epithelial transit to just prior to target cell internalization. Current formulation strategies have disproportionately optimized only the initial and final stages of delivery, focusing heavily on mucosal retention and epithelial permeation alongside ligand-directed target-cell engagement (Yokel 2022; Drath et al. 2025). Concurrently, they have largely neglected the intermediate post-epithelial channels, namely CSF/perivascular space (PVS)-mediated redistribution and deep parenchymal penetration (Yokel 2020; Yokel 2022). As a result, the lack of strategies to navigate these intermediate biological bottlenecks can render even sophisticated targeting ligands ineffective, relegating otherwise promising technologies to mere conceptual possibilities. Therefore, bridging this translational gap requires a paradigm shift toward multistage-aware formulation design capable of orchestrating the entire transport cascade.

Because N2B transport is a sequence of interconnected stages, maximizing the efficiency of a single stage can inadvertently introduce physicochemical trade-offs that compromise subsequent transport phases (Lai et al. 2009; Suk et al. 2016; Yokel 2022). A representative example is robust mucoadhesion. While it effectively extends nasal residential time, it simultaneously occupies therapeutic cargoes within the dense mucus mesh, thereby hindering their diffusion toward the epithelial surface (Cone 2009; Lai et al. 2009). Conversely, PEGylation designed to facilitate mucus penetration often compromises subsequent cellular uptake efficiencies (Suk et al. 2016). Furthermore, the surface conjugation of targeting ligands frequently impairs the mucus-penetrating properties of the formulation (Lai et al. 2009; Suk et al. 2016). These contradictory requirements across sequential barriers highlight why a multistage-aware design that systematically harmonizes the entire transport cascade is a key mechanistic requirement.

Recent formulation design has evolved beyond single-function maximization toward the spatiotemporal integration of complementary functionalities. The primary stage of this progress focused on a simple bidirectional integration, typically combining a cationic mucoadhesive backbone with a brain-targeting ligand within a single platform to simultaneously enhance nasal retention and receptor-mediated transcytosis (Meng et al. 2018). It has recently advanced into multi-layered sequential cascades designed to

orchestrate triple-targeting properties, encompassing the mucus barrier, the epithelial cell layer, and specific intracellular uptake (Rassu et al. 2017). A single nanocarrier can be used to systematically link together different modular components. For example, the outermost mucoadhesive chitosan shell prolongs nasal residence time and opens epithelial paracellular junctions. Because N2B transport operates as an interconnected cascade, the isolated optimization of a single stage can inadvertently impose physicochemical trade-offs that compromise downstream transport phases (Rassu et al. 2017). This study demonstrated multistage recognizing architecture can orchestrate a sequential triple-targeting cascade. Beyond this simple multifunctional stacking, the cutting edge of multistage engineering has incorporated 'conditional activation' to resolve the dilemmas of systemic exposure and off-target interactions. A prominent example includes bio-responsive ferritin nano carrier engineered with protective polypeptide shields via matrix metalloproteinase-2/9 (MMP-2/9)-cleavable linkers (Marrocco et al. 2024). These platforms can maintain rigorous physical shielding within the nasal cavity and the initial fluidic pathways, unshielding the core targeting domains only upon encountering pathological enzyme gradients overexpressed in the tumor microenvironment. These sequential advancements demonstrate that N2B delivery engineering has transitioned from passive multifunctional assembly toward a systematic sequential design paradigm (Rassu et al. 2017; Meng et al. 2018; Marrocco et al. 2024).

Nevertheless, formulation platforms that actively target late-stage transport before final cellular uptake remain rare (Yokel 2020; Yokel 2022). Despite being the critical determinants of clinical efficacy, PVS/CSF-mediated redistribution and parenchymal penetration have largely been addressed only through external physical modalities, such as focused ultrasound (FUS) or magnetic field guidance (Chen et al. 2014; Xi et al. 2015; Ye et al. 2021; Li and Feng 2022). However, lessons from alternative CNS administration routes, such as convection-enhanced delivery (CED) or direct intrathecal injection, suggest that post-epithelial transport is not an uncontrollable, passive diffusion process (Nance et al. 2012; Lonser et al. 2015; Pizzo et al. 2018). Rather, it may represent a tunable bottleneck. CSF influx and glymphatic transport do not occur through linear anatomical conduits. Instead, they constitute a dynamic circulation network governed by physiological and hydrodynamic variables (Iliff et al. 2012, 2013; Mestre et al. 2018; Wang et al. 2025). Therefore, N2B formulation engineering must look beyond the epithelial boundary and capture the three columns of late-stage physiology (Influx, Exchange, and Outflow) as independent formulation design parameters (Figure 12) (Iliff et al. 2012, 2013; Mestre et al. 2018; Proulx 2021).

First, the design of the formulation can leverage hemodynamic drive and influx. Arterial pulsatility driven by cardiac cycles serves as the primary physical engine driving CSF into the perivascular channels (Iliff et al. 2013; Mestre et al. 2018). The dobutamine treatment, artificially amplifying arterial pulsatility, significantly accelerates paravascular CSF influx, whereas unilateral internal carotid artery ligation reduces pulsatility via drastically suppresses flow (Iliff et al. 2013). Secondly, modulating intra-tissue fluid exchange can be applied. For convective fluid to penetrate the dense brain parenchyma, efficient solute exchange between the CSF and ISF is mandatory (Iliff et al. 2012; Wang et al. 2025). Biologically, the expression and polarized localization of aquaporin-4 (AQP4) water channels at the astrocytic endfeet act as the molecular gatekeeper of this exchange (Iliff et al. 2012). Therefore, to maximize this fluid-to-tissue transfer, future co-delivery strategies could incorporate transient modulators of AQP4-dependent CSF-ISF exchange alongside the primary therapeutic cargo, or surface-functionalizing the nanocarrier itself with bio-responsive components designed to engage this perivascular exchange interface (Iliff et al. 2012; Simões et al. 2024). By temporally synchronizing the upregulation of this molecular gatekeeper with the arrival of the formulation in the CSF space, or by allowing the nanocarrier to actively breach the parenchymal gateway upon local contact with the astrocytic endfeet, these approaches enable highly precise, on-demand control over intra-tissue delivery kinetics. Lastly, to sustain continuous convective flow and prevent fluid stagnation, an unobstructed exit pathway is vital. CSF drainage is complexly wired not only to the arachnoid villi but also to perineural spaces, the cribriform plate route surrounding the olfactory nerve, and the nasal/dural lymphatic drainage networks (Proulx 2021; Spera et al. 2023). To address this, future formulations could be engineered to actively lower downstream hydrodynamic resistance. For example, nanocarriers designed for the sequential, spatiotemporal release of mild extracellular matrix-remodeling enzymes or lymphatic vasodilators (e.g. VEGF-C) at the exit sites could improve local obstruction, thereby regulating outflow pressure to ensure uninterrupted, deep-brain convective circulation (Song et al. 2020). Collectively, because CSF influx and glymphatic transport function as a dynamic circulation network responsive to physiological

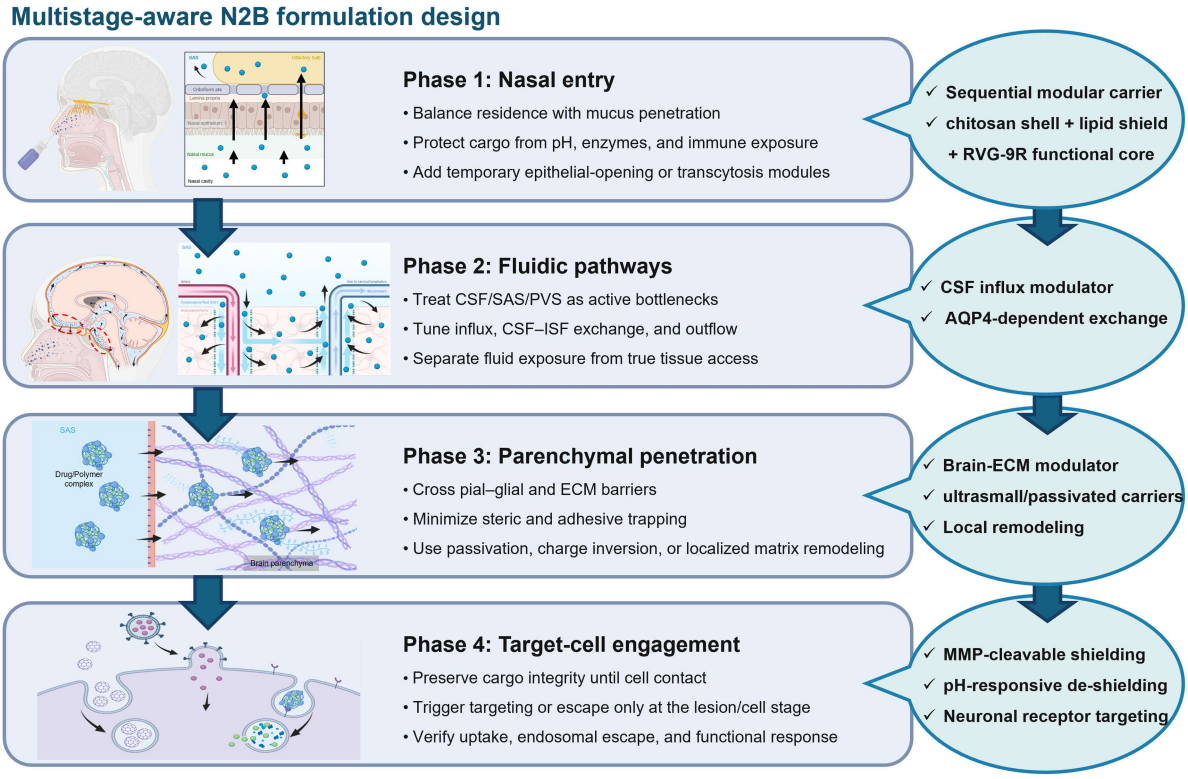

Figure 12. Conceptual framework for multistage-aware N2B formulation design. The framework organizes N2B engineering into four sequentially addressed phases. Phase 1 (nasal entry) addresses the balance between nasal residence and mucus penetration, cargo protection from pH, enzymatic, and immune exposure, and the incorporation of epithelial-opening or transcytosis-enabling modules. Phase 2 (fluidic pathways) treats CSF, SAS, and PVS as active, tunable bottlenecks, targeting influx modulation, CSF-ISF exchange via aquaporin-4 (AQP4), and outflow resistance. Phase 3 (parenchymal penetration) focuses on crossing the pial-glia limitans and ECM barriers through surface passivation, charge inversion, or localized matrix remodeling. Phase 4 (target-cell engagement) requires cargo integrity preservation until cell contact, conditional activation at the lesion site, and direct verification of uptake, endosomal escape, and functional response. A representative sequential modular carrier integrating a chitosan shell, lipid shield, and RVG-9R functional core is shown as an example of multistage integration. CSF, cerebrospinal fluid. SAS, subarachnoid space. PVS, perivascular space. ECM, extracellular matrix. MMP, matrix metalloproteinase. RVG, rabies virus glycoprotein. Created with BioRender.com.

variables, N2B delivery platforms must look beyond static cargo characteristics such as size and charge. Instead, they must actively integrate patient hemodynamics (pulsatility), anatomical alignment (posture and AQP4 gatekeepers), and lymphatic clearance capacity into their core architecture (Iliff et al. 2012, 2013; Mestre et al. 2018; Proulx 2021).

Finally, the surface properties of nanocarriers must be sophisticatedly modified to navigate the brain-specific ECM during parenchymal penetration (Nance et al. 2012; Lau et al. 2013). Beyond hyaluronan, the ECM of brain lesions and tumor microenvironments presents highly dense physical barriers composed of chondroitin sulfate proteoglycans (CSPGs), collagens, and tenascin-C (Lau et al. 2013). However, because healthy brain ECM is critical for maintaining neurological homeostasis and synaptic plasticity, indiscriminate enzymatic degradation is prohibited due to severe neurotoxicity risks. Therefore, smart N2B that executes localized, transient matrix-remodeling in response to pathological enzyme gradients can be a highly promising and biocompatible design trajectory. Alternatively, platforms utilizing charge-inversion can be employed to maximize diffusion kinetics across the negatively charged interstitial space. These vectors remain positively charged during epithelial translocation, but transit to a neutral or negative state upon entering the parenchymal interface. This temporary charge shift ensures deep tissue penetration without disrupting structural homeostasis.

A further translational consideration is the harmonization of intranasal administration itself. Clinically approved N2B products are delivered as metered nasal sprays or powder devices engineered for reproducible deposition, whereas preclinical studies rely on heterogeneous techniques, ranging from micropipette instillation into the nostril to catheter placement, frequently under anesthesia and supine positioning that maximize olfactory contact in ways human self-administration cannot replicate (Drath et al. 2025). This mismatch confounds cross-study comparison and inflates apparent delivery efficiency relative to what a clinical device could achieve, since conventional sprays deposit only a small fraction of the dose in the upper nasal region. where olfactory transport occurs. Narrowing this gap will require preclinical protocols to report deposition-relevant parameters, such as administered volume, head position, and the targeted nasal region. Harmonizing these approaches to ensure market viability requires a paradigm shift: future formulations can no longer be developed in isolation from physical device engineering and anatomical considerations. Instead, formulation chemistry must be co-developed with advanced delivery technologies, such as anatomically designed olfactory-targeting devices, breath-actuated dispensers, and human nasal cast benchmarking, early in the preclinical stage (Boyuklieva et al. 2023). By embracing this multidisciplinary convergence from the outset, researchers can bridge the gap between preclinical instillation and clinical reality, improving the odds that a promising nanomedicine successfully reaches the market.

Ultimately, advanced, multistage-aware N2B formulations must exceed their historical role as passive vehicles and evolve into dynamic transport systems capable of sequentially decoding the brain's fluidic pathways and pathological tissue barriers to navigate the CNS landscape intelligently.

4.2. Cargo-informed design

N2B delivery platforms cannot serve as universally applicable vehicles across disparate therapeutic modalities (Patel et al. 2022). From small molecule generics to peptides, nucleic acids, gene-editing machinery, and complex biological viral vectors, the intrinsic physicochemical and biological identity of each cargo fundamentally dictates both the type and the hierarchy of the biological barriers that the formulation must overcome. Therefore, alongside multi-stage aware, a cargo-informed design that establishes the inherent properties of the payload as the primary engineering starting point is an indispensable prerequisite.

N2B delivery platform for small molecules should overcome local clearance. The primary pharmacokinetic issue for relatively small, lipophilic molecules is ensuring adequate mucosal solubility and prolonged local residence time (Qian et al. 2014; Rassu et al. 2015; Agrawal et al., 2020; Kali et al. 2024). For these payloads, straightforward physicochemical interventions, such as the utilization of cyclodextrin derivatives for inclusion complexation or responsive in situ gelling matrices, are typically sufficient to yield meaningful improvements in global brain delivery efficiency.

Conversely, peptide and protein therapeutics face immediate enzymatic destruction by the dense repertoire of proteases and peptidases in the nasal mucosa, alongside low paracellular permeability due to their hydrophilicity (Hussain et al. 1985; Sarkar 1992; Aungst 2012; Patel et al. 2022). For intermediate peptides like insulin or oxytocin, chemical interventions must be precisely tailored to neutralize mucosal proteases and transiently modulate the epithelial barrier. Specifically, this is achieved by co-incorporating competitive protease inhibitors, such as bacitracin or amastatin, to shield the labile peptide backbone from enzymatic cleavage (Hussain et al. 1989; O'Hagan et al. 1990). Concurrently, specialized paracellular permeation enhancers including sodium glycocholate or medium-chain fatty acids like sodium caprate are utilized to transiently disrupt and dilate epithelial tight junctions, thereby facilitating passive mucosal transit (Aungst 2012). However, macromolecular proteins such as monoclonal antibodies face a more formidable barrier even after crossing the epithelium. The size-exclusion threshold of the pial-glial interface can be a big challenge during parenchymal entry (Pizzo et al. 2018). These therapeutic antibodies are inherently restricted from undergoing passive paracellular diffusion through the tight interstitial gaps. Consequently, formulation strategies for payload must reroute the transport pathway from a paracellular to a transcellular route. Incorporation of multifunctional targeting motifs, such as transferrin- or lactoferrin-receptor ligands, may support receptor-associated uptake or transcytosis pathways (Hu et al. 2009; Gabold et al. 2023).

Nucleic acid therapeutics, including siRNA, ASOs, and mRNA, present entirely different physicochemical hurdles. As highly polyanionic macromolecules, they are inherently incapable of passively crossing lipid

bilayers and are rapidly degraded by ubiquitous nucleases within the nasal and extracellular fluids (Howard et al. 2006; Fihurka et al. 2018). Moreover, the conventional engineering approach of using cationic carriers for electrostatic condensation often leads to severe entrapment within the negatively charged mucus mesh, inducing premature clearance (Cone 2009; Lai et al. 2009; Boegh and Nielsen 2015). Therefore, it would be highly advantageous to structurally encapsulate and shield the payload within advanced lipid nanoparticles (LNPs) or polyplex architectures (Howard et al. 2006; Bazargani et al. 2025; Maniyamgama et al., 2025). Furthermore, PEGylation integrating surface charge-masking for mucus penetration alongside stimuli-responsive mechanisms to trigger endosomal escape within a single platform represents a preferred strategy to maximize overall therapeutic efficacy (Suk et al. 2016; Simões et al. 2024).

CRISPR gene-editing systems, such as Cas9/Cas12 ribonucleoproteins (RNPs) and base/prime editors, present a unique physicochemical bottleneck that conflates the vulnerabilities of both protein and nucleic acid payloads (Simões et al. 2024). A fully assembled RNP complex, comprising guide RNA (gRNA) and the Cas protein, is a ~150–200 kDa of macromolecular complex characterized by a highly polyanionic charge and inherent immunogenicity. When utilizing non-viral polymeric or lipidic nanocarriers to condense these systems, researchers face dual constraints that hinder efficient transport. First, charge over-compensation frequently leads to premature entrapment within the negatively charged mucus network (Cone 2009; Lai et al. 2009; Boegh and Nielsen 2015). Subsequently, the payload's bulkiness induces severe steric exclusion by the pial-glial interface and parenchymal ECM (Nance et al. 2012; Pizzo et al. 2018). Consequently, cargo-informed CRISPR platform relies on structural concealing during mucosal and fluidic transit. Further, this carrier must be programmed with multi-stage stimuli-responsive components that trigger rapid endosomal escape and subsequent nuclear localization immediately upon target-cell internalization, maximizing gene-editing efficiency without inducing cellular toxicity (Simões et al. 2024).

Engineered viral vectors, encompassing a wide range of gene therapy vehicles and oncolytic viruses, represent the peak of formulation complexity (Quinn et al. 2011; Gadenstaetter et al. 2022; Zhao et al. 2025). These biological entities present unique engineering challenges based on their distinct physical dimensions. On one end of the physical continuum, small, non-enveloped vectors such as adeno-associated viruses (AAVs, ~25–30 nm) possess rigid capsids that sit near the upper cut-off threshold of glymphatic convective channels (Quinn et al. 2011; Gadenstaetter et al. 2022; Wang et al. 2025), allowing for relatively favorable fluidic transport. Conversely, larger viral vectors, ranging from intermediate enveloped particles like lentiviruses (~80–120 nm) to macroscopic oncolytic platforms including adenoviruses, vaccinia viruses, and herpes simplex viruses (HSVs, up to ~200 nm), suffer severe steric entrapment and immobilization within the dense interstitial mesh of the brain parenchyma (Nance et al. 2012; Yokel 2022; Zhao et al. 2025). Further, all viral modalities share the dual biological vulnerabilities of pronounced systemic immunogenicity and pre-existing host neutralizing antibodies (Quinn et al. 2011; Gadenstaetter et al. 2022), alongside an evolutionarily determined native tissue tropism that often misdirects the cargo away from the intended CNS lesion (Gadenstaetter et al. 2022). Consequently, when designing hybrid biopolymer coatings or supramolecular shielding envelopes to guide these diverse viral entities, core engineering objective is achieving a programmable dynamic equilibrium. The N2B formulation for viral vectors must comprehensively coat the vector's surface capsids or envelopes to evade immunological surveillance during mucosal and fluidic transit, yet seamlessly de-shield at the target site to fully restore the virus's native infectivity, membrane fusion, and cellular transduction capabilities (Quinn et al. 2011; Gadenstaetter et al. 2022).

Ultimately, the refinement of cargo-informed design can be achieved only when formulation engineering fully understands the mechanistic vulnerabilities of a payload (Table 7).

4.3. Disease-informed design

Another critical blind spot in current N2B delivery research is that most formulation platforms are developed and evaluated based on normal physiological barriers under homeostatic conditions (Yokel 2022; Drath et al. 2025; Park and Riew 2025). However, CNS disorders do not preserve static anatomy or physiological states. These are progressive pathologies that continuously remodel the physical, hydrodynamic, and biochemical barriers along the transport pathway over time (Kress et al. 2014; Rasmussen et al. 2018). To achieve successful clinical translation, formulation engineering must exceed the traditional view of anatomy as a static filter. Instead, a paradigm shift toward a ‘disease-informed design’ is required,

Table 7. Cargo-informed N2B formulation design: biophysical identity, stage-specific barriers, and engineering strategies by cargo class. For each payload class, the table lists the key biophysical properties, the stage-specific biological barriers imposed along the N2B transport cascade, and the corresponding formulation engineering strategies required to address them. Cargo classes covered include small molecules, peptide and protein therapeutics including monoclonal antibodies (mAbs), nucleic acid therapeutics such as siRNA, antisense oligonucleotides (ASOs), and mRNA, CRISPR ribonucleoprotein (RNP) complexes, and engineered viral vectors. LNP, lipid nanoparticle. mAb, monoclonal antibody. RNP, ribonucleoprotein complex. siRNA, small interfering RNA. Created with BioRender.com.

Cargo type	Key biophysical identity	Biological barriers and challenges	N2B formulation engineering strategies	Ref
Small molecule generics	• Low MW • Lipophilic • Solubility-dependent absorption	• Rapid mucociliary clearance • Low mucosal solubility • Short epithelial contact	• Cyclodextrin complexation • In situ gelling	Qian et al. (2014); Rassu et al. (2015); Agrawal et al., 2020; Kali et al. (2024)
Peptide and protein therapeutics (e.g. insulin, oxytocin)	• Hydrophilic macromolecule • Enzyme-labile backbone • Low passive permeability	• Enzymatic degradation • Low paracellular permeability • Short half-life	• Protease inhibitors (bacitracin, amastatin) • Permeation enhancers (glycocholate)	Hussain et al. (1985), (1989); O'Hagan et al. (1990); Sarkar (1992); Aungst (2012); Patel et al. (2022)
Macromolecular proteins (Monoclonal antibodies)	• Large MW (>100 kDa) • Charge-heterogeneous surface • No passive diffusion	• Pial-glial size exclusion • Restricted paracellular diffusion • ECM steric trapping	• Receptor ligands (transferrin, lactoferrin) for transcytosis	Hu et al. (2009); Pizzo et al. (2018); Gabold et al. (2023)
Nucleic acid therapeutics (siRNA, ASOs, mRNA)	• Polyanionic • No passive bilayer crossing • Nuclease-labile	• Nuclease degradation • No bilayer crossing • Cationic mucus entrapment • Endolysosomal sequestration	• LNP or polyplex encapsulation • PEGylation • Stimuli-responsive endosomal escape	Howard et al. (2006); Cone (2009); Lai et al. (2009); Boegh and Nielsen (2015); Suk et al. (2016); Fihurka et al. (2018); Bazargani et al. (2025); Maniyamgama et al., 2025)
CRISPR gene-editing systems (Cas9/Cas12 RNP, Base/Prime editors)	• Large RNP (~150–200 kDa) • Polyanionic • Cas immunogenicity • Nuclear access required	• Charge over-compensation • Bulky-RNP steric exclusion • Cas immunogenicity • Poor endosomal escape	• RNP concealment • Multi-stage responsive escape and nuclear delivery	Cone (2009); Lai et al. (2009); Nance et al. (2012); Boegh and Nielsen (2015); Pizzo et al. (2018); Seifelnasr et al. (2024); Simões et al. (2024)
Engineered viral vectors (AAVs, lentiviruses, adenoviruses, vaccinia viruses, HSVs/oncolytic viruses)	• AAV: ~25–30 nm • Lentivirus: ~80–120 nm • Adenovirus: ~90–100 nm • HSV: ~150–200 nm	• Steric ECM entrapment of large vectors • Immunogenicity • Native tropism misdirection	• Biopolymer capsid shielding • Target-site de-shielding	Quinn et al. (2011); Nance et al. (2012); Yokel (2022); Gadenstaetter et al. (2022); Zhao et al. (2025); Wang et al. (2025)

wherein pathologically induced barrier dynamics are integrated as core variables in N2B formulation engineering (Figure 13).

The very first gate, the nasal mucosa, is profoundly altered by pathological states (Gizurarson 1993; Merkus et al. 1998; Min et al. 2015). In patients with chronic neurodegenerative diseases, systemic neuroinflammation or aging-associated comorbidities often impair MCC and drastically alter intranasal pH and mucus rheology (Gizurarson 1993; Merkus et al. 1998). Under chronic inflammatory conditions, epithelial tight junctions may already be compromised, and altered concentrations of inflammatory proteins in the disease-induced mucus can abnormally amplify non-specific binding with cationic nanocarriers (Cone 2009; Lai et al. 2009; Boegh and Nielsen 2015; Min et al. 2015). In such a pathological environment, mucoadhesive formulations designed for healthy mucosal surfaces may cause excessive aggregation, which ironically impedes epithelial transmigration.

Following epithelial translocation, the hydrodynamic transport pathway undergoes the most dramatic remodeling. While CSF convection and glymphatic perivascular transport are critical drivers of post-epithelial N2B redistribution, these pathways are severely compromised in aging and neurodegenerative disorders such as Alzheimer's disease (AD) and Parkinson's disease (PD) (Kress et al. 2014; Rasmussen et al. 2018; Wang et al. 2025). The loss of aquaporin-4 (AQP4) polarization at the perivascular astroglial foot processes, coupled with diminished arterial pulsatility, weakens the hydrodynamic drivers that support

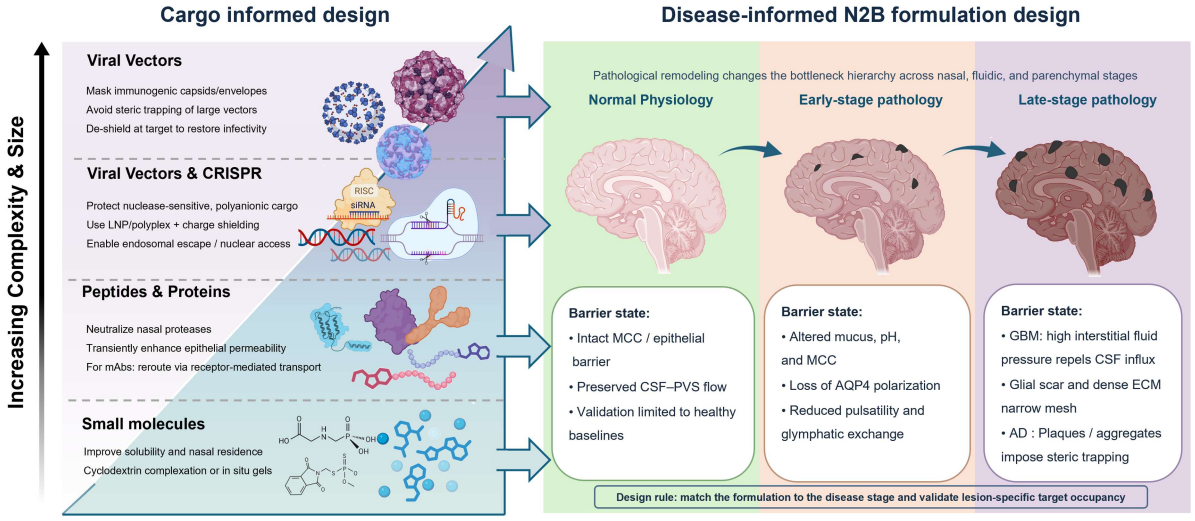

Figure 13. Integrated cargo-informed and disease-informed design framework for N2B delivery. Left panel (Cargo-informed design): Formulation strategies must scale with payload complexity. Small molecules require solubility and residence enhancement; peptides/proteins need protease protection and permeation enhancers (with mAbs requiring receptor-mediated transport). CRISPR and viral vectors demand advanced encapsulation (LNP/polyplex), charge shielding, endosomal escape, and dynamic de-shielding at target sites. Right panel (Disease-informed design): Biological barriers dynamically remodel with disease progression. While normal physiology serves as baseline control, early-stage pathologies exhibit altered mucus, MCC, and impaired glymphatic exchange. Late-stage conditions introduce high interstitial fluid pressure (IFP), dense ECM (glial scars), and steric trapping by protein plaques. Ultimately, formulations must be tailored to the specific disease stage and validated for lesion-specific target occupancy. AQP4, aquaporin-4, CSF, cerebrospinal fluid, ECM, extracellular matrix, GBM, glioblastoma multiforme, IFP, interstitial fluid pressure, LNP, lipid nanoparticle, mAb, monoclonal antibody, MCC, mucociliary clearance, PVS, perivascular space. Created with BioRender.com.

solute movement toward the brain parenchyma (Iliff et al. 2013; Kress et al. 2014; Mestre et al. 2018). Consequently, formulations designed for fluid-mediated targeting that perform well under intact physiological conditions can often fail to reach deep tissues when used in actual disease states. Therefore, formulations targeting late-stage neurodegeneration need to consider to incorporate active mechanisms, such as self-propelled nanomotor systems or transient glymphatic rejuvenators, to autonomously overcome or bypass damaged perivascular spaces (Rasmussen et al. 2018; Wang et al. 2025).

Furthermore, the microenvironment within the brain parenchyma is radically reorganized depending on the disease type and stage, creating a pivotal limitation for final tissue penetration. In malignant brain tumors like glioblastoma (GBM), abnormal neovascularization causes structural disruption of the BBB, leading to a leaky endothelium (Jain et al. 2007). While this hyperpermeability is advantageous for systemic intravenous delivery, it can be a formidable hydrodynamic barrier for N2B delivery. The continuous leakage of intravascular fluid and proteins into the tumor interstitium increases the interstitial fluid pressure (IFP) within the tumor microenvironment. This localized high-pressure environment functions as an outward fluidic barrier, physically repelling N2B cargoes attempting to diffuse into the tumor core from the surrounding CSF space or healthy parenchymal margins.

Simultaneously, pathological progression densely remodels the ECM, the structural scaffold of the brain parenchyma (Syková and Nicholson 2008; Sofroniew 2009; Lau et al. 2013). In ischemic stroke, traumatic brain injury (TBI), or zones of severe neuroinflammation, reactive astrocytes, together with microglial and inflammatory components, contribute to glial scar formation (Sofroniew 2009; Lau et al. 2013). This process involves the excessive deposition of inhibitory components, such as chondroitin sulfate proteoglycans (CSPGs) and collagens, which drastically constricts the interstitial mesh size and alters local electrostatic properties (Syková and Nicholson 2008; Sofroniew 2009). Similarly, in neurodegenerative pathologies, the accumulation of amyloid plaques or abnormal protein aggregates introduces massive steric hindrance within the interstitial space (Iliff et al. 2012; Zhang et al. 2023). Ultimately, nanocarriers that exhibit ideal

mobility *in vitro* may lose motility and become entrapped when confronting a fibrotic, pressurized lesion matrix (Syková and Nicholson 2008; Nance et al. 2012).

Taken together, a multistage-aware formulation must be coupled with a disease-informed design to ensure clinical efficacy. From the earliest stages of development, researchers must consider the altered states of the nasal, fluidic, and parenchymal barriers within the specific pathological window of the target disease. Furthermore, *in vitro* and *in vivo* validation frameworks must recapitulate microenvironmental pressures and biochemical remodeling. Only by redefining evaluation criteria from absolute bioavailability to lesion-specific target occupancy can N2B platforms evolve into viable clinical modalities.

4.4. Stage-resolved experimental validation

To date, many studies have relied on bulk, non-fractionated tissue readouts, such as whole-brain fluorescence imaging and total tissue homogenate assays, as proof of delivery success (Ahmad et al. 2017; Yokel 2020; Yokel 2022). Crucially, however, these compartment-blind metrics fail to reflect whether a vehicle is sequestered within intermediate boundary compartments, prematurely disrupted by pathological matrix forces, or rendered non-functional despite structural entry. Therefore, conventional readouts with a single quantitative value can create a general illusion of success that overestimates therapeutically relevant delivery. This methodological overestimation stems from three critical blind spots.

First, bulk readouts can obscure sub-anatomical compartment localization. Even when a robust brain signal or imaging is observed, it cannot discern whether the formulation has penetrated the deep brain parenchyma or remains sequestered within intermediate boundary compartments. As shown by Lochhead et al., intranasal tracers exploit the PVS as a low-resistance convective highway for rapid, brain-wide redistribution (Lochhead et al. 2015). However, while this glymphatic-associated transit is a vital macro-transport pathway, a widespread perivascular signal must not be conflated with widespread parenchymal entry. Without high-resolution confocal or sheet-illumination microscopy to verify paracellular extravasation out of the PVS and into the deep interstitial space, bulk readouts can lead to a misinterpretation of a vehicle on the vascular periphery as a successfully delivered therapeutic.

Secondly, conventional readouts often fail to address the carrier-cargo dissociation during the delivery process. As demonstrated by Ahmad et al. in intranasal nanoemulsion studies, a therapeutic payload can undergo rapid premature leakage or phase separation prior to reaching target sites, migrating through the tissue independently of its delivery vehicle (Ahmad et al. 2017). Consequently, observing a fluorescently labeled cargo within brain sections does not automatically imply the successful post-entry transport of an intact nanocarrier. To dismantle this illusion, future frameworks must implement dual-labeling strategies or advanced biophysical assays, such as Förster Resonance Energy Transfer (FRET), to differentiate between the signal of a structurally cohesive platform and that of a liberated, naked cargo (Ahmad et al. 2017; Yokel 2020).

Lastly, the physical accumulation of formulation within the brain does not warrant functional intracellular uptake or biological activation of therapeutics. Whether the delivered cargo undergoes productive target-cell penetration, endosomal escape, and pharmacological interaction remains an entirely separate biological hurdle. Therefore, experiments that directly assay cargo functionality provide more rigorous evidence of late-stage delivery success than simple fluorescent tracking (Harmon et al. 2014; Aly et al. 2023). For instance, Harmon et al. demonstrated functionally effective delivery by confirming that intranasally administered CK30PEG-compacted plasmid DNA nanoparticles successfully drove downstream eGFP expression in rat brains (Harmon et al. 2014). Similarly, Aly et al. showed that intranasal delivery of mutant huntingtin-lowering ASO-loaded apoA-I nanodiscs reduced toxic huntingtin protein levels in the cortex and striatum (Aly et al. 2023).

To address these limitations, future N2B studies should adopt a stage-resolved validation framework aligned with the transport cascade defined in Section 2. Each experimental setting should be matched to the specific stage it intends to support. In this framework, a whole-brain signal should be treated only as an initial screening endpoint, whereas claims of meaningful delivery require additional evidence of carrier integrity, compartment-resolved localization, true parenchymal entry, and functional target engagement. The recommended minimum and advanced validation criteria for each transport stage are summarized in Table 8.

Table 8. Stage-resolved experimental validation framework for mechanistically rigorous N2B delivery assessment. To overcome the limitations of compartment-blind bulk readouts, this table outlines a stage-specific validation framework corresponding to the N2B transport cascade. For each sequential delivery stage, the table identifies the primary interpretive risks of conventional assays and proposes both minimum and advanced experimental criteria required to substantiate precise delivery claims. ACQ, aggregation-caused quenching, ALI, air–liquid interface, DTE, drug targeting efficiency, DTP, direct transport percentage, LSFM, light-sheet fluorescence microscopy, MPT, multiple-particle tracking, Papp, apparent permeability coefficient.

Transport stage	Primary interpretive risk	Minimum validation criteria	Advanced validation criteria	Claim supported	Ref
Nasal deposition and mucosal retention	• Anterior impaction misread as retention • No olfactory-vs-respiratory resolution	• Gamma scintigraphy • Nasal cast mapping • Mucin-interaction assay • Franz/Ussing chamber	• CFD or cast simulation • Multiple-particle tracking • Ex vivo MCC assay • Large-animal deposition	Olfactory-accessible exposure and MCC bypass	Gizurarson (1993); Merkus et al. (1998); Cone (2009); Boegh and Nielsen (2015)
Epithelial crossing	• Lamina propria signal misread as transcytosis • Paracellular passage overestimated	• ALI model (Papp, TEER) • TJ-protein IF (ZO-1, claudin)	• Ex vivo TEM • Endocytic-marker co-localization • Inhibitor validation in 3D models	Mechanism and extent of translocation	Lin et al. (2016); Lochhead and Davis (2019); Yokel 2022; Drath et al. (2025); Qiu et al. (2025)
Olfactory and trigeminal nerve pathway transport	• Perineural diffusion misread as intraneuronal transport • No olfactory-vs-trigeminal separation	• Nerve IF (OMP, βIII-tubulin) • Excised-nerve fluorometry • Temporal dissection series	• Intact-carrier discrimination (ACQ, FRET) • CLSM of excised nerve	Route-specific and intact-carrier discrimination	Buchner et al. (1987); Thorne et al. (2004); Johnston et al. (2004); Nagra et al. (2006); Renner et al. (2012); Norwood and Zhang, 2019; Lochhead et al. (2019); Proulx (2021); Yokel (2022)
CSF and perivascular redistribution	• PVS/SAS signal misread as parenchymal entry • AQP4-glymphatic contribution unverified	• Cisterna magna CSF sampling • Regional brain dissection	• In vivo two-photon CSF tracking • AQP4-perturbation testing • Dynamic biodistribution	CSF transit and glymphatic dependence	Iliff et al. (2012); Iliff et al. (2013); Mestre et al. (2018); Proulx (2021)
Parenchymal penetration	• Perivascular/meningeal signal conflated with parenchymal entry • Artifact from intravascular adhesion	• Cardiac perfusion before harvest • IV control for BBB fraction • AQP4 boundary IF	• Light-sheet penetration mapping • AQP4-referenced depth profiling	True intraparenchymal distribution	Iliff et al. (2012); Pizzo et al. (2018); Proulx (2021)
Target-cell engagement and functional delivery	• Accumulation assumed as intracellular delivery • Off-target uptake undetected	• Cell-type IF (NeuN, GFAP, Iba1, CD31) • Competitive receptor blocking	• Receptor-blocking confirmation • In vivo integrity (FRET/ACQ) • Endosomal-escape imaging • Functional and behavioral readouts	Productive uptake and functional response	Schlachet and Sosnik (2019); Yokel (2022); Gabold et al. (2023)

While the stage-resolved framework is most informative when tailored to a given transport step, not every criterion applies to every formulation, so a minimal set of stage-agnostic requirements is useful as a common baseline that any N2B study should satisfy. First, direct nose-to-brain transport should be distinguished from systemic recirculation, for example by comparing intranasal with intravenous or a matched parenteral route and reporting a drug-targeting efficiency or direct-transport percentage rather than brain signal alone. Second, quantification must be normalized to the administered dose and be compartment-specific. Rather than analyzing whole-brain bulk homogenates, studies should use perfusion or tissue fractionation to distinguish actual brain tissue (parenchyma) from blood vessels and cerebrospinal fluid. Third, carrier and cargo should be tracked as distinct entities, so that measured brain signal reflects the intended species rather than a dissociated label or free payload. Finally, delivery should be linked to a functional or pharmacodynamic readout that confirms the cargo reaches its site of action in an active form. These four requirements, namely route-controlled transport, normalized compartment-aware

quantification, carrier-cargo discrimination, and functional confirmation, are applicable regardless of carrier chemistry and provide a comparable foundation onto which stage-specific validation can be layered.

On the other hand, the anatomical divergence between the rodent models and human nasal anatomy should be considered a translational constraint. As emphasized by Yokel the olfactory epithelium covers approximately 41%–52% of the nasal cavity surface in adult rats, whereas in humans it occupies only approximately 3.0%–10.5% (Yokel 2022). Unlike small molecules, for cargoes larger than 100 nm, only a small fraction is expected to deposit in the human olfactory region, making direct comparisons with rodent instillation studies complicated. This discrepancy is further amplified by common rodent protocols, in which formulations are often instilled under anesthesia and supine positioning, thereby increasing olfactory epithelial contact under conditions that do not reflect human self-administration. These anatomical and procedural disparities argue for complementing rodent efficacy data with human nasal cast deposition studies, primary human nasal epithelial cell air–liquid interface models, and large-animal nasal deposition models such as porcine or ovine systems.

Beyond these deposition-focused surrogates, nonhuman primate (NHP) models provide the closest approximation to human nasal physiology, since the olfactory region of macaques occupies a proportion of the nasal cavity comparable to that of humans and is similarly sequestered from the main airstream, allowing spray deposition, olfactory targeting, and systemic clearance to be evaluated under near-human geometry (Lee et al. 2020). Intranasal delivery of macromolecules and peptides to the primate CNS along olfactory and trigeminal pathways has been demonstrated on this basis, supporting the translational relevance of NHP data for deposition and transport (Sasaki et al. 2023). Human-derived three-dimensional systems, including nasal organoids and nose-on-a-chip platforms, provide a complementary but fundamentally different capability. These microphysiological models can recapitulate cell-level features such as epithelial barrier integrity, mucus turnover, and paracellular permeability that are difficult to control in vivo, yet they do not reproduce the macroscopic airflow, regional deposition, and whole-axis fluid transport that define the rodent-human anatomical gap in the first place. Their value therefore lies in dissecting stage-specific cellular mechanisms rather than in resolving the geometric and hydrodynamic discrepancies of the intact nasal pathway, for which in vivo NHP models remain indispensable.

In summary, although a whole-brain signal can serve as a useful experimental starting point, it is insufficient to confirm deep parenchymal penetration or productive target-cell engagement. The primary limitation of current N2B validation is the lack of stage-specific evidence capable of decoupling post-entry redistribution from true intra-tissue diffusion, carrier integrity, and functional uptake. Therefore, future N2B studies should move beyond the binary paradigm of total brain readout and adopt validation frameworks that verify vehicle integrity, compartment-resolved localization, parenchymal penetration, and functional target engagement in a stage-resolved manner (Harmon et al. 2014; Lochhead et al. 2015; Yokel 2020; Aly et al. 2023).

5. Conclusions

The current translational stagnation in N2B delivery is caused, in part, by a profound conceptual over-simplification. N2B transport is a formidable, sequential cascade encompassing mucosal retention, epithelial translocation, fluidic redistribution, and deep intraparenchymal extracellular diffusion. To bridge this translational gap, formulation engineering must shift toward an integrated paradigm built on three core principles. Future formulations must actively orchestrate multistage-aware designs to spatiotemporally harmonize sequential functionalities, cargo-informed architectures tailored to the payload's distinct vulnerabilities, and disease-informed approaches capable of adapting to pathologically remodeled physical and hydrodynamic barriers. Ultimately, even the most advanced delivery platforms will fail to achieve clinical maturity without a rigorous, stage-resolved validation framework. We recommend the adoption of compartment-resolved imaging, FRET-based dissociation assays, and functional readouts to explicitly decouple passive fluidic distribution from true parenchymal penetration and functional execution. Furthermore, recognizing the profound anatomical discrepancies in olfactory surface area between pre-clinical rodent models and humans is paramount. Equally important, the biofate, clearance, and long-term safety of these systems must be characterized alongside efficacy, since regulatory translation depends as much on how a carrier is eliminated from the brain as on how it is delivered. By integrating human-relevant anatomical evaluation models and strictly enforcing stage-specific validation, N2B delivery can move

beyond its status as a preclinical phenomenon and evolve into a reliable, transformative clinical modality for CNS therapeutics.

Author contributions

CRediT: **Youngbeom Kim:** Conceptualization, Formal analysis, Investigation, Visualization, Writing – original draft; **Chae-Ok Yun:** Conceptualization, Formal analysis, Funding acquisition, Investigation, Supervision, Writing – review & editing; **A-Rum Yoon:** Conceptualization, Formal analysis, Funding acquisition, Investigation, Project administration, Supervision, Writing – review & editing.

Disclosure statement

Chae-Ok Yun is the founder and CEO of GeneMedicine Co., Ltd. The remaining authors report no competing interests to declare.

Funding

This research was supported by a grant of the Korea Health Technology R&D Project through the Korea Health Industry Development Institute (KHIDI), funded by the Ministry of Health & Welfare, Republic of Korea (RS-2024-00439816, C-O. Y., RS-2025-02263117, A-R. Y.), Ministry of Food and Drug Safety, Republic of Korea (RS-2024-00395863, A-R. Y.) and Korea Basic Science Institute (National Research Facilities and Equipment Center) grant funded by the Ministry of Education. (2023R1A6C101A009). The funders had no role in the design of the review, literature interpretation, manuscript preparation, or decision to submit the article for publication.

Data availability statement

No new research data were generated or analyzed in this review. All information discussed in this article is available from the cited literature.

Declaration of generative AI and AI-assisted technologies in the manuscript preparation process

During the preparation of this work, the authors used ChatGPT (OpenAI, San Francisco, CA, USA) and Claude (Anthropic, San Francisco, CA, USA) to improve language clarity and readability. Conceptual schematic figures were prepared with the assistance of Manus (Monica, Singapore) and BioRender (BioRender, Toronto, Canada). After using these tools, the authors reviewed and edited all content and figures, verified all information, and took full responsibility for the content of the article.

Ethics approval

Not applicable. This article is a review and does not report new experiments involving human participants, animals, or biological samples performed by the authors.

References

Abbott NJ, Patabendige AA, Dolman DE, et al. 2010. Structure and function of the blood–brain barrier. Neurobiol Dis. 37(1):13–25. https://doi.org/10.1016/j.nbd.2009.07.030

Aceto A, Di Ilio C, Angelucci S, et al. 1989. Glutathione transferases in human nasal mucosa. Arch Toxicol. 63(6):427–431. https://doi.org/10.1007/BF00316443

Agrawal M, Saraf S, Dubey SK et al. 2020. Stimuli-responsive in situ gelling system for nose-to-brain drug delivery. J Control Release. 327:235–265. https://doi.org/10.1016/j.jconrel.2020.07.044

Ahmad E, Feng Y, Qi J, et al. 2017. Evidence of nose-to-brain delivery of nanoemulsions: cargoes but not vehicles. Nanos. 9(3):1174–1183. https://doi.org/10.1039/C6NR07581A

Alvarez-Erviti L, Seow Y, Yin H, et al. 2011. Delivery of siRNA to the mouse brain by systemic injection of targeted exosomes. Nat Biotechnol. 29(4):341–345. https://doi.org/10.1038/nbt.1807

Aly AE, Caron NS, Black HF, et al. 2023. Delivery of mutant huntingtin-lowering antisense oligonucleotides to the brain by intranasally administered apolipoprotein A-I nanodisks. J Control Release. 360:913–927. https://doi.org/10.1016/j.jconrel.2023.07.027

Aspden TJ, Mason JD, Jones NS, et al. 1997. Chitosan as a nasal delivery system: the effect of chitosan solutions on in vitro and in vivo mucociliary transport rates in human turbinates and volunteers. J Pharm Sci. 86(4):509–513. https://doi.org/10.1021/js960182o

Aungst BJ. 2012. Absorption enhancers: applications and advances. AAPS J. 14(1):10–18. https://doi.org/10.1208/s12248-011-9307-4

Bahadur S, Pardhi DM, Rautio J, et al. 2020. Intranasal nanoemulsions for direct nose-to-brain delivery of actives for CNS disorders. Pharmaceutics. 12(12):1230. https://doi.org/10.3390/pharmaceutics12121230

Baron J, Burke JP, Guengerich F, et al. 1988. Sites for xenobiotic activation and detoxication within the respiratory tract: implications for chemically induced toxicity. Toxicol Appl Pharmacol. 93(3):493–505. https://doi.org/10.1016/0041-008X(88)90053-1

Bazargani A, Hejazi M, Fernandez M, et al. 2025. PEGylated solid lipid nanoparticles for the intranasal delivery of combination antiretroviral therapy composed of atazanavir and elvitegravir to treat NeuroAIDS. Int J Pharm. 670:125166. https://doi.org/10.1016/j.ijpharm.2025.125166

Bi C, Wang A, Chu Y, et al. 2016. Intranasal delivery of rotigotine to the brain with lactoferrin-modified PEG-PLGA nanoparticles for Parkinson's disease treatment. Int J Nanomedicine. 11:6547–6559. https://doi.org/10.2147/IJN.S120939

Boegh M, Nielsen HM. 2015. Mucus as a barrier to drug delivery – understanding and mimicking the barrier properties. Basic Clin Pharmacol Toxicol. 116(3):179–186. https://doi.org/10.1111/bcpt.12342

Bonferoni MC, Rossi S, Sandri G, et al. 2019. Nanoemulsions for "Nose-to-Brain" drug delivery. Pharmaceutics. 11(2):84. https://doi.org/10.3390/pharmaceutics11020084

Boyuklieva R, Zagorchev P, Pilicheva B. 2023. Computational, in vitro, and in vivo models for nose-to-brain drug delivery studies. Biomedicines. 11(8):2198. https://doi.org/10.3390/biomedicines11082198

Bruinsmann FA, Pigana S, Aguirre T, et al. 2019. Chitosan-coated nanoparticles: effect of chitosan molecular weight on nasal transmucosal delivery. Pharmaceutics. 11(2):86. https://doi.org/10.3390/pharmaceutics11020086

Buchner K, Seitz-Tutter D, Schönitzer K, et al. 1987. A quantitative study of anterograde and retrograde axonal transport of exogenous proteins in olfactory nerve C-fibers. Neuroscience. 22(2):697–707. https://doi.org/10.1016/0306-4522(87)90366-6

Casettari L, Illum L. 2014. Chitosan in nasal delivery systems for therapeutic drugs. J Control Release. 190:189–200. https://doi.org/10.1016/j.jconrel.2014.05.003

Cattepoel S, Hanenberg M, Kulic L, et al. 2011. Chronic intranasal treatment with an anti-Abeta(30-42) scFv antibody ameliorates amyloid pathology in a transgenic mouse model of Alzheimer's disease. PLoS One. 6(4):e18296. https://doi.org/10.1371/journal.pone.0018296

Chae SY, Jang MK, Nah JW. 2005. Influence of molecular weight on oral absorption of water soluble chitosans. J Control Release. 102(2):383–394. https://doi.org/10.1016/j.jconrel.2004.10.012

Chae J, Choi M, Yoo S. 2024. The nasal lymphatic route of CSF outflow: implications for neurodegenerative disease diagnosis and monitoring. Anim Cells Syst (Seoul). 28(1):45–54. https://doi.org/10.1080/19768354.2024.2307559

Chatterjee B, Gorain B, Mohananaidu K, et al. 2019. Targeted drug delivery to the brain via intranasal nanoemulsion: available proof of concept and existing challenges. Int J Pharm. 565:258–268. https://doi.org/10.1016/j.ijpharm.2019.05.032

Chen H, Acosta C, Wu S, et al. 2014. A new brain drug delivery strategy: focused ultrasound-enhanced intranasal drug delivery. PLoS One. 9(10):e108880. https://doi.org/10.1371/journal.pone.0108880

Chen Y, Cheng G, Hu R, et al. 2019. A nasal temperature and pH dual-responsive in situ gel delivery system based on microemulsion of huperzine A: formulation, evaluation, and in vivo pharmacokinetic study. AAPS PharmSciTech. 20(7):301. https://doi.org/10.1208/s12249-019-1513-x

Chung S, Peters JM, Detyniecki K, et al. 2023. The nose has it: opportunities and challenges for intranasal drug administration for neurologic conditions including seizure clusters. Epilepsy Behav Rep. 21:100581. https://doi.org/10.1016/j.ebr.2022.100581

Cone RA. 2009. Barrier properties of mucus. Adv Drug Delivery Rev. 61(2):75–85. https://doi.org/10.1016/j.addr.2008.09.008

Costa C, Moreira J, Amaral M, et al. 2019. Nose-to-brain delivery of lipid-based nanosystems for epileptic seizures and anxiety crisis. J Control Release. 295:187–200. https://doi.org/10.1016/j.jconrel.2018.12.049

Cox B, Nicolai J, Williamson B. 2023. The role of the efflux transporter, P-glycoprotein, at the blood-brain barrier in drug discovery. Biopharm Drug Dispos. 44(1):113–126. https://doi.org/10.1002/bdd.2331

Craft S, Raman R, Chow TW, et al. 2020. Safety, efficacy, and feasibility of intranasal insulin for the treatment of mild cognitive impairment and alzheimer disease dementia: a randomized clinical trial. JAMA Neurol. 77(9):1099–1109. https://doi.org/10.1001/jamaneurol.2020.1840

Crowe TP, Hsu WH. 2022. Evaluation of recent intranasal drug delivery systems to the central nervous system. Pharmaceutics. 14(3):629. https://doi.org/10.3390/pharmaceutics14030629

Daly EJ, Singh JB, Fedgchin M, et al. 2018. Efficacy and safety of intranasal esketamine adjunctive to oral antidepressant therapy in treatment-resistant depression: a randomized clinical trial. JAMA Psychiatry. 75(2):139–148. https://doi.org/10.1001/jamapsychiatry.2017.3739

Danielyan L, Schäfer R, von Ameln-Mayerhofer A, et al. 2009. Intranasal delivery of cells to the brain. Eur J Cell Biol. 88(6):315–324. https://doi.org/10.1016/j.ejcb.2009.02.001

Detyniecki K, Van Ess PJ, Sequeira DJ, et al. 2019. Safety and efficacy of midazolam nasal spray in the outpatient treatment of patients with seizure clusters-a randomized, double-blind, placebo-controlled trial. Epilepsia. 60(9):1797–1808. https://doi.org/10.1111/epi.15159

Dey M, Yu D, Kanojia D, et al. 2016. Intranasal oncolytic virotherapy with CXCR4-Enhanced stem cells extends survival in mouse model of glioma. Stem Cell Reports. 7(3):471–482. https://doi.org/10.1016/j.stemcr.2016.07.024

Djupesland PG. 2013. Nasal drug delivery devices: characteristics and performance in a clinical perspective-a review. Drug Deliv Transl Res. 3(1):42–62. https://doi.org/10.1007/s13346-012-0108-9

Djupesland PG, Skretting A, Winderen M, et al. 2006. Breath actuated device improves delivery to target sites beyond the nasal valve. Laryngoscope. 116(3):466–472. https://doi.org/10.1097/01.MLG.0000199741.08517.99

Dlamini SM, Mahumane GD, Kumar P, et al. 2026. A review of nanoparticle-based astrocyte modulation in CNS disorders: evaluating the underexplored potential of intranasal delivery. Nano Select. 7(1):e70089. https://doi.org/10.1002/nano.70089

Drath I, Richter F, Feja M. 2025. Nose-to-brain drug delivery: from bench to bedside. Transl Neurodegener. 14(1):23. https://doi.org/10.1186/s40035-025-00481-w

El-Ayoubi A, Klawitter M, Rüttinger J, et al. 2023. Intranasal delivery of oncolytic adenovirus XVir-N-31 via optimized shuttle cells significantly extends survival of glioblastoma-bearing mice. Cancers. 15:4912. https://doi.org/10.3390/cancers15204912

Fan K, Cao C, Pan Y, et al. 2012. Magnetoferritin nanoparticles for targeting and visualizing tumour tissues. Nat Nanotechnol. 7(7):459–464. https://doi.org/10.1038/nnano.2012.90

Faubel R, Westendorf C, Bodenschatz E, et al. 2016. Cilia-based flow network in the brain ventricles. Sci. 353(6295):176–178. https://doi.org/10.1126/science.aae0450

Fihurka O, Sanchez-Ramos J, Sava V. 2018. Optimizing nanoparticle design for gene therapy: protection of oligonucleotides from degradation without impeding release of cargo. Nanomed Nanosci Res. 2(6).

Foo MY, Cheng Y, Su W, et al. 2007. The influence of spray properties on intranasal deposition. J Aerosol Med. 20(4):495–508. https://doi.org/10.1089/jam.2007.0638

Gabold B, Adams F, Brameyer S, et al. 2023. Transferrin-modified chitosan nanoparticles for targeted nose-to-brain delivery of proteins. Drug Deliv Transl Res. 13(3):822–838. https://doi.org/10.1007/s13346-022-01245-z

Gadenstaetter AJ, SCHMUTZLER L, GRIMM D, et al. 2022. Intranasal application of adeno-associated viruses: a systematic review. Transl Res. 248:87–110. https://doi.org/10.1016/j.trsl.2022.05.002

Gadhave D, Tupe S, Tagalpallewar A, et al. 2021. Nose-to-brain delivery of amisulpride-loaded lipid-based poloxamer-gellan gum nanoemulgel: in vitro and in vivo pharmacological studies. Int J Pharm. 607:121050. https://doi.org/10.1016/j.ijpharm.2021.121050

Galeano C, Qiu Z, Mishra A, et al. 2018. The route by which intranasally delivered stem cells enter the central nervous system. Cell Transplant. 27(3):501–514. https://doi.org/10.1177/0963689718754561

Gao M, Shen X, Mao S. 2020. Factors influencing drug deposition in thenasal cavity upon delivery via nasal sprays. Journal of Pharmaceutical Investigation. 50(3):251–259. https://doi.org/10.1007/s40005-020-00482-z

Gao X, Xiong Y, Chen H, et al. 2023. Mucus adhesion vs. Mucus penetration? Screening nanomaterials for nasal inhalation by MD simulation. J Control Release. 353:366–379. https://doi.org/10.1016/j.jconrel.2022.11.051

Gervasi PG, Longo V, Naldi F, et al. 1991. Xenobiotic-metabolizing enzymes in human respiratory nasal mucgsa. Biochem Pharmacol. 41(2):177–184. https://doi.org/10.1016/0006-2952(91)90474-J

Gizurarson S. 1993. The relevance of nasal physiology to the design of drug absorption studies. Adv Drug Delivery Rev. 11(3):329–347. https://doi.org/10.1016/0169-409X(93)90015-V

Steinmetz JD, Seeher KM, Schiess N et al. 2024. Global, regional, and national burden of disorders affecting the nervous system, 1990-2021: a systematic analysis for the global burden of disease study 2021. Lancet Neurol. 23(4):344–381. https://doi.org/10.1016/S1474-4422(24)00038-3

Harmon BT, Aly AE, Padegimas L, et al. 2014. Intranasal administration of plasmid DNA nanoparticles yields successful transfection and expression of a reporter protein in rat brain. Gene Ther. 21(5):514–521. https://doi.org/10.1038/gt.2014.28

Harris AS, Svensson E, Wagner Z, et al. 1988. Effect of viscosity on particle size, deposition, and clearance of nasal delivery systems containing desmopressin. J Pharm Sci. 77(5):405–408. https://doi.org/10.1002/jps.2600770510

Hatakawa Y, Tanaka A, Furubayashi T, et al. 2025. Efficient nose-to-brain delivery of nine residues peptide (JAL-TA9) exhibiting hydrolytic activity against amyloid-beta. Eur J Pharm Biopharm. 208:114661. https://doi.org/10.1016/j.ejpb.2025.114661

Higdon LM, Sperling MR. 2021. A review of a diazepam nasal spray for the treatment of acute seizure clusters and prolonged seizures. Expert Rev Neurother. 21(11):1207–1212. https://doi.org/10.1080/14737175.2021.1965880

Hong SP, Jin C, Yang MJ et al 2026. CSF clearance through arachnoid fenestrations to olfactory meningeal lymphatics. Cell. 189(18):5724–5742.

Howard KA, Rahbek UL, Liu X, et al. 2006. RNA interference in vitro and in vivo using a novel chitosan/siRNA nanoparticle system. Mol Ther. 14(4):476–484. https://doi.org/10.1016/j.ymthe.2006.04.010

Hu K, Li J, Shen Y, et al. 2009. Lactoferrin-conjugated PEG-PLA nanoparticles with improved brain delivery: in vitro and in vivo evaluations. J Control Release. 134(1):55–61. https://doi.org/10.1016/j.jconrel.2008.10.016
Huang Q, Chen Y, Zhang W, et al. 2024. Nanotechnology for enhanced nose-to-brain drug delivery in treating neurological diseases. J Controlled Release. 366:519–534. https://doi.org/10.1016/j.jconrel.2023.12.054
Hussain A, Faraj J, Aramaki Y, et al. 1985. Hydrolysis of leucine enkephalin in the nasal cavity of the rat--a possible factor in the low bioavailability of nasally administered peptides. Biochem Biophys Res Commun. 133(3):923–928. https://doi.org/10.1016/0006-291X(85)91224-0
Hussain MA, Shenvi AB, Rowe SM, et al. 1989. The use of α-Aminoboronic acid derivatives to stabilize peptide drugs during their intranasal absorption. Pharm Res. 6(2):186–189. https://doi.org/10.1023/A:1015949013644
Iliff JJ, Wang M, Liao Y et al. 2012. A paravascular pathway facilitates CSF flow through the brain parenchyma and the clearance of interstitial solutes, including amyloid β. Sci Transl Med. 4(147):147ra111. https://doi.org/10.1126/scitranslmed.3003748
Iliff JJ, Wang M, Zeppenfeld DM, et al. 2013. Cerebral arterial pulsation drives paravascular CSF-interstitial fluid exchange in the murine brain. J Neurosci. 33(46):18190–18199. https://doi.org/10.1523/JNEUROSCI.1592-13.2013
Illum L. 2000. Transport of drugs from the nasal cavity to the central nervous system. Eur J Pharm Sci. 11(1):1–18. https://doi.org/10.1016/S0928-0987(00)00087-7
Illum L, Farraj NF, Davis SS. 1994. Chitosan as a novel nasal delivery system for peptide drugs. Pharm Res. 11(8):1186–1189. https://doi.org/10.1023/A:1018901302450
Jain RK, di Tomaso E, Duda DG, et al. 2007. Angiogenesis in brain tumours. Nat Rev Neurosci. 8(8):610–622. https://doi.org/10.1038/nrn2175
Johnston M, Zakharov A, Papaiconomou C, et al. 2004. Evidence of connections between cerebrospinal fluid and nasal lymphatic vessels in humans, non-human primates and other mammalian species. Cerebrospinal Fluid Res. 1(1):2. https://doi.org/10.1186/1743-8454-1-2
Kali G, Haddadzadegan S, Bernkop-Schnürch A. 2024. Cyclodextrins and derivatives in drug delivery: new developments, relevant clinical trials, and advanced products. Carbohydr Polym. 324:121500. https://doi.org/10.1016/j.carbpol.2023.121500
Kamei N, Hashimoto A, Tanaka E, et al. 2022. Therapeutic effects of anti-amyloid beta antibody after intravenous injection and efficient nose-to-brain delivery in Alzheimer's disease mouse model. Drug Deliv Transl Res. 12(11):2667–2677. https://doi.org/10.1007/s13346-022-01117-6
Kapoor A, Hafeez A, Kushwaha P, et al. 2025. Chitosan-coated nanostructured lipid carriers of amantadine for nose-to-brain delivery: formulation optimization, in vitro-ex vivo characterization, and in vivo anti-parkinsonism assessment. Int J Biiol Macromol. 316:144497. https://doi.org/10.1016/j.ijbiomac.2025.144497
Keller LA, Merkel O, Popp A. 2022. Intranasal drug delivery: opportunities and toxicologic challenges during drug development. Drug Deliv Transl Res. 12(4):735–757. https://doi.org/10.1007/s13346-020-00891-5
Khafagy ES, Kamei N, Fujiwara Y, et al. 2020. Systemic and brain delivery of leptin via intranasal coadministration with cell-penetrating peptides and its therapeutic potential for obesity. J Control Release. 319:397–406. https://doi.org/10.1016/j.jconrel.2020.01.016
Kimbell JS, Segal RA, Asgharian B, et al. 2007. Characterization of deposition from nasal spray devices using a computational fluid dynamics model of the human nasal passages. J Aerosol Med. 20(1):59–74. https://doi.org/10.1089/jam.2006.0531
Koh M, Lee JE, Ye E, et al. 2026. Intranasal administration of temozolomide conjugated nanoparticles with transcranial magnetic stimulation improves the survival in glioblastoma xenograft models. Drug Deliv Transl Res. 16(2):509–521. https://doi.org/10.1007/s13346-025-01895-9
Krauland AH, Guggi D, Bernkop-Schnurch A. 2006. Thiolated chitosan microparticles: a vehicle for nasal peptide drug delivery. Int J Pharm. 307(2):270–277. https://doi.org/10.1016/j.ijpharm.2005.10.016
Kress BT, Iliff JJ, Xia M, et al. 2014. Impairment of paravascular clearance pathways in the aging brain. Ann Neurol. 76(6):845–861. https://doi.org/10.1002/ana.24271
Laffleur F, Hörmann N, Gust R, et al. 2023. Synthesis, characterization and evaluation of hyaluronic acid-based polymers for nasal delivery. Int J Pharm. 631:122496. https://doi.org/10.1016/j.ijpharm.2022.122496
Lai SK, Wang YY, Hanes J. 2009. Mucus-penetrating nanoparticles for drug and gene delivery to mucosal tissues. Adv Drug Deliv Rev. 61(2):158–171. https://doi.org/10.1016/j.addr.2008.11.002
Lau LW, Cua R, Keough MB, et al. 2013. Pathophysiology of the brain extracellular matrix: a new target for remyelination. Nat Rev Neurosci. 14(10):722–729. https://doi.org/10.1038/nrn3550
Lee MR, Shnitko TA, Blue SW, et al. 2020. Labeled oxytocin administered via the intranasal route reaches the brain in rhesus macaques. Nat Commun. 11(1):2783. https://doi.org/10.1038/s41467-020-15942-1
Li B, Feng Y. 2022. In silico study to enhance delivery efficiency of charged nanoscale nasal spray aerosols to the olfactory region using external magnetic fields. Bioengineering (Basel). 9(1):40. https://doi.org/10.3390/bioengineering9010040
Li H, Shen X, Zhang B, et al. 2025. Brain-targeted intranasal delivery of biologics: a perspective for Alzheimer's disease treatment. RSC Pharmaceutics. 2(6):1323–1348. https://doi.org/10.1039/D5PM00148J
Lin T, Liu E, He H, et al. 2016. Nose-to-brain delivery of macromolecules mediated by cell-penetrating peptides. Acta Pharm Sin B. 6(4):352–358. https://doi.org/10.1016/j.apsb.2016.04.001

Lipton RB, Croop R, Stock DA, et al. 2023. Safety, tolerability, and efficacy of zavegepant 10 mg nasal spray for the acute treatment of migraine in the USA: a phase 3, double-blind, randomised, placebo-controlled multicentre trial. Lancet Neurol. 22(3):209–217. https://doi.org/10.1016/S1474-4422(22)00517-8

Lochhead JJ, Davis TP. 2019. Perivascular and perineural pathways involved in brain delivery and distribution of drugs after intranasal administration. Pharmaceutics. 11(11):598. https://doi.org/10.3390/pharmaceutics11110598

Lochhead JJ, Wolak DJ, Pizzo ME, et al. 2015. Rapid transport within cerebral perivascular spaces underlies widespread tracer distribution in the brain after intranasal administration. J Cereb Blood Flow Metab. 35(3):371–381. https://doi.org/10.1038/jcbfm.2014.215

Lochhead JJ, Kellohen KL, Ronaldson PT, et al. 2019. Distribution of insulin in trigeminal nerve and brain after intranasal administration. Sci Rep. 9(1):2621. https://doi.org/10.1038/s41598-019-39191-5

Longo V, Citti L, Gervasi PG. 1986. Metabolism of diethylnitrosamine by nasal mucosa and hepatic microsomes from hamster and rat: species specificity of nasal mucosa. Carcinogenesis. 7(8):1323–1328. https://doi.org/10.1093/carcin/7.8.1323

Lonser RR, Sarntinoranont M, Morrison PF, et al. 2015. Convection-enhanced delivery to the central nervous system. J Neurosurg. 122(3):697–706. https://doi.org/10.3171/2014.10.JNS14229

Madara JL, Dharmsathaphorn K. 1985. Occluding junction structure-function relationships in a cultured epithelial monolayer. J Cell Biol. 101(6):2124–2133. https://doi.org/10.1083/jcb.101.6.2124

Malhotra M, Tomaro-Duchesneau C, Saha S et al. 2013. Intranasal, siRNA delivery to the brain by TAT/MGF tagged PEGylated chitosan nanoparticles. J Pharm (Cairo). 2013:812387.

Maniyamgama N, Bae KH, Chang ZW et al. 2025. *Muco-penetrating lipid nanoparticles having a liquid core for enhanced intranasal mrna delivery*. Adv Sci (Weinh). 12(11):e2407383.

Marrocco F, Falvo E, Mosca L, et al. 2024. Nose-to-brain selective drug delivery to glioma via ferritin-based nanovectors reduces tumor growth and improves survival rate. Cell Death Dis. 15(4):262. https://doi.org/10.1038/s41419-024-06653-2

Marttin E, Verhoef JC, Spies F et al. 1999. The effect of methylated beta-cyclodextrins on the tight junctions of the rat nasal respiratory epithelium: electron microscopic and confocal laser scanning microscopic visualization studies. J Control Release. 57(2):205–213. https://doi.org/10.1016/S0168-3659(98)00115-1

Mehta MR, Surve SA, Menon MD. 2009. Novel nasal in situ gelling system for treatment of sinusitis. Indian J Pharm Sci. 71(6):721–722.

Meng Q, Wang A, Hua H, et al. 2018. Intranasal delivery of huperzine A to the brain using lactoferrin-conjugated N-trimethylated chitosan surface-modified PLGA nanoparticles for treatment of Alzheimer's disease. Int J Nanomedicine. 13:705–718. https://doi.org/10.2147/IJN.S151474

Merkus FWHM, Verhoef JC, Marttin E et al. 1999. Cyclodextrins in nasal drug delivery. Adv Drug Delivery Rev. 36(1):41–57. https://doi.org/10.1016/S0169-409X(98)00054-4

Merkus FW, Marttin E, Schipper NG, et al. 1998. Nasal mucociliary clearance as a factor in nasal drug delivery. Adv Drug Deliv Rev. 29(1-2):13–38. https://doi.org/10.1016/S0169-409X(97)00059-8

Mestre H, Tithof J, Du T, et al. 2018. Flow of cerebrospinal fluid is driven by arterial pulsations and is reduced in hypertension. Nat Commun. 9(1):4878. https://doi.org/10.1038/s41467-018-07318-3

Min HJ, Kim TH, Yoon J. 2015. Hypoxia increases epithelial permeability in human nasal epithelia. Yonsei Med J. 56(3):825–831. https://doi.org/10.3349/ymj.2015.56.3.825

Moglia I, Santiago M, Guerrero S, et al. 2021. Enhanced cellular uptake of H-Chain human ferritin containing gold nanoparticles. Pharmaceutics. 13(11):1966. https://doi.org/10.3390/pharmaceutics13111966

Nagra G, Koh L, Zakharov A, et al. 2006. Quantification of cerebrospinal fluid transport across the cribriform plate into lymphatics in rats. Am J Physiol Regul Integr Comp Physiol. 291(5):R1383–9. https://doi.org/10.1152/ajpregu.00235.2006

Nance EA, Woodworth GF, Sailor KA et al. 2012. A dense poly(ethylene glycol) coating improves penetration of large polymeric nanoparticles within brain tissue. Sci Transl Med. 4(149):149ra119. https://doi.org/10.1126/scitranslmed.3003594

Norwood JN, Zhang Q, Card D. 2019. Anatomical basis and physiological role of cerebrospinal fluid transport through the murine cribriform plate. eLife. 8:e44278. https://doi.org/10.7554/eLife.44278

O'Hagan DT, Critchley H, Farraj NF, et al. 1990. Nasal absorption enhancers for biosynthetic human growth hormone in rats. Pharm Res. 7(7):772–776. https://doi.org/10.1023/A:1015884026056

Pardridge WM. 2005. The blood-brain barrier: bottleneck in brain drug development. NeuroRx. 2(1):3–14. https://doi.org/10.1602/neurorx.2.1.3

Park J, Riew T-R. 2025. Nanoparticle-mediated nose-to-brain delivery for ischemic stroke therapy: preclinical insights. Pharmaceutics. 17:1447. https://doi.org/10.3390/pharmaceutics17111447

Patel D, Patel B, Wairkar S. 2022. Intranasal delivery of biotechnology-based therapeutics. Drug Discov Today. 27(12):103371. https://doi.org/10.1016/j.drudis.2022.103371

Pizzo ME, Wolak DJ, Kumar NN, et al. 2018. Intrathecal antibody distribution in the rat brain: surface diffusion, perivascular transport and osmotic enhancement of delivery. J Physiol. 596(3):445–475. https://doi.org/10.1113/JP275105

du Plessis LH, Kotze AF, Junginger HE. 2010. Nasal and rectal delivery of insulin with chitosan and N-trimethyl chitosan chloride. Drug Deliv. 17(6):399–407. https://doi.org/10.3109/10717541003762888
Porfiryeva NN, Semina II, Salakhov IA, et al. 2021. Mucoadhesive and mucus-penetrating interpolyelectrolyte complexes for nose-to-brain drug delivery. Nanomedicine. 37:102432. https://doi.org/10.1016/j.nano.2021.102432
Prego C, Torres D, Alonso MJ. 2006. Chitosan nanocapsules: a new carrier for nasal peptide delivery. J Drug Delivery Sci Technol. 16(5):331–337. https://doi.org/10.1016/S1773-2247(06)50061-9
Pritchard K, Lansley AB, Martin GP, et al. 1996. Evaluation of the bioadhesive properties of hyaluronan derivatives: detachment weight and mucociliary transport rate studies. Int J Pharm. 129(1):137–145. https://doi.org/10.1016/0378-5173(95)04280-6
Proulx ST. 2021. Cerebrospinal fluid outflow: a review of the historical and contemporary evidence for arachnoid villi, perineural routes, and dural lymphatics. Cell Mol Life Sci. 78(6):2429–2457. https://doi.org/10.1007/s00018-020-03706-5
Qian S, Wong YC, Zuo Z. 2014. Development, characterization and application of in situ gel systems for intranasal delivery of tacrine. Int J Pharm. 468(1-2):272–282. https://doi.org/10.1016/j.ijpharm.2014.04.015
Qiu Y, Huang S, Peng L, et al. 2025. The nasal-brain drug delivery route: mechanisms and applications to central nervous system diseases. MedComm (2020). 6(6):e70213. https://doi.org/10.1002/mco2.70213
Quinn K, Quirion MR, Lo C, et al. 2011. Intranasal administration of adeno-associated virus type 12 (AAV12) leads to transduction of the nasal epithelia and can initiate transgene-specific immune response. Mol Ther. 19(11):1990–1998. https://doi.org/10.1038/mt.2011.146
Rao Q, Xu Y, Wang X, et al. 2024. Construction of an intranasal drug delivery system with hypothalamus-targeting nanoparticles. SusMat. 4(4):e222. https://doi.org/10.1002/sus2.222
Rasmussen MK, Mestre H, Nedergaard M. 2018. The glymphatic pathway in neurological disorders. Lancet Neurol. 17(11):1016–1024. https://doi.org/10.1016/S1474-4422(18)30318-1
Rassu G, Soddu E, Cossu M, et al. 2015. Solid microparticles based on chitosan or methyl-beta-cyclodextrin: a first formulative approach to increase the nose-to-brain transport of deferoxamine mesylate. J Control Release. 201:68–77. https://doi.org/10.1016/j.jconrel.2015.01.025
Rassu G, Soddu E, Posadino AM, et al. 2017. Nose-to-brain delivery of BACE1 siRNA loaded in solid lipid nanoparticles for Alzheimer's therapy. Colloids Surf B Biointerfaces. 152:296–301. https://doi.org/10.1016/j.colsurfb.2017.01.031
Renner DB, Svitak AL, Gallus NJ, et al. 2012. Intranasal delivery of insulin via the olfactory nerve pathway. J Pharm Pharmacol. 64(12):1709–1714. https://doi.org/10.1111/j.2042-7158.2012.01555.x
Riani LR, Seno GFB, Silva DM, et al. 2026. Chitosan-based nanoparticles for nose-to-brain drug delivery: a real path toward effective CNS therapy? ACS Biomaterials Science & Engineering. 12(5):2567–2589. https://doi.org/10.1021/acsbiomaterials.6c00137
Saini S, Sharma T, Jain A, et al. 2021. Systematically designed chitosan-coated solid lipid nanoparticles of ferulic acid for effective management of Alzheimer's disease: a preclinical evidence. Colloids Surf B Biointerfaces. 205:111838. https://doi.org/10.1016/j.colsurfb.2021.111838
Salade L, Wauthoz N, Deleu M, et al. 2017. Development of coated liposomes loaded with ghrelin for nose-to-brain delivery for the treatment of cachexia. Int J Nanomedicine. 12:8531–8543. https://doi.org/10.2147/IJN.S147650
Salzman R, Manson JE, Griffing GT, et al. 1985. Intranasal aerosolized insulin. N Engl J Med. 312(17):1078–1084. https://doi.org/10.1056/NEJM198504253121702
Samaridou E, Alonso MJ. 2018. Nose-to-brain peptide delivery - the potential of nanotechnology. Bioorg Med Chem. 26(10):2888–2905. https://doi.org/10.1016/j.bmc.2017.11.001
Sarin H. 2015. Permeation thresholds for hydrophilic small biomolecules across microvascular and epithelial barriers are predictable on basis of conserved biophysical properties. In Silico Pharmacol. 3(1):5. https://doi.org/10.1186/s40203-015-0009-y
Sarkar MA. 1992. Drug metabolism in the nasal mucosa. Pharm Res. 9(1):1–9. https://doi.org/10.1023/A:1018911206646
Sasaki K, Fukakusa S, Torikai Y, et al. 2023. Effective nose-to-brain drug delivery using a combination system targeting the olfactory region in monkeys. J Controlled Release. 359:384–399. https://doi.org/10.1016/j.jconrel.2023.06.005
Sava V, Fihurka O, Khvorova A, et al. 2020. Enriched chitosan nanoparticles loaded with siRNA are effective in lowering Huntington's disease gene expression following intranasal administration. Nanomedicine. 24:102119. https://doi.org/10.1016/j.nano.2019.102119
Schlachet I, Sosnik A. 2019. Mixed mucoadhesive amphiphilic polymeric nanoparticles cross a model of nasal septum epithelium in vitro. ACS Appl Mater Interfaces. 11(24):21360–21371. https://doi.org/10.1021/acsami.9b04766
Seifelnasr A, Si X, Xi J. 2024. Assessing nasal epithelial dynamics: impact of the natural nasal cycle on intranasal spray deposition. Pharmaceuticals (Basel). 17(1):73. https://doi.org/10.3390/ph17010073
Shingaki T, Hidalgo IJ, Furubayashi T, et al. 2009. The transnasal delivery of 5-fluorouracil to the rat brain is enhanced by acetazolamide (the inhibitor of the secretion of cerebrospinal fluid). Int J Pharm. 377(1-2):85–91. https://doi.org/10.1016/j.ijpharm.2009.05.009
Shingaki T, Inoue D, Furubayashi T, et al. 2010. Transnasal delivery of methotrexate to brain tumors in rats: a new strategy for brain tumor chemotherapy. Mol Pharm. 7(5):1561–1568. https://doi.org/10.1021/mp900275s
Simões S, Lino M, Barrera A, et al. 2024. Near-infrared light activated formulation for the spatially controlled release of CRISPR-Cas9 ribonucleoprotein for brain gene editing. Angew Chem Int Ed Engl. 63(21):e202401004. https://doi.org/10.1002/anie.202401004

Soane RJ, Frier M, Perkins A, et al. 1999. Evaluation of the clearance characteristics of bioadhesive systems in humans. Int J Pharm. 178(1):55–65. https://doi.org/10.1016/S0378-5173(98)00367-6
Sofroniew MV. 2009. Molecular dissection of reactive astrogliosis and glial scar formation. Trends Neurosci. 32(12):638–647. https://doi.org/10.1016/j.tins.2009.08.002
Song E, Mao T, Dong H, et al. 2020. VEGF-C-driven lymphatic drainage enables immunosurveillance of brain tumours. Natur. 577(7792):689–694. https://doi.org/10.1038/s41586-019-1912-x
Spera I, Cousin N, Ries M, et al. 2023. Open pathways for cerebrospinal fluid outflow at the cribriform plate along the olfactory nerves. EBioMedicine. 91:104558. https://doi.org/10.1016/j.ebiom.2023.104558
Steinbach JM, Seo YE, Saltzman WM. 2016. Cell penetrating peptide-modified poly(lactic-co-glycolic acid) nanoparticles with enhanced cell internalization. Acta Biomater. 30:49–61. https://doi.org/10.1016/j.actbio.2015.11.029
Steinke A, Meier-Stiegen S, Drenckhahn D, et al. 2008. Molecular composition of tight and adherens junctions in the rat olfactory epithelium and fila. Histochem Cell Biol. 130(2):339–361. https://doi.org/10.1007/s00418-008-0441-8
Suk JS, Xu Q, Kim N, et al. 2016. PEGylation as a strategy for improving nanoparticle-based drug and gene delivery. Adv Drug Deliv Rev. 99(Pt A):28–51. https://doi.org/10.1016/j.addr.2015.09.012
Syková E, Nicholson C. 2008. Diffusion in brain extracellular space. Physiol Rev. 88(4):1277–1340. https://doi.org/10.1152/physrev.00027.2007
Thorne RG, Pronk G, Padmanabhan V, et al. 2004. Delivery of insulin-like growth factor-I to the rat brain and spinal cord along olfactory and trigeminal pathways following intranasal administration. Neuroscience. 127(2):481–496. https://doi.org/10.1016/j.neuroscience.2004.05.029
Vasiliu O. 2023. Esketamine for treatment-resistant depression: a review of clinical evidence (Review). Exp Ther Med. 25(3):111. https://doi.org/10.3892/etm.2023.11810
Vu VP, Gifford GB, Chen F, et al. 2019. Immunoglobulin deposition on biomolecule corona determines complement opsonization efficiency of preclinical and clinical nanoparticles. Nat Nanotechnol. 14(3):260–268. https://doi.org/10.1038/s41565-018-0344-3
Wagner S, Zensi A, Wien SL, et al. 2012. Uptake mechanism of ApoE-modified nanoparticles on brain capillary endothelial cells as a blood-brain barrier model. PLoS One. 7(3):e32568. https://doi.org/10.1371/journal.pone.0032568
Wang Z, Xiong G, Tsang WC, et al. 2019. Nose-to-brain delivery. J Pharmacol Exp Ther. 370(3):593–601. https://doi.org/10.1124/jpet.119.258152
Wang X, Yin Y, Zhou H, et al. 2025. Drug delivery pathways to the central nervous system via the brain glymphatic system circumventing the blood-brain barrier. Exploration (Beijing). 5(2):20240036. https://doi.org/10.1002/EXP.20240036
Ways TMM, Filippov SK, Maji S, et al. 2022. Mucus-penetrating nanoparticles based on chitosan grafted with various non-ionic polymers: synthesis, structural characterisation and diffusion studies. JCIS. 626:251–264. https://doi.org/10.1016/j.jcis.2022.06.126
Wheless JW, Miller I, Hogan RE, et al. 2021. Final results from a phase 3, long-term, open-label, repeat-dose safety study of diazepam nasal spray for seizure clusters in patients with epilepsy. Epilepsia. 62(10):2485–2495. https://doi.org/10.1111/epi.17041
Xi J, Zhang Z, Si XA. 2015. Improving intranasal delivery of neurological nanomedicine to the olfactory region using magnetophoretic guidance of microsphere carriers. Int J Nanomedicine. 10:1211–1222. https://doi.org/10.2147/IJN.S77520
Xie L, Kang H, Xu Q, et al. 2013. Sleep drives metabolite clearance from the adult brain. Sci. 342(6156):373–377. https://doi.org/10.1126/science.1241224
Yang T, Hussain A, Paulson J, et al. 2004. Cyclodextrins in nasal delivery of low-molecular-weight heparins: in vivo and in vitro studies. Pharm Res. 21(7):1127–1136. https://doi.org/10.1023/B:PHAM.0000032998.84488.7a
Ye D, Yuan J, Yue Y, et al. 2021. Focused ultrasound-enhanced delivery of intranasally administered anti-programmed cell death-ligand 1 antibody to an intracranial murine glioma model. Pharmaceutics. 13(2):190. https://doi.org/10.3390/pharmaceutics13020190
Ye E, Park E, Kim E, et al. 2023. Transcranial application of magnetic pulses for improving brain drug delivery efficiency via intranasal injection of magnetic nanoparticles. Biomed Eng Lett. 13(3):417–427. https://doi.org/10.1007/s13534-023-00272-0
Yokel RA. 2020. Nanoparticle brain delivery: a guide to verification methods. Nanomedicine (Lond). 15(4):409–432. https://doi.org/10.2217/nnm-2019-0169
Yokel RA. 2022. Direct nose to the brain nanomedicine delivery presents a formidable challenge. Wiley Interdiscip Rev Nanomed Nanobiotechnol. 14(2):e1767. https://doi.org/10.1002/wnan.1767
Yu X, Deng X, Lin Y, et al. 2026. Nose-to-brain delivery of mRNA-Loaded lipid nanoparticles bypasses the Blood–Brain barrier for effective brain disease therapy. ACS Nano. 20(21):15589–15605. https://doi.org/10.1021/acsnano.6c04580
Zhang YJ, MA C, LU W, et al. 2005. Permeation-enhancing effects of chitosan formulations on recombinant hirudin-2 by nasal delivery in vitro and in vivo. Acta Pharmacol Sin. 26(11):1402–1408. https://doi.org/10.1111/j.1745-7254.2005.00174.x
Zhang H, Chen Y, Yu M, et al. 2023. Nasal delivery of polymeric nanoDisc mobilizes a synergy of central and peripheral amyloid-beta clearance to treat Alzheimer's disease. Proc Natl Acad Sci U S A. 120(51):e2304213120. https://doi.org/10.1073/pnas.2304213120

Zhang Y, Zhao F, Jiang Z, et al. 2023. Mitochondrial-targeted and ROS-responsive nanocarrier via nose-to-brain pathway for ischemic stroke treatment. Acta Pharm Sin B. 13(12):5107–5120. https://doi.org/10.1016/j.apsb.2023.06.011

Zhao C, Zhang J, Hu H, et al. 2018. Design of lactoferrin modified lipid nano-carriers for efficient brain-targeted delivery of nimodipine. Mater Sci Eng C Mater Biol Appl. 92:1031–1040. https://doi.org/10.1016/j.msec.2018.02.004

Zhao Y, Kasala D, Jiao A, et al. 2025. Potent antitumor effect of intranasally administrable ph-sensitive and photothermal polymeric oncolytic adenovirus for the treatment of brain cancer. Chem Eng J. 505:159770. https://doi.org/10.1016/j.cej.2025.159770

Zhuang X, Xiang X, Grizzle W, et al. 2011. Treatment of brain inflammatory diseases by delivering exosome encapsulated anti-inflammatory drugs from the nasal region to the brain. Mol Ther. 19(10):1769–1779. https://doi.org/10.1038/mt.2011.164